BIBLIOGRAPHY

Chapter I

[1] Lehn, J. M., Atwood, J. L., Davies, J. E. D., Mac Nicol D. D. & Vögtle, F. 1st Ed., Pergamon, Comprehensive Supramolecular Chemistry, Oxford, **1996**.

[2] Fischer, E. Einfluss der Configuration auf die Wirkung der Enzyme. *Ber. Deutch. Chem. 2*. **1894**, *27*, 2985–2993.

[3] Pedersen,C.J. Cyclic polyethers and their complexes with metal salts. *J. Am. Chem. Soc.* **1967**, *89*, 7017–7036.

[4] Cram, D.J. Preorganization–from solvents to spherands. *Angew. Chem. Int. Ed. Engl.* **1986**, *25*, 1039-1157.

[5] Vaidya, S. Clathrates — An exploration of the chemistry of caged compounds. *Resonance.* **2004**, *9,* 18–31.

[6] Gould, S. & Scott, R. C. 2-Hydroxypropyl-β-cyclodextrin (HP-β-CD) : A toxicology review. *Food Chem. Toxicol.* **2005**, *43*, 1451–1459.

[7] Whitesides, G.M. & Boncheva, M. Beyond molecules: self-assembly of mesoscopic and macroscopic components. *Proc. Natl. Acad. Sci. U S A*. **2002**, *99*, 4769-4774.

[8] Blokzijl, W. & Engberts, J.B. Hydrophobic effects. Opinions and facts. *Angew. Chem. Int. Ed. Engl.* **1993,** *32*, 1545-79.

[9] Aakeröy, C.B. & Seddon, K.R. The hydrogen bond and crystal engineering. *Chem. Soc. Rev. Chem. Soc. Rev.* **1993**, *22*, 397-407.

[10] Metrangolo, P. & Resnati, G. Halogen bonding: a paradigm in supramolecular chemistry. *Chem. Eur. J.* **2001**, *7*, 2511-2519.

[11] Oshovsky, G. V., Reinhoudt, D. N. & Verboom, W. Supramolecular Chemistry in Water. *Angew. Chem. Int. Ed. Engl.* **2007**, *46*, 2366–93.

[12] Dsouza, R.N., Pischel, U. & Nau, W.M. Fluorescent Dyes and Their Supramolecular Host/Guest Complexes with Macrocycles in Aqueous Solution. *Chem. Rev.* **2011**, *111*, 7941–7980.

[13] Guo, D.S. & Liu, Y. Supramolecular Chemistry of p-Sulfonatocalix[n]arenes and Its Biological Applications. *Acc. Chem. Res.* **2014**, *47*, 1925–1934.

[14] Song, X., Wen, Y., Zhu, J. L., Zhao, F., Zhang, Z. X. & Li, J. Thermoresponsive Delivery of Paclitaxel by β-Cyclodextrin-Based Poly(N-isopropylacrylamide) Star Polymer via Inclusion Complexation. *Biomacromolecules.* **2016,** *17*, 3957–3963.

[15] Bagabas, A. A., Frasconi, M., Iehl, J., Hauser, B., Farha, O. K., Hupp, J. T., Hartlieb, K. J., Botrosand, Y. Y. & Stoddart, J. F. γ-Cyclodextrin Cuprate Sandwich-Type Complexes. *Inorg. Chem.* **2013,** *52*, 2854–2861.

[16] Xiao, T., Elmes, R. & Yao, Yong. Editorial: Host-Guest Chemistry of Macrocycles. *Front*. *Chem*.**2020**, *8*, 1174.

[17] Guo, D.S. & Liu, Y. Supramolecular chemistry of p-Sulfonatocalix[n]arenes and its biological applications. *Acc*. *Chem*. *Res*. **2014**, *47*, 1925–1934.

[18] Ogoshi, T., Kakuta, T. & Yamagishi, T. A. Applications of pillar[n]arene based supramolecular assemblies. *Angew*. *Chem*. *Int*. *Ed*. **2018**, *58*, 2197–2206.

[19] Xiao, T., Zhou, L.,Wei, X., Li, Z., & Sun, X. Supramolecular copolymers driven by quadruple hydrogen bonding and host-guest interactions. *Chin*. *J*. *Org*. *Chem*. **2020**, *40*, 944–949.

[20] Antoniuk, I., and Amiel, C. Cyclodextrin-mediated hierarchical selfassembly and its potential in drug delivery applications. *J*. *Pharm*. *Sci*. **2016**, *105*, 2570–2588.

[21] Murray, J., Kim, K., Ogoshi, T., Yao, W., & Gibb, B. C. The aqueous supramolecular chemistry of cucurbit[n]urils, pillar[n]arenes and deep-cavity cavitands. *Chem*. *Soc*. *Rev*. **2017**, *46*, 2479–2496.

[22] Wang, Y., Wang, C., Long, R., Cao, Y., Fan, D., Cen, M., Cao, L., Chen, Y. & Yao, Y. Synthesis and controllable self-assembly of 3D amphiphilic organoplatinum (ii) metallacages in water. *Chem. Commun*. **2019**, *55*, 5167-5170.

[23] Yu, G., Jie, K. & Huang, F. Supramolecular Amphiphiles Based on Host–Guest Molecular Recognition Motifs. *Chem. Rev.* **2015**, *115*, 7240-7303.

[24] Iglesias, E. Inclusion Complexation of Novocaine by β-Cyclodextrin in Aqueous Solutions. *J. Org. Chem*. **2006**, *71*, 4383-4392.

[25] Liu, J., Hennink, W. E., van Steenbergen, M. J., Zhuo, R. & Jiang, X. Versatile Supramolecular Gene Vector Based on Host–Guest Interaction. *Bioconjug. Chem.* **2016**, *27*, 1143-1152.

[26] Aytac, Z., Yildiz, Z.I., Kayaci-Senirmak, F., San Keskin, N.O., Kusku, S.I., Durgun, E., Tekinay, T. & Uyar, T. Fast-dissolving, prolonged release, and antibacterial cyclodextrin/limonene-inclusion complex nanofibrous webs via polymer-free electrospinning. *J. Agric. Food Chem.* **2016**, *64*, 7325-7334.

[27] Chen, X., Liu, Z., Parker, S.G., Zhang, X., Gooding, J.J., Ru, Y., Liu, Y. & Zhou, Y. Light-induced hydrogel based on tumor-targeting mesoporous silica nanoparticles as a theranostic platform for sustained cancer treatment. *ACS Appl. Mater. Interfaces*. **2016**, *8*, 15857-15863.

[28] Lin, N. & Dufresne, A. Supramolecular hydrogels from in situ host-guest inclusion between chemically modified cellulose nanocrystals and cyclodextrin. *Biomacromolecules.* **2013**, *14*, 871-880.

[29] Kida, T., Iwamoto, T., Asahara, H., Hinoue, T. & Akashi, M. Chiral Recognition and Kinetic Resolution of Aromatic Amines via Supramolecular Chiral Nanocapsules in Nonpolar Solvents. *J. Am. Chem. Soc.* **2013**, *135*, 3371-3374.

[30] Shi, Z. Q., Cai, Y. T., Deng, J., Zhao, W. F. & Zhao, C. S. Host-Guest Self-Assembly Toward Reversible Thermoresponsive Switching for Bacteria Killing and Detachment. *ACS Appl. Mater. Interfaces.* **2016**, *8*, 23523-23532.

[31] Zhu, W., Zhang, K., Chen, Y. & Xi, F. Simple, Clean Preparation Method for Cross-Linked α-Cyclodextrin Nanoparticles via Inclusion Complexation. *Langmuir.* **2013**, *29*, 5939-5943.

[32] Li, H., Li, F., Zhang, B., Zhou, X., Yu, F. & Sun, L. Visible light-driven water oxidation promoted by host–guest interaction between photosensitizer and catalyst with a high quantum efficiency. *J. Am. Chem. Soc.* **2015**, *137*, 4332-5.

[33] Bakirhan, N. K., Tok, T. T. & Ozkan, S. A. The redox mechanism investigation of non-small cell lung cancer drug: Erlotinib via theoretical and experimental techniques and its host–guest detection by β-Cyclodextrin nanoparticles

modified glassy carbon electrode. *Sens*. *Actuators B*: *Chem*. **2019**, *278*, 172-180.

[34] Rodríguez-López, M.I., Mercader-Ros, M.T., López-Miranda, S., Pellicer, J.A., Pérez-Garrido, A., Pérez-Sánchez, H., Núñez-Delicado, E. & Gabaldón, J.A. Thorough characterization and stability of HP-β-cyclodextrin thymol inclusion complexes prepared by microwave technology: A required approach to a successful application in food industry. *J. Sci*. *Food Agric*. **2019**, *99*, 1322-33.

[35] Kfoury, M., Geagea, C., Ruellan, S., Greige-Gerges, H. & Fourmentin, S. Effect of cyclodextrin and cosolvent on the solubility and antioxidant activity of caffeic acid. *Food Chem*. **2019**, *278*, 163-169.

[36] Mourtzinos, I., Prodromidis, P., Grigorakis, S., Makris, D.P., Biliaderis, C.G. & Moschakis, T. Natural food colorants derived from onion wastes: Application in a yoghurt product. *Electrophoresis*. **2018**. *39*, 1975-1983.

[37] Strokopytov, B., Penninga, D., Rozeboom, H.J., Kalk, K.H., Dijkhuizen, L. & Dijkstra, B.W., 1995. X-ray structure of cyclodextrin glycosyltransferase complexed with acarbose. Implications for the catalytic mechanism of glycosidases. *Biochemistry*. **1995**, *34*, 2234-2240.

[38] Bellringer, M. E., Smith, T. G., Read, R., Gopinath, C. & Olivier, P. β-Cyclodextrin: 52-Week toxicity studies in the rat and dog. *Food Chem*. *Toxicol*. **1995**, *33*, 367-376.

[39] Gould, S. and Scott, R.C. 2-Hydroxypropyl-β-cyclodextrin (HP-β-CD): a toxicology review. *Food Chem. Toxicol*. **2005**,*43*, 1451-1459.

[40] Sayed, M., Gubbala, G. K. & Pal, H. Contrasting interactions of DNA-intercalating dye acridine orange with hydroxypropyl derivatives of β-cyclodextrin and γ-cyclodextrin hosts. *New J. Chem*. **2019**, *43*, 724-736.

[41] Ho, S., Thoo, Y. Y., Young, D. J. & Siow, L. F. Stability and recovery of cyclodextrin encapsulated catechin in various food matrices. *Food Chem*. **2019**, *275*, 594-599.

[42] Bohmer, V. Calixarenes, macrocycles with (almost) unlimited possibilities. *Angew. Chem. Int. Ed.* **1995**, *34*, 713–745.

[43] Gutsche, C.D. Ed., Stoddart, J. F., Calixarenes Revisited, Monographs in Supramolecular Chemistry, The Royal Society of Chemistry, Cambridge, UK, **1998**.

[44] Ikeda, A. & Shinkai, S. Novel cavity design using calix [n] arene skeletons: toward molecular recognition and metal binding. *Chem. Rev.* **1997**, *97*, 1713-1734.

[45] Du, S., Yu, T.Q., Liao, W. & Hu, C. Structure modeling, synthesis and X-ray diffraction determination of an extra-large calixarene-based coordination cage and its application in drug delivery. *Dalton Trans*. **2015**, *44*, 14394-14402.

[46] Gutsche, C.D. Calixarenes. Ed., Stoddart, J.F., Royal Society of Chemistry, Cambridge, UK, **1989**.

[47] Perret, F., Lazar, A.N. and Coleman, A.W. Biochemistry of the para-sulfonato-calix [n] arenes. *Chem. Commun.* **2006**, *23*, 2425-2438.

[48] Abd El-Rahman, M. K. & Mahmoud, A. M. A novel approach for spectrophotometric determination of succinylcholine in pharmaceutical formulation via host–guest complexation with water-soluble p-sulfonatocalixarene, *RSC Adv*. **2015**, *5*, 62469–62476.

[49] Makha, M. & Raston, C.L. Direct synthesis of calixarenes with extended arms: p-phenylcalix [4, 5, 6, 8] arenes and their water-soluble sulfonated derivatives. *Tetrahedron Lett.* **2001**, *42*, 6215-6217.

[50] Yang, W. & de Villiers, M.M. Aqueous solubilization of furosemide by supramolecular complexation with 4-sulphonic calix [n] arenes. *J. Pharm. Pharmacol.* **2004**, *56*, 703-708.

[51] Da Silva, E., Lazar, A.N. & Coleman, A.W. Biopharmaceutical applications of calixarenes. *J. Drug Deliv. Sci. Technol.* **2004**, *14*, 3-20.

[52] Shinkai, S., Mori, S., Koreishi, H., Tsubaki, T. & Manabe, O. Hexasulfonated calix [6] arene derivatives: a new class of catalysts, surfactants, and host molecules. *J. Am. Chem. Soc.* **1986**, *108*, 2409-2416.

[53] Shinkai, S., Kawabata, H., Arimura, T., Matsuda, T., Satoh, H. & Manabe, O. New water-soluble calixarenes bearing sulphonate groups on the 'lower rim': the

relation between calixarene shape and binding ability. *J. Chem. Soc. Perkin Trans.* **1989**, *1*, 1073-1074.

[54] Guo, D.S., Wang, K. & Liu, Y. Selective binding behaviors of p-sulfonatocalixarenes in aqueous solution. *J. Inclusion Phenom. Macrocyclic Chem.* **2008**, *62*, 1-21.

[55] Wintgens, V., Biczók, L. & Miskolczy, Z. Thermodynamics of host–guest complexation between p-sulfonatocalixarenes and 1-alkyl-3-methylimidazolium type ionic liquids. *Thermochim. Acta*. **2011**, *523*, 227-231.

[56] Megyesi, M. & Biczók, L. Considerable change of fluorescence properties upon multiple binding of coralyne to 4-sulfonatocalixarenes. *J. Phys. Chem. B*. **2010**, *114*, 2814-2819.

[57] Wintgens, V., Amiel, C., Biczók, L., Miskolczy, Z. & Megyesi, M. Host–guest interactions between 4-sulfonatocalix [8] arene and 1-alkyl-3-methylimidazolium type ionic liquids. *Thermochim. Acta*, **2012**, *548*, 76-80.

[58] Miskolczy, Z. & Biczók, L. Photochromism of a Merocyanine Dye Bound to Sulfonatocalixarenes: Effect of pH and the Size of Macrocycle on the Kinetics. *J. Phys. Chem. B*. **2013**, *117*, 648-653.

[59] Wang, K., Guo, D.S., Zhang, H.Q., Li, D., Zheng, X.L. & Liu, Y. Highly effective binding of viologens by p-sulfonatocalixarenes for the treatment of viologen poisoning. *J. Med. Chem*. **2009**, *52*, 6402-6412.

[60] Perret, F. & Coleman, A.W. Biochemistry of anionic calix [n] arenes. *Chem. Commun.* **2011**, *47*, 7303-7319.

[61] Basilio, N., Francisco, V. & Garcia-Rio, L. Aggregation of p-sulfonatocalixarene-based amphiphiles and supra-amphiphiles. *Int. J. Mol. Sci*. **2013**, *14*, 3140-3157.

[62] Wang, K., Guo, D.S., Wang, X. & Liu, Y. Multistimuli responsive supramolecular vesicles based on the recognition of p-sulfonatocalixarene and its controllable release of doxorubicin. *Acs Nano*. **2011**, *5*, 2880-2894.

[63] Bakirci, H. & Nau, W.M. Fluorescence regeneration as a signaling principle for choline and carnitine binding: a refined supramolecular sensor system based on a fluorescent azoalkane. *Adv. Funct. Mater.* **2006**, *16*, 237-242.

[64] Hennig, A., Bakirci, H. & Nau, W.M. Label-free continuous enzyme assays with macrocycle-fluorescent dye complexes. *Nat. Methods*. **2007**, *4*, 629-632.

[65] Guo, D.S., Uzunova, V.D., Su, X., Liu, Y. & Nau, W.M. Operational calixarene-based fluorescent sensing systems for choline and acetylcholine and their application to enzymatic reactions. *Chem. Sci.* **2011**, *2*, 1722-1734.

[66] Basílio, N. & Garcia-Rio, L. Calixarene-Based Surfactants: Conformational-Dependent Solvation Shells for the Alkyl Chains. *Chem. Phys. Chem*. **2012**, *13*, 2368-2376.

[67] Guo, D.S., Wang, K., Wang, Y.X. & Liu, Y. Cholinesterase-responsive supramolecular vesicle. *J. Am. Chem. Soc*. **2012**,*134*, 10244-10250.

[68] Wang, Y.X., Guo, D.S., Duan, Y.C., Wang, Y.J. & Liu, Y. Amphiphilic p-sulfonatocalix [4] arene as "drug chaperone" for escorting anticancer drugs. *Sci. Rep*. **2015**, *5*, 1-7.

[69] McGovern, R.E., Fernandes, H., Khan, A.R., Power, N.P. & Crowley, P.B. Protein camouflage in cytochrome c–calixarene complexes. *Nat. Chem.* **2012**, *4*, 527-533.

[70] Dalgarno, S.J., Atwood, J.L. & Raston, C.L. Sulfonatocalixarenes: molecular capsule and 'Russian doll'arrays to structures mimicking viral geometry. *Chem. Commun.* **2006**, *44*, 4567-4574.

[71] Yuan, D., Wu, M., Wu, B., Xu, Y., Jiang, F. & Hong, M. Guest-induced molecular capsule assembly of p-sulfonatothiacalix [4] arene. *Cryst. Growth Des*. **2006**, *6*, 514-518.

[72] Selkti, M., Coleman, A.W., Nicolis, I., Douteau-Guével, N., Villain, F., Tomas, A. & de Rango, C. The first example of a substrate spanning the calix [4] arene bilayer: the solid state complex of p-sulfonatocalix [4] arene with l-lysine. *Chem*. *Commun*. **2000**, *2,* 161-162.

[73] Guo, D., & Liu, Y. Supramolecular chemistry of p-sulfonatocalix[n]arenes and its biological applications. *Acc. Chem. Res.* **2014**, *47*, 1925-34.

[74] Aggarwal, B.B. & Ichikawa, H. Molecular targets and anticancer potential of indole-3-carbinol and its derivatives. *Cell cycle*. **2005**, *4*, 1201-1215.

[75] Fujioka, N., Fritz, V., Upadhyaya, P., Kassie, F. & Hecht, S.S. Research on cruciferous vegetables, indole-3-carbinol, and cancer prevention: A tribute to Lee W. Wattenberg. *Mol. Nutr. Food Res.* **2016**, *60*, 1228-1238.

[76] Verhoeven, D.T., Verhagen, H., Goldbohm, R.A., van den Brandt, P.A. & van Poppel, G. A review of mechanisms underlying anticarcinogenicity by brassica vegetables. *Chem. Biol. Interact.* **1997**, *103*, 79-129.

[77] Kim, S.Y., Kim, D.S., Jeong, Y.M., Moon, S.I., Kwon, S.B. & Park, K.C. Indole-3-carbinol and ultraviolet B induce apoptosis of human melanoma cells via down-regulation of MITF. *Pharmazie.* **2011**, *66*, 982-987.

[78] El-Naga, R.N., Ahmed, H.I. & Abd Al Haleem, E.N. Effects of indole-3-carbinol on clonidine-induced neurotoxicity in rats: impact on oxidative stress, inflammation, apoptosis and monoamine levels. *Neurotoxicology*. **2014**, *44*, 48-57.

[79] Song, J.M., Qian, X., Molla, K., Teferi, F., Upadhyaya, P., OSullivan, G., Luo, X. & Kassie, F. Combinations of indole-3-carbinol and silibinin suppress inflammation-driven mouse lung tumorigenesis by modulating critical cell cycle regulators. *Carcinogenesis*. **2015**, *36*, 666-675.

[80] Bradlow, H.L. Indole-3-carbinol as a chemoprotective agent in breast and prostate cancer. *In Vivo*. **2008**, *22*, 441-445.

[81] Rao, A.K. Acquired disorders of platelet function. *Platelets*. **2013**, 1049-1073.

[82] Ferri, N., Corsini, A. & Bellosta, S. Pharmacology of the new P2Y12 receptor inhibitors: insights on pharmacokinetic and pharmacodynamic properties. *Drugs*. **2013**, *73*, 1681-1709.

[83] Wu, Y.J. Heterocycles and medicine: a survey of the heterocyclic drugs approved by the US FDA from 2000 to present. *Prog*. *Heterocycl*. *Chem*. **2012**, *24*, 1-53.

[84] de Lorgeril, M., Bordet, J.C., Salen, P., Durbin, S., Defreyn, G., Delaye, J. & Boissonnat, P. Ticlopidine increases nitric oxide generation in heart-transplant recipients: a possible novel property of ticlopidine. *J. Cardiovasc. Pharmacol.* **1998**, *32*, 225-230.

[85] Hayakawa, M. & Kuzuya, F. Effects of ticlopidine on erythrocyte aggregation in thrombotic disorders. *Angiology*. **1991**, *42*, 747-753.

[86] Mazoyer, E., Ripoll, L., Boisseau, M.R. and Drouet, L. How does ticlopidine treatment lower plasma fibrinogen? *Thromb. Res.* **1994**, *75*, 361-370.

[87] Zeng, X.X., Zheng, R.L., Zhou, T., He, H.Y., Liu, J.Y., Zheng, Y., Tong, A.P., Xiang, M.L., Song, X.R., Yang, S.Y. & Yu, L.T. Novel thienopyridine derivatives as specific anti-hepatocellular carcinoma (HCC) agents: synthesis, preliminary structure–activity relationships, and in vitro biological evaluation. *Bioorg*. *Med*. *Chem*. *Lett*. **2010**, *20*, 6282-6285.

[88] Calvisi, D.F. Inhibition of hepatitis B virus–associated liver cancer by antiplatelet therapy: A revolution in hepatocellular carcinoma prevention? *Hepatology*, **2013**, *57*, 848-850.

[89] Saltiel, E. & Ward, A. Ticlopidine. A review of its pharmacodynamic and pharmacokinetic properties, and therapeutic efficacy in platelet-dependent disease states. *Drugs*. **1987**, *34*, .222-262.

[90] Gachet, C., Stierlé, A., Cazenave, J.P., Ohlmann, P., Lanza, F., Bouloux, C. & Maffrand, J.P. The thienopyridine PCR 4099 selectively inhibits ADP-induced platelet aggregation and fibrinogen binding without modifying the membrane glycoprotein IIb–IIIa complex in rat and in man. *Biochem. Pharmacol.* **1990**, *40*, 229-238.

[91] Veloso, T.R., Oechslin, F., Que, Y.A., Moreillon, P., Entenza, J.M. & Mancini, S. Aspirin plus ticlopidine prevented experimental endocarditis due to *Enterococcus faecalis* and *Streptococcus gallolyticus*. *Pathog. Dis.* **2015**, *73*, ftv060.

[92] Wojtukiewicz, M.Z., Hempel, D., Sierko, E., Tucker, S.C. & Honn, K.V. Antiplatelet agents for cancer treatment: a real perspective or just an echo from the past? *Cancer Metastasis Rev.* **2017**, *36*, 305-329.

[93] Ram, V., Kher, G., Dubal, K., Dodiya, B. & Joshi, H. Development and validation of a stability indicating UPLC method for determination of ticlopidine hydrochloride in its tablet formulation. *Saudi Pharm. J.* **2011**, *19*, 159-164.

[94] Chhabra, R.S. NTP technical report on the toxicity studies of benzophenone (CAS No. 119-61-9). Administered in feed to F344/N rats and B6C3F mice. *Toxic. Rep. Ser.* **2000**, *1*, 1-53.

[95] Rietschel, R.L., Fowler, J.F. Jr. 5th Ed., Philadelphia: Lippincott Williams & Wilkins, Fisher's contact dermatitis, **2001**.

[96] Colás-Ruiz, N.R., Ramirez, G., Courant, F., Gomez, E., Hampel, M. & Lara-Martín, P.A. Multi-omic approach to evaluate the response of gilt-head sea bream (*Sparus aurata*) exposed to the UV filter sulisobenzone. *Sci. Total Environ.* **2022**, *803*, 150080.

Chapter II

[1] Szejtli, J. Introduction and general overview of cyclodextrin chemistry. *Chem. Rev.* **1998**, *98*, 1743-1754.

[2] Cramer, F., Saenger, W. & Spatz, H.C. Inclusion compounds. XIX. 1a The formation of inclusion compounds of α-cyclodextrin in aqueous solutions. Thermodynamics and kinetics. *J. Am. Chem. Soc.* **1967**, *89*, 14-20.

[3] Szejtli, J. & Osa, T. Cyclodextrins, 1999, 189-203 (Elsevier).

[4] Kang, Y., Guo, K., Li, B.J. & Zhang, S. Nanoassemblies driven by cyclodextrin-based inclusion complexation. *Chem. Comm.* **2014**, *50*, 11083-11092.

[5] Tian, B. & Liu, J. The classification and application of cyclodextrin polymers: a review. *New J. Chem.* **2020**, *44*, 9137-9148.

[6] Sun, Y.X., Zhu, J.Y., Qiu, W.X., Lei, Q., Chen, S. & Zhang, X.Z. Versatile supermolecular inclusion complex based on host–guest interaction for targeted gene delivery. *ACS Appl. Mater. Interfaces*. **2017**, *9*, 42622-42632.

[7] Alsbaiee, A., Smith, B.J., Xiao, L., Ling, Y., Helbling, D.E. & Dichtel, W.R. Rapid removal of organic micropollutants from water by a porous β-cyclodextrin polymer. *Nature*. 2016, *529*, 190-194.

[8] Liu, G., Yuan, Q., Hollett, G., Zhao, W., Kang, Y. & Wu, J. Cyclodextrin-based host–guest supramolecular hydrogel and its application in biomedical fields. *Polym. Chem*. **2018**, *9*, 3436-3449.

[9] Goswami, S., Majumdar, A. & Sarkar, M. Painkiller Isoxicam and Its Copper Complex Can Form Inclusion Complexes with Different Cyclodextrins: A Fluorescence, Fourier Transform Infrared Spectroscopy, and Nuclear Magnetic Resonance Study. *J. Phys. Chem. B*. **2017**, *121*, 8454-8466.

[10] Su, W., Liang, Y., Meng, Z., Chen, X., Lu, M., Han, X., Deng, X., Zhang, Q., Zhu, H. & Fu, T. Inhalation of Tetrandrine-hydroxypropyl-β-cyclodextrin inclusion complexes for pulmonary fibrosis treatment. *Mol. Pharm.* **2020**, *17*, 1596-1607.

[11] Patra, D., Zhang, H., Sengupta, S. & Sen, A. Dual stimuli-responsive, rechargeable micropumps via "host–guest" interactions. *ACS Nano*. **2013**, *7*, 7674-7679.

[12] Wang, Y., Zhuo, S., Hou, J., Li, W. & Ji, Y. Construction of β-cyclodextrin covalent organic framework-modified chiral stationary phase for chiral separation. *ACS Appl. Mater. Interfaces*. **2019**, *11*, 48363-48369.

[13] Sun, R., Xue, C., Ma, X., Gao, M., Tian, H. & Li, Q. Light-driven linear helical supramolecular polymer formed by molecular-recognition-directed self-assembly of bis (p-sulfonatocalix [4] arene) and pseudorotaxane. *J. Am. Chem. Soc.* **2013**, *135*, 5990-5993.

[14] Guo, D.S., Uzunova, V.D., Su, X., Liu, Y. & Nau, W.M. Operational calixarene-based fluorescent sensing systems for choline and acetylcholine and their application to enzymatic reactions. *Chem. Sci.* **2011**, *2*, 1722-1734.

[15] Wang, K., Guo, D.S., Wang, X. & Liu, Y. Multistimuli responsive supramolecular vesicles based on the recognition of p-sulfonatocalixarene and its controllable release of doxorubicin. *ACS Nano*. **2011**, *5*, 2880-2894.

[16] Cheignon, C., Heurté, M., Knighton, R.C., Kassir, A.A., Lecointre, A., Nonat, A., Boos, A., Christine, C., Asfari, Z. & Charbonnière, L.J. Investigation of the Supramolecular Assembly of Luminescent Lanthanide Nanoparticles Surface Functionalized by p-Sulfonato-Calix [4] arenes with Charged Aromatic Compounds. *Eur. J. Inorg. Chem.* **2021**, *2021*, 3761-3770.

[17] Wang, Y.X., Guo, D.S., Duan, Y.C., Wang, Y.J. & Liu, Y. Amphiphilic p-sulfonatocalix [4] arene as "drug chaperone" for escorting anticancer drugs. *Sci. Rep.* **2015**, *5*, 1-7.

Chapter III

[1] Vo, Q.V., Van Bay, M., Nam, P.C. & Mechler, A. Hydroxyl radical scavenging of indole-3-carbinol: a mechanistic and kinetic study. *ACS omega.* **2019**, *4*, 19375-19381.

[2] Bomzan, P., Roy, N., Sharma, A., Rai, V., Ghosh, S., Kumar, A. & Roy, M.N. Molecular encapsulation study of indole-3-methanol in cyclodextrins: Effect on antimicrobial activity and cytotoxicity. *J. Mol. Struct.* **2021**, *1225*, 129093.

[3] Martins, F.T., deLima, P.V., Azarias, L.C., de Abreu, P.J., Neves, P.P., Legendre, A.O., de Andrade, F.M., de Oliveira, G.R., Ellena, J. & Doriguetto, A.C. Increasing the symmetry of drug crystals: a monoclinic conformational polymorph of the platelet antiaggregating agent ticlopidine hydrochloride. *Cryst. Eng. Comm.* **2011**, *13*, 5737-5743.

[4] Bomzan, P., Roy, N., Rai, V., Roy, D., Ghosh, S., Kumar, A., Roy, K., Chakrabarty, R., Das, J., Dakua, V.K. & Basnet, K. Inclusion of an antiplatelet agent inside into β-cyclodextrin for biochemical applications with diverse authentications. *Food Chem.* **2022**, *1*,100015.

[5] Paredes, E., Pérez, S., Rodil, R., Quintana, J.B. & Beiras, R. Ecotoxicological evaluation of four UV filters using marine organisms from different trophic levels Isochrysis galbana, Mytilus galloprovincialis, Paracentrotus lividus, and Siriella armata. *Chemosphere.* **2014**, *104*, 44-50.

[6] Kurul, E. and Hekimoğlu, S. Skin permeation of two different benzophenone derivatives from various vehicles. *Int. J. Cosmet. Sci*. **2001**, *23*, 211-218.

[7] Gao, H., Tuyishime, P., Zhang, X., Yang, T., Xu, M. & Rao, Z. Engineering of microbial cells for L-valine production: challenges and opportunities. *Microb. Cell Factories.* **2021**, *20*, 1-16.

[8] D'Aniello, A. D-Aspartic acid: an endogenous amino acid with an important neuroendocrine role. *Brain Res. Rev.* **2007.** *53*, 215-234.

[9] Roy, N., Bomzan, P. & Roy, M.N. Probing Host-Guest inclusion complexes of Ambroxol Hydrochloride with α-& β-Cyclodextrins by physicochemical contrivance subsequently optimized by molecular modeling simulations. *Chem. Phys. Lett.* **2020**, *748*, 137372.

[10] Kurkov, S.V. & Loftsson, T. Cyclodextrins. *Int. J. Pharm.* **2013**, *453*, 167-180.

[11] Loftsson, T., Jarho, P., Másson, M. & Järvinen, T. Cyclodextrins in drug delivery. *Expert Opin. Drug Deliv.* **2005**, *2*, 335-351.

[12] Onishi, M., Ozasa, K., Kobiyama, K., Ohata, K., Kitano, M., Taniguchi, K., Homma, T., Kobayashi, M., Sato, A., Katakai, Y. & Yasutomi, Y. Hydroxypropyl-β-cyclodextrin spikes local inflammation that induces Th2 cell and T follicular helper cell responses to the coadministered antigen. *J. Immunol.* **2015**, *194*, 2673-2682.

[13] Chen, B., Yuan, D., Wu, M., Jiang, F. & Hong, M. Two Coordination Networks Built from p-Sulfonatothiacalix [4] arene Tetranuclear Clusters. *Z. fur Anorg. Allg. Chem.* **2009**, *635*, 1669-1672.

[14] Patil, S.V., Athare, S.V., Jagtap, A., Kodam, K.M., Gejji, S.P. & Malkhede, D.D. Encapsulation of rhodamine-6G within p-sulfonatocalix [n] arenes: NMR, photophysical behaviour and biological activities. *RSC Adv.* **2016**, *6*, 110206-110220.

Chapter IV

[1] Li, H., Chen, D.X., Sun, Y.L., Zheng, Y.B., Tan, L.L., Weiss, P.S. & Yang, Y.W. Viologen-mediated assembly of and sensing with carboxylatopillar [5] arene-modified gold nanoparticles. *J. Am. Chem. Soc.* **2013**, *135*, 1570-1576.

[2] Qiu, N., Shen, B., Li, X., Zhang, X., Sang, Z., Yang, T., An, L., Liu, J., Chen, L. & Wang, L. Inclusion complex of magnolol with hydroxypropyl-β-cyclodextrin: characterization, solubility, stability and cell viability. *J. Incl. Phenom. Macrocycl. Chem.* **2016**, *85*, 289-301.

[3] Saenger, W. Cyclodextrin inclusion compounds in research and industry. *Angew. Chem. Int. Ed.* **1980**, *19*, 344-362.

[4] Del Valle, E.M. Cyclodextrins and their uses: a review. *Process Biochem.* **2004**, *39*, 1033-1046.

[5] Mathapa, B.G. & Paunov, V.N. Cyclodextrin stabilised emulsions and cyclodextrinosomes. *Phys. Chem. Chem. Phys.* **2013**, *15,* 17903-17914.

[6] Kang, Y., Guo, K., Li, B.J. & Zhang, S. Nanoassemblies driven by cyclodextrin-based inclusion complexation. *Chem. Comm.* **2014**, *50*, 11083-11092.

[7] Alberti, S., Soler-Illia, G.J. & Azzaroni, O. Gated supramolecular chemistry in hybrid mesoporous silica nanoarchitectures: controlled delivery and molecular transport in response to chemical, physical and biological stimuli. *Chem. Comm.* **2015**, *51*, 6050-6075.

[8] Liu, Y. & Chen, Y. Cooperative binding and multiple recognition by bridged bis (β-cyclodextrin) s with functional linkers. *Acc. Chem. Res.* **2006**, *39*, 681-691.

[9] Misiuk, W. & Zalewska, M. Investigation of inclusion complex of trazodone hydrochloride with hydroxypropyl-β-cyclodextrin. *Carbohydr. Polym.* **2009**, *77*, 482-488.

[10] Wu, H., Liang, H., Yuan, Q., Wang, T. & Yan, X. Preparation and stability investigation of the inclusion complex of sulforaphane with hydroxypropyl-β-cyclodextrin. *Carbohydr. Polym.* **2010**, *82*, 613-617.

[11] Pinho, E., Grootveld, M., Soares, G. & Henriques, M. Cyclodextrins as encapsulation agents for plant bioactive compounds. *Carbohydr. Polym.* **2014**, *101*, 121-135.

[12] Bian, H., Chen, J., Cai, X., Liu, P., Liu, H., Qiao, X. & Huang, L. Inclusion complex of butachlor with β-cyclodextrin: characterization, solubility, and speciation-dependent adsorption. *J. Agric. Food Chem.* **2009**, *57*, 7453-7458.

[13] Uekama, K., Hirayama, F. & Irie, T. Cyclodextrin-based controlled drug release system. *Chem. Rev.* **1998**, *98*, 2045-2076.

[14] Wang, J.H. & Cai, Z. Investigation of inclusion complex of miconazole nitrate with β-cyclodextrin. *Carbohydr. Polym.* **2008**, *72*, 255-260.

[15] Ueno, A. Fluorescent cyclodextrins for molecule sensing. *Supramolecular Science*, **1996**, *3*, 31-36.

[16] Breslow, R. & Dong, S.D. Biomimetic reactions catalyzed by cyclodextrins and their derivatives. *Chem. Rev.* **1998**, *98*, 1997-2012.

[17] Szejtli, J. Introduction and general overview of cyclodextrin chemistry. *Chem. Rev.* **1998**, *98*, 1743-1754.

[18] Yu, G., Jie, K. & Huang, F. Supramolecular amphiphiles based on host–guest molecular recognition motifs. *Chem. Rev.* **2015**, *115*, 7240-7303.

[19] Aytac, Z., Yildiz, Z.I., Kayaci-Senirmak, F., San Keskin, N.O., Kusku, S.I., Durgun, E., Tekinay, T. & Uyar, T. Fast-dissolving, prolonged release, and antibacterial cyclodextrin/limonene-inclusion complex nanofibrous webs via polymer-free electrospinning. *J. Agric. Food Chem*. **2016**, *64*, 7325-7334.

[20] Zhou, H., Yamada, T. & Kimizuka, N. Supramolecular thermo-electrochemical cells: enhanced thermoelectric performance by host–guest complexation and salt-induced crystallization. *J. Am. Chem. Soc.* **2016**, *138*, 10502-10507.

[21] Stricker, L., Fritz, E.C., Peterlechner, M., Doltsinis, N.L. & Ravoo, B.J. Arylazopyrazoles as light-responsive molecular switches in cyclodextrin-based supramolecular systems. *J. Am. Chem. Soc.* **2016**, *138*, 4547-4554.

[22] Xue, M., Wei, W., Su, Y., Johnson, D. & Heath, J.R. Supramolecular probes for assessing glutamine uptake enable semi-quantitative metabolic models in single cells. *J. Am. Chem. Soc.* **2016**, *138*, 3085-3093.

[23] Díez, P., Sánchez, A., Gamella, M., Martínez-Ruíz, P., Aznar, E., De La Torre, C., Murguía, J.R., Martínez-Máñez, R., Villalonga, R. & Pingarrón, J.M. Toward the design of smart delivery systems controlled by integrated enzyme-based biocomputing ensembles. *J. Am. Chem. Soc.* **2014**,*136*, 9116-9123.

[24] Aggarwal, B.B. & Ichikawa, H. Molecular targets and anticancer potential of indole-3-carbinol and its derivatives. *Cell Cycle.* **2005**, *4*, 1201-1215.

[25] Fujioka, N., Fritz, V., Upadhyaya, P., Kassie, F. & Hecht, S.S. Research on cruciferous vegetables, indole-3-carbinol, and cancer prevention: A tribute to Lee W. Wattenberg. *Mol Nutr Food Res*. **2016**, *60*, 1228-1238.

[26] Verhoeven, D.T., Verhagen, H., Goldbohm, R.A., van den Brandt, P.A. & van Poppel, G. A review of mechanisms underlying anticarcinogenicity by brassica vegetables. *Chem. Biol. Interact.* **1997**, *103*, 79-129.

[27] Kim, S.Y., Kim, D.S., Jeong, Y.M., Moon, S.I., Kwon, S.B. & Park, K.C. Indole-3-carbinol and ultraviolet B induce apoptosis of human melanoma cells via down-regulation of MITF. *Pharmazie.* **2011**, *66*, 982-987.

[28] Bradlow, H.L. Indole-3-carbinol as a chemoprotective agent in breast and prostate cancer. *In Vivo* **2008**, *22*, 441-445.

[29] El-Naga, R.N., Ahmed, H.I. & Abd Al Haleem, E.N. Effects of indole-3-carbinol on clonidine-induced neurotoxicity in rats: impact on oxidative stress, inflammation, apoptosis and monoamine levels. *Neurotoxicology.* **2014**, *44*, 48-57.

[30] Song, J.M., Qian, X., Molla, K., Teferi, F., Upadhyaya, P., OSullivan, G., Luo, X. & Kassie, F. Combinations of indole-3-carbinol and silibinin suppress inflammation-driven mouse lung tumorigenesis by modulating critical cell cycle regulators. *Carcinogenesis.* **2015**, *36*, 666-675.

[31] Grose, K.R. & Bjeldanes, L.F. Oligomerization of indole-3-carbinol in aqueous acid. *Chem. Res. Toxicol.* **1992**, *5*, 188-193.

[32] Vallejo, F., Tomás-Barberán, F. & García-Viguera, C. Glucosinolates and vitamin C content in edible parts of broccoli florets after domestic cooking. *Eur. Food Res. Technol.* **2002**, *215*, 310-316.

[33] Adeoye, O., Conceição, J., Serra, P.A., da Silva, A.B., Duarte, N., Guedes, R.C., Corvo, M.C., Aguiar-Ricardo, A., Jicsinszky, L., Casimiro, T. & Cabral-Marques, H. Cyclodextrin solubilization and complexation of antiretroviral drug lopinavir: In silico prediction; Effects of derivatization, molar ratio and preparation method. *Carbohydr. Polym.* **2020**, *227*, 115287.

[34] Geng, Q., Li, T., Wang, X., Chu, W., Cai, M., Xie, J. & Ni, H. The mechanism of bensulfuron-methyl complexation with β-cyclodextrin and 2-hydroxypropyl-β-cyclodextrin and effect on soil adsorption and bio-activity. *Sci. Rep.* **2019**, *9*, 1-11.

[35] Wintola, O.A. & Afolayan, A.J. The antibacterial, phytochemicals and antioxidants evaluation of the root extracts of *Hydnora africana* Thunb. used as antidysenteric in Eastern Cape Province, South Africa. *BMC Complement Altern. Med.* **2015**, *15*, 1-12.

[36] Balouiri, M., Sadiki, M. & Ibnsouda, S.K. Methods for in vitro evaluating antimicrobial activity: A review. *J. Pharm. Anal.* **2016**, *6*, 71-79.

[37] Job, P. Formation and stability of inorganic complexes in solution. *Ann. Chim.* **1928**, *9*, 113-134.

[38] Caso, J.V., Russo, L., Palmieri, M., Malgieri, G., Galdiero, S., Falanga, A., Isernia, C. & Iacovino, R. Investigating the inclusion properties of aromatic amino acids complexing beta-cyclodextrins in model peptides. *Amino acids.* **2015**, *47*, 2215-2227.

[39] Gao, Y.A., Zhao, X., Dong, B., Zheng, L., Li, N. & Zhang, S. Inclusion complexes of β-cyclodextrin with ionic liquid surfactants. *J. Phys. Chem. B.* **2006**, *110*, 8576-8581.

[40] Piñeiro, Á., Banquy, X., Pérez-Casas, S., Tovar, E., García, A., Villa, A., Amigo, A., Mark, A.E. & Costas, M. On the characterization of host– guest complexes: surface tension, calorimetry, and molecular dynamics of cyclodextrins with a non-ionic surfactant. *J. Phys. Chem. B* **2007**, *111*, 4383-4392.

[41] Roy, A., Saha, S. & Roy, M.N. Study to explore host-guest inclusion complexes of cyclodextrins with biologically active molecules in aqueous environment. *Fluid Ph. Equilibria.* **2016**, *425*, 252-258.

[42] Roy, M.N., Saha, S., Kundu, M., Saha, B.C. & Barman, S. Exploration of inclusion complexes of neurotransmitters with β-cyclodextrin by physicochemical techniques. *Chem. Phys. Lett.* **2016**, *655*, pp.43-50.

[43] Roy, A., Saha, S., Datta, B. & Roy, M.N. Insertion behavior of imidazolium and pyrrolidinium based ionic liquids into α and β-cyclodextrins: mechanism and factors leading to host–guest inclusion complexes. *RSC Adv.* **2016**, *6*, 100016-100027.

[44] Roy, M.N., Saha, S., Barman, S. & Ekka, D. Host–guest inclusion complexes of RNA nucleosides inside aqueous cyclodextrins explored by physicochemical and spectroscopic methods. *RSC Adv.* **2016**, *6*, 8881-8891.

[45] Roy, M.N., Ekka, D., Saha, S. & Roy, M.C. Host–guest inclusion complexes of α and β-cyclodextrins with α-amino acids. *RSC Adv.* **2014**, *4*, 42383-42390.

[46] Saha, S., Roy, A., Roy, K. & Roy, M.N. Study to explore the mechanism to form inclusion complexes of β-cyclodextrin with vitamin molecules. *Sci. Rep.* **2016**, *6*, 1-12.

[47] Roy, M.N., Saha, S., Barman, S. & Ekka, D. Host–guest inclusion complexes of RNA nucleosides inside aqueous cyclodextrins explored by physicochemical and spectroscopic methods. *RSC Adv.* **2016**, *6*, 8881-8891.

[48] Cramer, F., Saenger, W. & Spatz, H.C. Inclusion compounds. XIX. 1a The formation of inclusion compounds of α-cyclodextrin in aqueous solutions. Thermodynamics and kinetics. *J. Am. Chem. Soc.* **1967**, *89*, 14-20.

[49] Benesi, H.A. & Hildebrand, J.H.J. A spectrophotometric investigation of the interaction of iodine with aromatic hydrocarbons. *J. Am. Chem. Soc.* **1949**, *71*, 2703-2707.

[50] Dotsikas, Y., Kontopanou, E., Allagiannis, C. & Loukas, Y.L. Interaction of 6-p-toluidinylnaphthalene-2-sulphonate with β-cyclodextrin. *J. Pharm. Biomed. Anal.* **2000**, *23*, 997-1003.

[51] He, Y. & Shen, X. Interaction between β-cyclodextrin and ionic liquids in aqueous solutions investigated by a competitive method using a substituted 3H-indole probe. *J. Photochem. Photobiol. A: Chem.* **2008**, *197*, 253-259.

[52] Ignaczak, A., Pałecz, B. & Belica-Pacha, S. Quantum chemical study and isothermal titration calorimetry of β-cyclodextrin complexes with mianserin in aqueous solution. *Org. Biomol. Chem.* **2017**, *15*, 1209-1216.

[53] Prabu, S., Swaminathan, M., Sivakumar, K. & Rajamohan, R. Preparation, characterization and molecular modeling studies of the inclusion complex of Caffeine with Beta-cyclodextrin. *J. Mol. Struct.* **2015**, *1099*, 616-624.

[54] Sanramé, C.N., de Rossi, R.H. & Argüello, G.A. Effect of β-cyclodextrin on the excited state properties of 3-substituted indole derivatives. *J. Phys. Chem.* **1996**, *100*, 8151-8156.

[55] Oana, M., Tintaru, A., Gavriliu, D., Maior, O. & Hillebrand, M. Spectral study and molecular modeling of the inclusion complexes of β-cyclodextrin with some phenoxathiin derivatives. *J. Phys. Chem. B.* **2002**, *106*, 257-263.

[56] Zhang, Q.F., Jiang, Z.T., Guo, Y.X. & Li, R. Complexation study of brilliant cresyl blue with β-cyclodextrin and its derivatives by UV–vis and fluorospectrometry. *Spectrochim. Acta A Mol. Biomol. Spectrosc.* **2008**, *69*, 65-70.

[57] Zhang, M., Li, J., Jia, W., Chao, J. & Zhang, L. Theoretical and experimental study of the inclusion complexes of ferulic acid with cyclodextrins. *Supramol. Chem.* **2009**, *21,* 597-602.

[58] Li, W., Liu, X., Yang, Q., Zhang, N., Du, Y. & Zhu, H. Preparation and characterization of inclusion complex of benzyl isothiocyanate extracted from papaya seed with β-cyclodextrin. *Food Chem.* **2015**, *184*, 99-104.

[59] Srinivasan, K., Sivakumar, K. & Stalin, T. 2, 6-Dinitroaniline and β-cyclodextrin inclusion complex properties studied by different analytical methods. *Carbohydr. Polym.* **2014**, *113*, 577-587.

[60] Sindelar, V., Cejas, M.A., Raymo, F.M., Chen, W., Parker, S.E. & Kaifer, A.E., 2005. Supramolecular assembly of 2, 7-dimethyldiazapyrenium and cucurbit [8] uril: A new fluorescent host for detection of catechol and dopamine. *Chem. Eur. J.* **2005**, *11*, 7054-7059.

[61] Kim, K.H. & Park, Y.H. Enantioselective inclusion between terbutaline enantiomers and hydroxypropyl-β-cyclodextrin. *Int. J. Pharm.* **1998**, *175*, 247-253.

[62] Ribeiro, L., Carvalho, R.A., Ferreira, D.C. & Veiga, F.J. Multicomponent complex formation between vinpocetine, cyclodextrins, tartaric acid and water-soluble polymers monitored by NMR and solubility studies. *Eur. J. Pharm. Sci.* **2005**, *24*, 1-13.

[63] Yang, L.J., Ma, S.X., Zhou, S.Y., Chen, W., Yuan, M.W., Yin, Y.Q. & Yang, X.D. Preparation and characterization of inclusion complexes of naringenin with β-cyclodextrin or its derivative. *Carbohydr. Polym.* **2013**, *98*, 861-869.

[64] Veiga, F.J.B., Fernandes, C.M., Carvalho, R.A. & Geraldes, C.F.G.C. Molecular modelling and 1H-NMR: ultimate tools for the investigation of tolbutamide: β-cyclodextrin and tolbutamide: hydroxypropyl-β-cyclodextrin complexes. *Chem. Pharm. Bull.* **2001**, *49*, 1251-1256.

[65] Fernandes, A., Ivanova, G., Brás, N.F., Mateus, N., Ramos, M.J., Rangel, M. & de Freitas, V. Structural characterization of inclusion complexes between cyanidin-3-O-glucoside and β-cyclodextrin. *Carbohydr. Polym.* **2014**, *102*, 269-277.

[66] Yang, B., Lin, J., Chen, Y. & Liu, Y. Artemether/hydroxypropyl-β-cyclodextrin host–guest system: characterization, phase-solubility and inclusion mode. *Bioorg. Med. Chem.* **2009**, *17*, 6311-6317.

[67] Xiao, C.F., Li, K., Huang, R., He, G.J., Zhang, J.Q., Zhu, L., Yang, Q.Y., Jiang, K.M., Jin, Y. & Lin, J. Investigation of inclusion complex of Epothilone A with cyclodextrins. *Carbohydr. Polym.* **2014**, *102*, 297-305.

[68] Wang, T., Wang, M., Ding, C. & Fu, J. Mono-benzimidazole functionalized β-cyclodextrins as supramolecular nanovalves for pH-triggered release of p-coumaric acid. *Chem. Comm.* **2014**, *50*, 12469-12472.

[69] Okada, Y., Ueyama, K., Nishikawa, J.I., Semma, M. & Ichikawa, A. Effect of 6-O-α-maltosyl-β cyclodextrin and its cholesterol inclusion complex on cellular cholesterol levels and ABCA1 and ABCG1 expression in mouse mastocytoma P-815 cells. *Carbohydr. Res.* **2012**, *357*, 68-74.

[70] Zhang, J.Q., Jiang, K.M., An, K., Ren, S.H., Xie, X.G., Jin, Y. & Lin, J. Novel water-soluble fisetin/cyclodextrins inclusion complexes: Preparation, characterization, molecular docking and bioavailability. *Carbohydr. Res.* **2015**, *418*, 20-28.

[71] Zhang, W., Gong, X., Cai, Y., Zhang, C., Yu, X., Fan, J. & Diao, G. Investigation of water-soluble inclusion complex of hypericin with β-cyclodextrin polymer. *Carbohydr. Polym.* **2013**, *95*, 366-370.

[72] Wang, J., Cao, Y., Sun, B. & Wang, C. Characterisation of inclusion complex of trans-ferulic acid and hydroxypropyl-β-cyclodextrin. *Food Chem.* **2011**, *124*, 1069-1075.

[73] Ghosh, R., Ekka, D., Rajbanshi, B., Yasmin, A. & Roy, M.N. Synthesis, characterization of 1-butyl-4-methylpyridinium lauryl sulfate and its inclusion phenomenon with β-cyclodextrin for enhanced applications. *Colloids Surf. A: Physicochem. Eng. Asp.* **2018**, *548*, 206-217.

[74] Basak, S., Mondal, S., Dey, S., Bhattacharya, P., Saha, A., Deep Punetha, V., Abbas, A. & Gopal Sahoo, N. Fabrication of β-cyclodextrin-mediated single bimolecular inclusion complex: characterization, molecular docking, in-vitro release and bioavailability studies for gefitinib and simvastatin conjugate. *J. Pharm. Pharmacol.* **2017**, *69*, 1304-1317.

[75] Issaraseriruk, N., Shitangkoon, A. & Aree, T. Molecular docking study for the prediction of enantiodifferentiation of chiral styrene oxides by octakis (2, 3-di-O-acetyl-6-O-tert-butyldimethylsilyl)-γ-cyclodextrin. *J. Mol. Graphics Modell.* **2010**, *28*, 506-512.

[76] Sompornpisut, P., Deechalao, N. & Vongsvivut, J. An inclusion complex of β-Cyclodextrin-L-Phenylalanine: 1H NMR and molecular docking studies. *Sci. Asia* **2002**, *28*, 263-270.

[77] Sanramé, C.N., de Rossi, R.H. & Argüello, G.A. Effect of β-cyclodextrin on the excited state properties of 3-substituted indole derivatives. *J. Phys. Chem.* **1996**, *100*, 8151-8156.

[78] Al-Sou'od, K.A., Zughul, M.B. & Badwan, A.A. Experimental and molecular mechanical studies of complexation of some 2H-and 3H-indole derivatives with aqueous β-cyclodextrin. *J. Solution Chem.* **2006**, *35*, 1377-1388.

[79] Mady, F.M. & Aly, U.F. Experimental, molecular docking investigations and bioavailability study on the inclusion complexes of finasteride and cyclodextrins. *Drug Des. Dev. Ther* **2017**, *11*, 1681.

[80] Zhang, C.L., Liu, J.C., Yang, W.B., Chen, D.L. & Jiao, Z.G. Experimental and molecular docking investigations on the inclusion mechanism of the complex of phloridzin and hydroxypropyl-β-cyclodextrin. *Food Chem.* **2017**, *215*, 124-128.

[81] Walsh, T.R., Toleman, M.A., Poirel, L. & Nordmann, P. Metallo-β-lactamases: the quiet before the storm? *Clin. Microbiol. Rev.* **2005**, *18*, 306-325.

[82] Maki, M.A.A., Kumar, P.V., Cheah, S.C., Siew Wei, Y., Al-Nema, M., Bayazeid, O. & Majeed, A.B.B.A. Molecular modeling-based delivery system enhances everolimus-induced apoptosis in Caco-2 cells. *ACS Omega.* **2019**, *4*, 8767-8777.

[83] Ren, L., Wang, J. & Chen, G. Preparation, optimization of the inclusion complex of glaucocalyxin A with sulfobutylether-β-cyclodextrin and antitumor study. *Drug Deliv.* **2019**, *26*, 309-317.

Chapter V

[1] Wu,Y. J. Heterocycles and Medicine:A Survey of the Heterocyclic Drugs Approved by the U.S. FDA from 2000 to present. *Prog. Heterocycl. Chem.***2012**, *24*, 1–53.

[2] Rao, A. K. Acquired Disorders of Platelet Function. *Platelets* **2013**, 1049–1073.

[3] Ferri, N., Corsini, A. & Bellosta,S. Pharmacology of the new P2Y12 receptor inhibitors: insights on pharmacokinetic and pharmacodynamic properties. *Drugs.* **2013**, *73*, 1681–1709.

[4] Mazoyer, E., Ripoll, L., Boisseau, M.R. & Drouet, L. How does ticlopidine treatment lower plasma fibrinogen? *Thromb. Res*. **1994**, *75*, 361–370.

[5] Hayakawa, M. & Kuzuya, F. Effects of ticlopidine on erythrocyte aggregation in thrombotic Disorders. *Angiology.* **1991**, 42, 747–753.

[6] De Lorgeril, M., Bordet, J.C., Salen, P., Durbin, S., Defreyn, G., Delaye, J. & Boissonnat, P. Ticlopidine increases nitric oxide generation in heart-transplant recipients: a possible novel property of ticlopidine. *J. Cardiovasc. Pharmacol.* **1998**, *32*, 225–230.

[7] Calvisi, D.F. Inhibition of hepatitis B virus-associated liver cancer by antiplatelet therapy: a revolution in hepatocellular carcinoma prevention? *Hepatology.* **2013**, *57,* 848–850.

[8] Zeng, X.X., Zheng, R.L., Zhou, T., He, H.Y., Liu, J.Y., Zheng, Y., Tong, A.P., Xiang, M.L., Song, X.R., Yang, S.Y., Yu, L.T., Wei, Y.Q., Zhao, Y.L. & Yang, L. Novel thienopyridine derivatives as specific anti-hepatocellular carcinoma (HCC) agents: synthesis, preliminarystructure-activity relationships, and in vitro biological evaluation. *Bioorg. Med. Chem. Lett*. **2010**, *20*, 6282–6285.

[9] Saltiel, E. & Ward, A. Ticlopidine. A review of its pharmacodynamic and pharmacokinetic properties, and therapeutic efficacy in platelet-dependent disease states. *Drugs.* **1987**, *34*, 222–262.

[10] Gachet, C., Stierle, A., Cazenave, J.P., Ohlmann, P., Lanza, F., Bouloux, C. & Maffrand, J.P. The thienopyridine PCR 4099 selectively inhibits ADP-induced platelet aggregationand fibrinogen binding without modifying the membrane glycoprotein IIb-IIIa complexin rat and in man. *Biochem. Pharmacol.* **1990,** *40*, 229–238.

[11] Veloso, T. R., Oechslin, F., Que, Y., Moreillon, P., Entenza, J. M. & Mancini, S. Aspirin plus ticlopidine prevented experimental endocarditis due to *Enterococcus faecalis* and *Streptococcus gallolyticus*. *FEMS Pathog. Dis.* **2015**, *73*, ftv060.

[12] Wojtukiewicz, M. Z., Hempel, D., Sierko, E., Tucker, S. C. & Honn, K. V. Antiplatelet agents for cancer treatment: a real perspective or justan echo from the past? *Cancer Metastasis Rev*. **2017**, *36*, 305–329.

[13] Ram, V., Kher, G., Dubal, K., Dodiya, B. & Joshi, H. Development and validation of a stability indicating UPLC method for determination of ticlopidinehydrochloride in its tablet formulation. *Saudi Pharm. J*.**2011**, *19*, 159–164.

[14] Ozdemira, N., Polab, C.C., Teixeirac, B.N., Hilld, L.E., Bayraka, A. & Gomesd, C.L. Preparation of black pepper oleoresin inclusion complexes based on beta-cyclodextrinfor antioxidant and antimicrobial delivery applications using kneading and freeze drying methods: a comparative study. *LWT-Food Sci. Technol.***2018**, *91*, 439–445.

[15] Magalhães, T. S. S. A., Macedo, P. C. O., Pacheco, S. Y. K., Sofia Santos da Silva, S. S. S., Barbosa, E. G., Pereira, R. R., Costa, R. M. R., Junior, J. O. C. S., Ferreira, M. A. S. & Almeida, J. C. Development and Evaluation of Antimicrobial and Modulatory Activity of Inclusion Complex of *Euterpe oleracea* Mart Oil and β-Cyclodextrin or HP-β–Cyclodextrin. *Int. J. Mol. Sci.* **2020**, *21*, 942.

[16] Zhang, L., Man, S., Qiu, H., Liu, Z.., Zhang, M., Ma, L. & Gao, W. Curcumin-cyclodextrincomplexes enhanced the anti-cancer effects of curcumin. *Environ. Toxicol. Pharmacol.* **2016**, *48*, 31–38.

[17] Liu, D.D., Guo, Y.F., Zhang, J.Q., Yang, Z.K., Li, X., Yang, B. & Yang, R. Inclusion of lycorine with natural cyclodextrins (α-, β- and γ-CD): experimental and in vitro evaluation. *J. Mol. Struct.* **2017**, *1130*, 669–676.

[18] USFDA, 2001. U.S. Food and Drug Administration. Agency response letter GRAS notice 000074. CFSAN/Office of Food Additive Safety. <https://www. fda.gov/downloads/food/ingredientspackaginglabeling/gras/noticeinventor y/ ucm261320.pdf/> (Accessed date: 5 May 2017).

[19] Gong, L., Li, T., Chen, F., Duan, X., Yuan, Y., Zhang, D. & Jiang, Y. An inclusion complex of eugenol into β-cyclodextrin: preparation, and physicochemical and antifungal characterization. *Food Chem.* **2016**, *196*, 324–330.

[20] Li, Q., Pu, H., Tang, P., Tang, B., Sun, Q. & Li, H. Propyl gallate/cyclodextrinsupramolecular complexes with enhanced solubility and radical scavenging capacity. *Food Chem*. **2018**, *245*, 1062–1069.

[21] Rajbanshi, B., Saha, S., Das, K., Barman, B. K., Sengupta, S., Bhattacharjee, A. & Roy, M. N. Study to Probe Subsistence of Host-Guest Inclusion Complexes of α and β-Cyclodextrins with Biologically Potent Drugs for Safety Regulatory Dischargement. *Sci. Rep.* **2018**, *8*, 13031.

[22] Alshehri, S., Imam, S. S., Hussain, A. & Altamimi, M. A. Formulation of Piperine Ternary Inclusion Complex Using β-CD and HPMC: Physicochemical Characterization, Molecular Docking, and Antimicrobial Testing. *Processes* **2020**, *8*, 1450.

[23] Rai, V., Kumar, A., Das, V., & Ghosh, S. Evaluation of chemical constituents and in vitro antimicrobial, antioxidant and cytotoxicity potential of rhizome of *Astilbe rivularis* (Bodho-okhati), an indigenous medicinal plant from Eastern Himalayan region of India. *BMC complementary and alternative medicine* **2019**, *19*, 1-10.

[24] Cramer, F., Saenger, W., Spatz, H. Inclusion Compounds. XIX 1a. The formation of inclusion compounds of α-cyclodextrin in aqueous solutions, Thermodynamics and kinetics. *J. Am. Chem. Soc.***1967**, *89*, 14-20.

[25] Alshaer, W., Zraikat, M., Amer, A., Nsairat, H., Lafi, Z., Alqudah, D. A., Al Qadi, E., Alsheleh, T., Odeh, F., Alkaraki, A., Zihlif, M., Bustanji, Y., Fattal, E. & Awidi,

A. Encapsulation of echinomycin in cyclodextrin inclusion complexes into liposomes : in vitro antiproliferative and anti-invasive activity in glioblastoma. *RSC Adv.* **2019**, *9*, 30976-30988.

[26] Benkovics, G., Afonso, D., Darcsi, A., Béni, S., Conoci, S., Fenyvesi, É., Szente, L.., Malanga, M. & Sortino, S. Novel β-cyclodextrin–eosin conjugates. Beilstein. *J. Org. Chem*. **2017**, *13*, 543–551.

[27] Rani, D., Sethi, A., Kaur, K. & Agarwal, J. Ultrasonication-Assisted Synthesis of a D-Glucosamine-Based β-CD Inclusion Complex and Its Application as an Aqueous Heterogeneous Organocatalytic System. .*J. Org. Chem.***2020**, *85,* 9548-9557.

[28] Roy, N., Ghosh, B., Roy, D., Bhaumik, B. & Roy, M. N. Exploring the Inclusion Complex of a Drug (Umbelliferone) withα-Cyclodextrin Optimized by Molecular Docking and Increasing Bioavailability with Minimizing the Doses in Human Body. *ACS Omega.* **2020**, *5*, 30243-30251.

[29] Pal, A., Roy, S., Kumar, A., Mahmood, S., Khodapanah, N.,Thomas, S., Agatemor, C. & Ghosal, K. Physicochemical Characterization, Molecular Docking, and *In Vitro* Dissolution of Glimepiride–Captisol Inclusion Complexes. *ACS Omega.* **2020**, *5,* 19968-19977.

[30] Ren, L., Wang, J. & Chen, G. Preparation, optimization of the inclusion complex of glaucocalyxin Awith sulfobutylether-β-cyclodextrin and antitumor study. *Drug Deliv.* **2019**, *26,* 309-317.

[31] Loftsson, T. Drug permeation through biomembranes: cyclodextrins and the unstirred water layer. *Die Pharm.***2012**, *67*, 363-370.

[32] Deavall, D.G., Martin, E.A., Horner, J.M. & Roberts, R. Drug-induced oxidative stress and toxicity. *J. Toxicol*.2012, 1–13.

[33] Tian, L., Yin, D., Ren, Y., Gong, C., Chen, A. & Guo, F. Plumbagin induces apoptosis via the p53 pathway and generation of reactive oxygen species in human osteosarcoma cells. *Mol. Med. Rep.***2012**, *5,* 126-132.

[34] Bhat, S., Muthunatarajan, S., Mulki, S. S., Bhat, K. A. & Kotian, K. H. Bacterial Infection among Cancer Patients: Analysis of Isolates and Antibiotic Sensitivity Pattern. *Int. J. Microbiol.* **2021**, *2021*.

[35] Inoue, Y., Suzuki, R., Murata, I., Nomura, H., Isshiki, Y. & Kanamoto, I. Evaluation of Antibacterial Activity Expression of the Hinokitiol/Cyclodextrin Complex against Bacteria. *ACS Omega.* **2020**, *5*, 27180-27187.

[36] Savic, I. M., Jocic, E., Nikolic, V. D., Popsavin, M. M., Rakic, S. J. & Savic-Gajic, I. M. The effect of complexation with cyclodextrins on the antioxidant and antimicrobial activity of ellagic acid. *Pharm. Dev. Technol.* **2019**, *24*, 410-418.

Chapter VI

[1] Ainbinder, D. & Touitou, E. 1st Ed., Farage, M.A., Kenneth W. Miller, K.W. & Howard I. Maibach, H.I, Skin photodamage prevention: state of the art and new prospects. Textbook of aging skin, Springer Berlin, Heidelberg, 2010, 429-440.

[2] Doktorovova, S., Marques, C., Barbosa, C., Lopes, C.M. & Souto, E.B. Novel carriers for sunscreen formulations. *Househ. Pers. Care Today*. **2009**, *3*.

[3] Egambaram, O.P., Kesavan Pillai, S. & Ray, S.S. Materials science challenges in skin UV protection: A review. *Photochem. Photobiol*. **2020**, *96*, 779-797.

[4] Baker, L.A., Marchetti, B., Karsili, T.N., Stavros, V.G. & Ashfold, M.N. Photoprotection: extending lessons learned from studying natural sunscreens to the design of artificial sunscreen constituents. *Chem. Soc. Rev*. **2017**, *46*, 3770-3791.

[5] Oh, J.J., Kim, J.Y., Son, S.H., Jung, W.J., Seo, J.W. & Kim, G.H. Fungal melanin as a biocompatible broad-spectrum sunscreen with high antioxidant activity. *RSC Adv.* **2021**, *11*, 19682-19689.

[6] Murphy, R.B., Staton, J., Rawal, A. & Darwish, T.A.The effect of deuteration on the keto–enol equilibrium and photostability of the sunscreen agent avobenzone. *Photochem. Photobiol. Sci.* **2020**, *19*, 1410-1422.

[7] Lee, S.Y., San Lim, H., Lee, N.E. & Cho, S.O. Biocompatible UV-absorbing polymer nanoparticles prepared by electron irradiation for application in sunscreen. *RSC Adv.* **2020**, *10*, 356-361.

[8] Chan, C.T.L., Ma, C., Chan, R.C.T., Ou, H.M., Xie, H.X., Wong, A.K.W., Wang, M.L. & Kwok, W.M. A long lasting sunscreen controversy of 4-aminobenzoic acid

and 4-dimethylaminobenzaldehyde derivatives resolved by ultrafast spectroscopy combined with density functional theoretical study. *Phys. Chem. Chem. Phys.* **2020**, *22*, 8006-8020.

[9] Li, Y., Yang, D., Lu, S., Qiu, X., Qian, Y. & Li, P. Encapsulating TiO_2 in lignin-based colloidal spheres for high sunscreen performance and weak photocatalytic activity. *ACS Sustain. Chem. Eng.* **2019**, *7*, 6234-6242.

[10] Semones, M.C., Sharpless, C.M., MacKay, A.A. & Chin, Y.P. Photodegradation of UV filters oxybenzone and sulisobenzone in wastewater effluent and by dissolved organic matter. *Appl. Geochemistry.* **2017**, *83*,150-157.

[11] Colás-Ruiz, N.R., Ramirez, G., Courant, F., Gomez, E., Hampel, M. & Lara-Martín, P.A. Multi-omic approach to evaluate the response of gilt-head sea bream (Sparus aurata) exposed to the UV filter sulisobenzone. *Sci.Total Environ.* **2022,** *803*, 150080.

[12] Beel, R., Lütke Eversloh, C. & Ternes, T.A. Biotransformation of the UV-filter sulisobenzone: challenges for the identification of transformation products. *Environ. Sci. Technol.* **2013**, *47*, 6819-6828.

[13] Richard, C., Cassel, S. & Blanzat, M. Vesicular systems for dermal and transdermal drug delivery. *RSC Adv.* **2021**, *11*, 442-451.

[14] Yan, Y., Xing, J., Xu, W., Zhao, G., Dong, K., Zhang, L. & Wang, K. Hydroxypropyl-β-cyclodextrin grafted polyethyleneimine used as transdermal penetration enhancer of diclofenac sodium. *Int. J. Pharm.* **2014**, *474*, 182-192.

[15] Hayden, D.R., Kibbelaar, H.V., Imhof, A. & Velikov, K.P. Size and optically tunable ethyl cellulose nanoparticles as carriers for organic UV filters. *Chem. Nano. Mat.* **2018**, *4*, 301-308.

[16] Tran, M.H., Phan, D.P. & Lee, E.Y. Review on lignin modifications toward natural UV protection ingredient for lignin-based sunscreens. *Green Chem.* **2021**, *23*, 4633-4646.

[17] Xu, Q., Geng, S., Dai, Y., Qin, G. & Wang, J.Y. CDBA-liposome as an effective sunscreen with longer UV protection and longer shelf life. *J. Photochem. Photobiol. B: Biol.* **2013**, *129*, 78-86.

[18] d'Agostino, S., Azzali, A., Casali, L., Taddei, P. & Grepioni, F. Environmentally friendly sunscreens: Mechanochemical synthesis and characterization of β-CD inclusion complexes of avobenzone and octinoxate with improved photostability. *ACS Sustain. Chem. Eng.* **2020**, *8*, 13215-13225.

[19] Kellici, S., Acord, J., Vaughn, A., Power, N.P., Morgan, D.J., Heil, T., Facq, S.P. & Lampronti, G.I. Calixarene assisted rapid synthesis of silver-graphene nanocomposites with enhanced antibacterial activity. *ACS Appl. Mater. Interfaces.* **2016**, *8*, 19038-19046.

[20] Hayden, D.R., Kibbelaar, H.V., Imhof, A. and Velikov, K.P.Size and optically tunable ethyl cellulose nanoparticles as carriers for organic UV filters. *Chem. Nano. Mat.* **2018**, *4*, 301-308.

[21] Chen, M.X., Li, T., Peng, S. & Tao, D. Supramolecular nanocapsules from the self-assembly of amphiphilic calixarene as a carrier for paclitaxel. *New J. Chem.* **2016**, *40*, 9923-9929.

[22] Dahabra, L., Broadberry, G., Le Gresley, A., Najlah, M. & Khoder, M. Sunscreens containing cyclodextrin inclusion complexes for enhanced efficiency: A strategy for skin cancer prevention. *Molecules.* **2021**, *26*, 1698.

[23] Wintgens, V., Lorthioir, C., Miskolczy, Z., Amiel, C. & Biczók, L. Substituent effects on the inclusion of 1-alkyl-6-alkoxy-quinolinium in 4-sulfonatocalix [n] arenes. *ACS Omega.* **2018**, *3*, 8631-8637.

[24] Kumar, R., Lee, Y.O., Bhalla, V., Kumar, M. & Kim, J.S. Recent developments of thiacalixarene based molecular motifs. *Chem. Soc. Rev.* **2014**, *43*, 4824-4870.

[25] Kunda, U.M.R., Yamada, M., Kimuro, T., Katagiri, H., Kondo, Y. & Hamada, F. A hetero-alkali metallic (Na, K) three-dimensional supramolecular assembly based on p-sulfonatothiacalix [4] arene. *RSC Adv.* **2015**, *5*, 30140-30144.

[26] Le Loh, S., Sobolev, A.N., Lim, S.H. & Ling, I. Influence of ortho-and meta-substituted N-heterocyclic dications towards the self-assembly of p-sulfonatocalix [4] arene. *Cryst. Eng. Comm.* **2020**, *22*, 52-60.

[27] Chen, B., Yuan, D., Wu, M., Jiang, F. & Hong, M. Two Coordination Networks Built from p-Sulfonatothiacalix [4] arene Tetranuclear Clusters. *Z. fur Anorg. Allg. Chem***. 2009**, *635*, 1669-1672.

[28] Gong, H., Luo, W.W. & Jiang, H. Preparation and characterization of inclusion complex of 2-hydroxy-4-methoxybenzophenone-5-sulfonic acid with β-cyclodextrin. *China Surfactant Detergent and Cosmetics*. **2006**, 36, 358-360.

[29] Jing, J., Szarpak-Jankowska, A., Guillot, R., Pignot-Paintrand, I., Picart, C. & Auzély-Velty, R. Cyclodextrin/paclitaxel complex in biodegradable capsules for breast cancer treatment. *Chem. Mater.* **2013**, *25*, 3867-3873.

[30] Arancibia, J.A. & Escandar, G.M. Complexation study of diclofenac with β-cyclodextrin and spectrofluorimetric determination. *Analyst.* **1999**, *124*, 1833-1838.

[31] Wu, H., Liang, H., Yuan, Q., Wang, T. & Yan, X. Preparation and stability investigation of the inclusion complex of sulforaphane with hydroxypropyl-β-cyclodextrin. *Carbohydr. Polym.* **2010**, *82*, 613-617.

[32] Liu, Y., Guo, D.S., Yang, E.C., Zhang, H.Y. & Zhao, Y.L. The structures and thermodynamics of complexes between water-soluble Calix [4] arenes and Dipyridinium Ions. *Eur. J. Org. Chem.* **2005**, *2005*, 162-170.

[33] Frisch, M. J., Trucks, G. W., Schlegel, H. B., Scuseria, G. E., Robb, M. A., Cheeseman, J. R., Scalmani, G., Barone, V., Petersson, G.A., Nakatsuji, H., Li, X., Caricato, M., Marenich, A., Bloino, J., Janesko, B.G., Gomperts, R., Mennucci, B., Hratchian, H.P., Ortiz, J.V., Izmaylov, A. F., Sonnenberg, J.L., Williams-Young, D., Ding, F., Lipparini, F., Egidi, F., Goings, J., Peng, B., Petrone, A., Henderson, T., Ranasinghe, D., Zakrzewski, V.G., Gao, J., Rega, N., Zheng, G., Liang, W., Hada, M., Ehara, M., Toyota, K., Fukuda, R., Hasegawa, J., Ishida, M., Nakajima, T., Honda, Y., Kitao, O., Nakai, H., Vreven, T., Throssell, K., Montgomery, J.A., Peralta, Jr., J. E., Ogliaro, F., Bearpark, M., Heyd, J.J., Brothers, E., Kudin, K.N., Staroverov, V.N., Keith, T., Kobayashi, R., Normand, J., Raghavachari, K., Rendell, A., Burant, J.C., Iyengar, S.S., Tomasi, J., Cossi, M., Millam, J.M., Klene, M., Adamo, C., Cammi, R., Ochterski, J.W., Martin, R.L., Morokuma, K., Farkas, O., Foresman, J.B. & D. J. Fox, *Gaussian 09, Revision D.01*, Gaussian, Inc., Wallingford CT, **2016**.

[34] Ghosh, B., Roy, N., Roy, D., Mandal, S., Ali, S., Bomzan, P., Roy, K. & Roy, M.N. An extensive investigation on supramolecular assembly of a drug (MEP) with βCD for innovative applications. *J. Mol. Liq.* **2021**, *344*, 117977.

[35] Dallakyan, S. & Olson, A.J. Small-molecule library screening by docking with PyRx. In *Chemical biology*. Humana Press, New York, NY, **2015**, 243-250.

[36] The PyMol Molecular Graphics System, Version 2.0 Schrodinger, LLC.

[37] Zhang, W., Gong, X., Cai, Y., Zhang, C., Yu, X., Fan, J. & Diao, G. Investigation of water-soluble inclusion complex of hypericin with β-cyclodextrin polymer. *Carbohydr. Polym.* **2013**, *95*, 366-370.

[38] Ghosh, B., Roy, N., Roy, D., Mandal, S., Ali, S., Bomzan, P., Roy, K. & Roy, M.N. An extensive investigation on supramolecular assembly of a drug (MEP) with βCD for innovative applications. *J. Mol. Liq.* **2021**, *344*, 117977.

[39] Bomzan, P., Roy, N., Sharma, A., Rai, V., Ghosh, S., Kumar, A. & Roy, M.N. Molecular encapsulation study of indole-3-methanol in cyclodextrins: Effect on antimicrobial activity and cytotoxicity. *J. Mol. Struct.* **2021**, *1225*, 129093.

[40] Ol'khovich, M.V., Sharapova, A.V., Perlovich, G.L., Skachilova, S.Y. & Zheltukhin, N.K. Inclusion complex of antiasthmatic compound with 2-hydroxypropyl-β-cyclodextrin: preparation and physicochemical properties. *Journal of Molecular Liquids* **2017**, *237*, 185-192.

[41] Ghosh, R., Roy, N., Saha, S., Das, S., Barman, B.K., Roy, D., Dakua, V.K. & Roy, M.N. Synthesis and characterization of an industrially significant ionic liquid and its inclusion complex with β-cyclodextrin and its soluble derivative for their advanced applications. *Chem. Phys. Lett.* **2021**, *769*, 138401.

[42] Roy, N., Ghosh, R., Das, K., Roy, D., Ghosh, T. & Roy, M.N. Study to synthesize and characterize host-guest encapsulation of antidiabetic drug (TgC) and hydroxy propyl-β-cyclodextrin augmenting the antidiabetic applicability in biological system. *J. Mol. Struct.* **2019**, *1179*, 642-650.

[43] Williams, M. Eds., MJO'Neil, The Merck Index: An Encyclopedia of Chemicals, Drugs, and Biologicals, Royal Society of Chemistry, Cambridge, UK ISBN 9781849736701, **2013**, 2708.

[44] Ashwin, B.C.M.A., Vinothini, A., Stalin, T. & Muthu Mareeswaran, P. Synthesis of a Safranin T-p-Sulfonatocalix [4] arene Complex by Means of Supramolecular Complexation. *Chemistry Select.* **2017**, *2*, 931-936.

[45] Patil, S.V., Gejji, S.P., Kalyani, V.S. & Malkhede, D.D. Hydroxycoumarin encapsulated sulfonatothiacalix [4] arene: 1H NMR, steady state fluorescence and theory. *J. Mol. Liq.* **2021**, *339*, 116760.

[46] Roy, N., Ghosh, B., Roy, D., Bhaumik, B. & Roy, M.N. Exploring the Inclusion Complex of a Drug (Umbelliferone) with α-Cyclodextrin Optimized by Molecular Docking and Increasing Bioavailability with Minimizing the Doses in Human Body. *ACS Omega.* **2020**, *5*, 30243-30251.

[47] Jarange, A.B., Patil, S.V., Malkhede, D.D., Deodhar, S.M., Nandre, V.S., Athare, S.V., Kodam, K.M. & Gejji, S.P. p-Sulfonatocalixarene versus p-thiasulfonatocalixarene: encapsulation of tenofovir disoproxil fumarate and implications to ESI-MS, HPLC, NMR, DFT and anti-MRSA activities. *J. Incl. Phenom. Macrocycl. Chem*. **2021**, *99*, 43-59.

[48] Galindo-Murillo, R., Sandoval-Salinas, M.E. & Barroso-Flores, J. In silico design of monomolecular drug carriers for the tyrosine kinase inhibitor drug imatinib based on calix-and thiacalix [n] arene host molecules: a DFT and molecular dynamics study. *J. Chem. Theory Comput.* **2014**, *10*, 825-834.

[49] Hanson, K.M., Cutuli, M., Rivas, T., Antuna, M., Saoub, J., Tierce, N.T. & Bardeen, C.J. Effects of solvent and micellar encapsulation on the photostability of avobenzone. *Photochem. Photobiol. Sci.* **2020**, *19*, 390-398.

Chapter VII

[1] Böhmer, V. Calixarenes, macrocycles with (almost) unlimited possibilities. *Angew. Chem. Int. Ed.* **1995**, *34*, 713-745.

[2] Gutsche, C.D. Ed., Stoddart, J. F., Calixarenes Revisited, Monographs in Supramolecular Chemistry, The Royal Society of Chemistry, Cambridge, UK, **1998**.

[3] Ikeda, A. & Shinkai, S. Novel cavity design using calix [n] arene skeletons: toward molecular recognition and metal binding. *Chem. Rev.* **1997**, *97*, 1713-1734.

[4] Du, S., Yu, T.Q., Liao, W. & Hu, C. Structure modeling, synthesis and X-ray diffraction determination of an extra-large calixarene-based coordination

cage and its application in drug delivery. *Dalton Trans.* **2015**, *44*, 14394-14402.

[5] Gutsche, C.D. Calixarenes. Ed., Stoddart, J.F., Royal Society of Chemistry, Cambridge, UK, **1989**.

[6] Perret, F., Lazar, A.N. & Coleman, A.W. Biochemistry of the para-sulfonato-calix [n] arenes. *Chem. Comm.* **2006**, 2425-2438.

[7] Abd El-Rahman, M.K. & Mahmoud, A.M. A novel approach for spectrophotometric determination of succinylcholine in pharmaceutical formulation via host–guest complexation with water-soluble p-sulfonatocalixarene. *RSC Adv.* **2015**, *5*, 62469-62476.

[8] Makha, M. & Raston, C.L. Direct synthesis of calixarenes with extended arms: p-phenylcalix [4, 5, 6, 8] arenes and their water-soluble sulfonated derivatives. *Tetrahedron Lett.* **2001**, *42*, 6215-6217.

[9] Yang, W. & de Villiers, M.M. Aqueous solubilization of furosemide by supramolecular complexation with 4-sulphonic calix [n] arenes. *J. Pharm. Pharmacol.* **2004**, *56*, 703-708.

[10] Da Silva, E., Lazar, A.N. & Coleman, A.W. Biopharmaceutical applications of calixarenes. *J. Drug Del. Sci. Tech.* **2004**, *14*, 3-20.

[11] Shinkai, S., Mori, S., Koreishi, H., Tsubaki, T. & Manabe, O. Hexasulfonated calix [6] arene derivatives: a new class of catalysts, surfactants, and host molecules. *J. Am. Chem. Soc.* **1986**, *108*, 2409-2416.

[12] Shinkai, S., Kawabata, H., Arimura, T., Matsuda, T., Satoh, H. & Manabe, O. New water-soluble calixarenes bearing sulphonate groups on the 'lower rim': the relation between calixarene shape and binding ability. *J. Chem. Soc., Perkin trans. 1.***1989**, 1073-1074.

[13] Guo, D.S., Wang, K. & Liu, Y. Selective binding behaviors of p-sulfonatocalixarenes in aqueous solution. *J. Incl. Phenom. Macrocycl. Chem.* **2008**, *62*, 1-21.

[14] Wintgens, V., Biczók, L. & Miskolczy, Z. Thermodynamics of host–guest complexation between p-sulfonatocalixarenes and 1-alkyl-3-methylimidazolium type ionic liquids. *Thermochim. Acta.* **2011**, *523*, 227-231.

[15] Megyesi, M. & Biczók, L. Considerable change of fluorescence properties upon multiple binding of coralyne to 4-sulfonatocalixarenes. *J. Phys. Chem. B.* **2010**, *114*, 2814-2819.

[16] Wintgens, V., Amiel, C., Biczók, L., Miskolczy, Z. & Megyesi, M. Host–guest interactions between 4-sulfonatocalix [8] arene and 1-alkyl-3-methylimidazolium type ionic liquids. *Thermochim. Acta.* **2012**, *548*, 76-80.

[17] Miskolczy, Z. & Biczók, L. Photochromism of a Merocyanine Dye Bound to Sulfonatocalixarenes: Effect of pH and the Size of Macrocycle on the Kinetics. *J. Phys. Chem. B.* **2013**, *117*, 648-653.

[18] Wang, K., Guo, D.S., Zhang, H.Q., Li, D., Zheng, X.L. & Liu, Y. Highly effective binding of viologens by p-sulfonatocalixarenes for the treatment of viologen poisoning. *J. Med. Chem.* **2009**, *52*, 6402-6412.

[19] Perret, F. & Coleman, A.W. Biochemistry of anionic calix [n] arenes. *Chem. Comm.* **2011**, *47*, 7303-7319.

[20] Basilio, N., Francisco, V. & Garcia-Rio, L. Aggregation of p-sulfonatocalixarene-based amphiphiles and supra-amphiphiles. *Int. J. Mol. Sci.* **2013**, *14*, 3140-3157.

[21] Wang, K., Guo, D.S., Wang, X. & Liu, Y. Multistimuli responsive supramolecular vesicles based on the recognition of p-sulfonatocalixarene and its controllable release of doxorubicin. *ACS Nano.* **2011**, *5*, 2880-2894.

[22] Bakirci, H. & Nau, W.M. Fluorescence regeneration as a signaling principle for choline and carnitine binding: a refined supramolecular sensor system based on a fluorescent azoalkane. *Adv. Funct. Mater.* **2006**, *16*, 237-242.

[23] Hennig, A., Bakirci, H. & Nau, W.M. Label-free continuous enzyme assays with macrocycle-fluorescent dye complexes. *Nat. Methods* **2007**, *4*, 629-632.

[24] Guo, D.S., Uzunova, V.D., Su, X., Liu, Y. & Nau, W.M. Operational calixarene-based fluorescent sensing systems for choline and acetylcholine and their application to enzymatic reactions. *Chem. Sci.* **2011**, *2*, 1722-1734.

[25] Basílio, N. & Garcia-Rio, L. Calixarene-Based Surfactants: Conformational-Dependent Solvation Shells for the Alkyl Chains. *Chem. Phys. Chem.* **2012**, *13*, 2368-2376.

[26] Guo, D.S., Wang, K., Wang, Y.X. & Liu, Y. Cholinesterase-responsive supramolecular vesicle. *J. Am. Chem. Soc.* **2012**, *134*, 10244-10250.

[27] Wang, Y.X., Guo, D.S., Duan, Y.C., Wang, Y.J. & Liu, Y. Amphiphilic p-sulfonatocalix [4] arene as "drug chaperone" for escorting anticancer drugs. *Sci. Rep.* **2015**, *5*, 1-7.

[28] McGovern, R.E., Fernandes, H., Khan, A.R., Power, N.P. & Crowley, P.B. Protein camouflage in cytochrome c–calixarene complexes. *Nat. Chem.* **2012**, *4*, 527-533.

[29] Dalgarno, S.J., Atwood, J.L. & Raston, C.L. Sulfonatocalixarenes: molecular capsule and 'Russian doll'arrays to structures mimicking viral geometry. *Chem. Comm.* **2006**, 4567-4574.

[30] Yuan, D., Wu, M., Wu, B., Xu, Y., Jiang, F. & Hong, M. Guest-induced molecular capsule assembly of p-sulfonatothiacalix [4] arene. *Cryst. Growth Des.* **2006**, *6*, 514-518.

[31] Selkti, M., Coleman, A.W., Nicolis, I., Douteau-Guével, N., Villain, F., Tomas, A. & de Rango, C. The first example of a substrate spanning the calix [4] arene bilayer: the solid state complex of p-sulfonatocalix [4] arene with L-lysine. *Chem. Comm.* 161-162.

[32] Guo, D.S. & Liu, Y. Supramolecular chemistry of p-sulfonatocalix [n] arenes and its biological applications. *Acc. Chem. Res.* **2014**, *47*, 1925-1934.

[33] Morohashi, N., Narumi, F., Iki, N., Hattori, T. & Miyano, S. Thiacalixarenes. *Chem. Rev.* **2006**, *106*, 5291-5316.

[34] Iki, N., Morohashi, N., Narumi, F. & Miyano, S. High complexation ability of thiacalixarene with transition metal ions. The effects of replacing methylene bridges of tetra (p-t-butyl) calix [4] arenetetrol by epithio groups. *Bulletin of the Chemical Society of Japan* **1998**, *71*, 1597-1603.

[35] Li, X., Gong, S.L., Yang, W.P., Li, Y., Chen, Y.Y. & Meng, X.G. Aminopyridyl derivative of thiacalix [4] arene-carboxylic acid as ionizable highly selective Ag+ ionophore. *J. Incl. Phenom. Macrocycl. Chem.* **2010**, *66*, 179-184.

[36] Agrawal, Y.K. & Pancholi, J.P. Analytical applications of thiacalixarenes: A review. *Ind. J. Chem.* **2007**, *46A*, 1373-1382.

[37] Nelson, D.L & M.M. Cox, M.M. Lehninger Principles of Biochemistry, third ed., Worth Publishing, New York, 2000. ISBN 1-57259-153-6.

[38] Lynch, C.J. & Adams, S.H. Branched-chain amino acids in metabolic signalling and insulin resistance. *Nat. Rev. Endocrinol.* **2014**. *10*, 723-736.

[39] Taya, Y., Ota, Y., Wilkinson, A.C., Kanazawa, A., Watarai, H., Kasai, M., Nakauchi, H. & Yamazaki, S. Depleting dietary valine permits nonmyeloablative mouse hematopoietic stem cell transplantation. *Science.* **2016**, *354*, 1152-1155.

[40] Gao, S., Bie, C., Ji, Q., Ling, H., Li, C., Fu, Y., Zhao, L. & Ye, F. Preparation and characterization of cyanazine–hydroxypropyl-beta-cyclodextrin inclusion complex. *RSC Adv.* **2019**, *9*, 26109-26115.

[41] Wang, K., Yang, E.C., Zhao, X.J., Dou, H.X. & Liu, Y. Molecular binding behaviors of sulfonated calixarenes with phenanthroline-diium in aqueous solution and solid state: Cavity size governing capsule formation. *Cryst. Growth Des.* **2014**, *14*, 4631-4639.

[42] Senthilkumaran, M., Chitumalla, R.K., Vigneshkumar, G., Rajkumar, E., Muthu Mareeswaran, P. & Jang, J. Investigation of the upper rim binding of triphenylpyrylium cation with p-sulfonatocalix [4] arene. *J. Incl. Phenom. Macrocycl. Chem.* **2018**, *91*, 161-169.

[43] Roy, M.N., Roy, A. & Saha, S. Probing inclusion complexes of cyclodextrins with amino acids by physicochemical approach. *Carbohydr. Polym.* **2016**, *151*, 458-466.

[44] Saravanan, C., Ashwin, B.C.M.A., Senthilkumaran, M. & Mareeswaran, P.M. Supramolecular Complexation of Biologically Important Thioflavin-T with p-Sulfonatocalix [4] arene. *Chemistry Select.* **2018**, *3*, 2528-2535.

[45] Rani, D., Sethi, A., Kaur, K. & Agarwal, J. Ultrasonication-Assisted Synthesis of a d-Glucosamine-Based β-CD Inclusion Complex and Its Application as an Aqueous Heterogeneous Organocatalytic System. *J. Org. Chem.* **2020**, *85*, 9548-9557.

[46] Valand, N.N., Patel, M.B. & Menon, S.K. Curcumin-p-sulfonatocalix [4] resorcinarene (p-SC [4] R) interaction: thermo-physico chemistry, stability and biological evaluation. *RSC Adv.* **2015**, *5*, 8739-8752.

[47] Ghosh, B., Roy, N., Roy, D., Mandal, S., Ali, S., Bomzan, P., Roy, K. & Roy, M.N. An extensive investigation on supramolecular assembly of a drug (MEP) with βCD for innovative applications. *J. Mol. Liq.* **2021**, *344*, 117977.

[48] Dallakyan, S., & Olson, A. J. Small-molecule library screening by docking with PyRx. *Methods Mol. Biol.* **2015**, *1263*, 243–250.

INDEX

Journal of Molecular Structure 1225 (2021) 129093

Contents lists available at ScienceDirect

Journal of Molecular Structure

journal homepage: www.elsevier.com/locate/molstr

Molecular encapsulation study of indole-3-methanol in cyclodextrins: Effect on antimicrobial activity and cytotoxicity

Pranish Bomzan[a], Niloy Roy[a], Antara Sharma[a], Vijeta Rai[b], Shilpi Ghosh[b], Anoop Kumar[b], Mahendra Nath Roy[a,*]

[a] Department of Chemistry, University of North Bengal, Darjeeling 734013, India
[b] Department of Biotechnology, University of North Bengal, Darjeeling 734013, India

ARTICLE INFO

Article history:
Received 21 June 2020
Revised 12 August 2020
Accepted 14 August 2020
Available online 15 August 2020

Keywords:
Indole-3-methanol
B-cyclodextrin
Hydroxypropyl-β-cyclodextrin
Molecular docking
In vitro biological activity study

ABSTRACT

We investigated the encapsulation of indole-3-methanol(IM) within the nanocage of β-cyclodextrin(β-CD) and hydroxypropyl-β-cyclodextrin(HP-β-CD). The formation of encapsulated complexes have been confirmed by the experimental studies such as UV-Visible, Fluorescence, ^{1}H NMR, DSC, SEM, surface tension, FT-IR and mass spectrometry. DSC study revealed that the inclusion into CDs can enhance the thermal stability of IM. Molecular docking studies provided useful insight on the encapsulation mode of IM molecule into the cavity of CDs. The antimicrobial activity of IM was considerably improved after encapsulation. Further, the encapsulated complexes expressed low cytotoxic effect than free IM on the normal liver cell line WRL-68.

1. Introduction

In supramolecular chemistry, cyclodextrins (CDs) are interesting ideal host molecules [1]. They are cyclic oligosaccharides composed of six (α-CD), seven (β-CD & HP-β-CD) and eight (γ-CD) glucopyranose units linked by $\alpha-1,4$-linkages with a hydrophobic cavity and a hydrophilic external surface [2,3]. They can form host–guest complexes by encapsulation of various organic, biological and pharmacological guest molecules into their internal hydrophobic cavity [4,5]. This usually enhances the chemical stability, solubility and bioavailability of the drug molecule [6–11]. Due to this interesting property, CDs have been used as drug carriers [12–14], photochemical sensors [15], enzyme mimics [16], and separation reagents [17], etc. CDs have been extensively exploited as excellent receptors and also applied to build stimuli-responsive supramolecular materials [18]. Inclusion with CD is the best way for the advancement of drug molecule's physicochemical properties [19]. The discharge of guest molecules from the ICs can be achieved by applying different external stimuli, such as, temperature, competitive binding, photosensing, enzyme activation and changes in pH [20–23].

Indole-3-methanol (IM) is a phytochemical compound obtained from hydrolysis of glucosinolate glucobrassicin catalyzed by myrosinase. A comparatively high level of IM can be found in vegetables of the Brassica genus [24]. IM has been examined concerning important role in cancer management [24–26]. In human melanoma cells, IM result in proliferation arrest and apoptosis [27]. In situ and in vivo studies identifies a role of IM in breast and prostate cancer as a chemoprotective agent [28]. The anti-inflammatory effect of IM was also described [29,30]. These findings have showed that IM exhibits significant potential for biological purpose. However, in spite of its potential in pharmacology, IM is unstable to acidic environment, light and temperature changes [31,32], which may restrict its broader applications in pharmaceutical science. Therefore, in order to retain or facilitate the biological activity of IM and enhance its stability from harsh environmental conditions, IM should be encapsulated in CDs forming host-guest ICs. Thus, CD can act as an encapsulating vehicle by forming IC for delivering the drug at the targeted site retaining its bioactivity [11].

In our present work, we have studied the encapsulation of IM within the nanocage of β-CD and HP-β-CD. Job's plot and surface tension study have been used to explain the 1:1 encapsulation. We have employed the spectroscopic method to evaluate association constant along with thermodynamic parameters. The ICs have been prepared and characterized by Fourier Transform Infrared (FTIR) spectroscopy, High-Resolution Mass spectrometry (HRMS), ^{1}H Nuclear Magnetic Resonance (NMR) spectroscopy, Differential Scanning Calorimetry and Scanning Electron Microscopy (SEM). Molecular modeling technique was utilized to get an insight into the possible interaction between IM and β-CD or HP-β-CD. Moreover, the antimicrobial activity against some pathogenic bacteria and in

* Corresponding author.
E-mail address: mahendraroy2002@yahoo.co.in (M.N. Roy).

https://doi.org/10.1016/j.molstruc.2020.129093
0022-2860/

vitro cytotoxic activity on normal liver cell line were tested out to investigate the benefits of IM encapsulation.

2. Experimental section

2.1. Materials

Indole-3-methanol with purity>98% and 2-Hydroxypropyl-β-cyclodextrin were procured from TCI chemicals India Pvt. Ltd. β-Cyclodextrin with purity 98% was purchased from Sigma-Aldrich, India and used as received.

2.2. Methods

UV–visible spectra were obtained by Agilent 8453 UV–VIS spectrophotometer. The temperature of the cell was kept fixed by an automated thermostat.

Surface tension experiments were performed using a digital K9 Tensiometer (Kruss, Germany) at 298.15 K with the accuracy of ± 0.1 mNm^{-1}.

Fluorescence spectra were taken by Agilent 8453 Spectrophotometer, at 298 K in a Hellma quartz cuvette.

^{1}H NMR measurements were carried out in DMSO–d_6 using Bruker Avance 300 MHz NMR spectrometer at 298.15 K.

HRMS spectra were recorded with positive-mode electrospray ionization in high-resolution Q-TOF instrument.

IR spectra were obtained by KBr disk method at room temperature on a Perkin-Elmer FTIR spectrometer.

Thermal analysis was performed in the temperature range of 30–300^{0}C under nitrogen gas atmosphere (1.5 atm.) on Perkin Elmer DSC-6 thermal analyzer.

Microscopic morphological structure analysis was carried out with JSM-6360 Scanning Electron Microscope (SEM).

2.3. Molecular modeling study

The possible binding mode as well as binding affinity of IM with β-CD and HP-β-CD was simulated by employing MOE2015 software. The 3D optimized structures of IM and β-CD were extracted from Chembridge Crystal data centre (CCDC) as CIF file and used as received. The structure of HP-β-CD was constructed by MOE Builder function by attaching seven hydroxypropyl substituents in 2-position of β-CD. Energy minimization of HP-β-CD was performed using MOE QuickPrep protocol. The MOE2015 software available in the Chemical Computing Group (CCG) was used to dock the guest molecule IM into the cavity of β-CD and HP-β-CD. Molecular modelling calculations were performed with molecular mechanics MMFF94x force field. The charges and hydrogens were kept fixed, and the root mean square (RMS) gradient was put to 0.005 kcal/mol. The Triangle Matcher method and the London ΔG scoring function were used respectively for fitting and ranking the ligand (cyclodextrins) conformations. Based on the docking scores, the produced poses were given rank. Finally, the inclusion complex was opted according to the optimum scoring pose and docking energy [33,34].

2.4. Antimicrobial activity assay

The antimicrobial activity of pure IM along with its inclusion complexes [IM-β-CD (IC1) and IM-HP-β-CD (IC2)] has been studied using the agar well diffusion technique. Bacterial cultures of *Bacillus subtilis, Bacillus amyloliquefaciens, Pseudomonas* sp. and *Proteus vulgaris*, grown overnight at 37^{0}C were spread over the nutrient agar plates. Using a sterile cork-borer, wells were made in the plates. To these wells, 40μl of DMSO as a control and 40μl 5 mM DMSO solutions of IM and its complexes were added. The plates were incubated at 24 hrs at 37^{0}C. The solvent DMSO used to dissolve IM and its complexes, was kept as a control. Following the incubation, the zone of inhibition was computed [35,36].

2.5. In vitro cytotoxicity assay with normal cell line WRL-68

The cytotoxic activity of the compound IM and its inclusion complexes [IM-β-CD (IC1), IM-HP-β-CD (IC2)], against the normal cell line were resolved by employing the 3-(4,5-dimethylthiazol-2-yl)−2,5-diphenyl tetrazolium bromide (MTT) based colorimetric assay. To initiate the assay, sterilized Dulbecco's Modified Eagle media was taken in a 100 mm petridish and inoculated with the normal liver cell line (WRL-68). This media was also enriched by the addition of 5% fetal bovine serum (FBS), antibiotics such as penicillin (100 IU/ml) and streptomycin (100 μg/ml) and incubated at 37°C in a CO_2(5%) humidified incubator. To a 96 welled microtiter plates, 100 μl each of the cell culture at a concentration of 1×10^5 cells/ml were added and incubated in a CO_2humidified incubator, temperature set to 37^{0}C for 24 h. Following incubation, the cells in each wells were subjected to treatment with varying concentrations of 5μl DMSO solutions of IM and its complexes. Past 24 h of incubation in a 37^{0}C set CO_2incubator, the media in the wells of the microtiter plate was replaced with fresh medium and thereafter 10μl from the working solution of MTT (5 mg/ml in phosphate buffer) was introduced to the wells. This was followed by the incubation of the microplate for 4 h at 37^{0}C set CO_2 incubator. The medium was subjected to aspiration and the formazan crystals formed in each wells of the microplate were dissolved using 50μl isopropanol. The degree to which the MTT was reduced to formazan crystals was assessed by computing the absorbance at 540 nm with the help of a microplate reader (Spectrostar nano, BMG Labtech). Lastly, the percentage of inhibition was computed by the formula; $(A_u\text{-}A_t/A_u) \times 100$, where A_u means the control's (cells subjected to DMSO treatment) average absorbance value and A_t means the average absorbance value of the cells subjected to the treatment with IM and its inclusion complexes. The stock solutions of IM and its inclusion complexes were prepared using DMSO and also the final dilutions (to the desired concentrations) were made in DMSO.

2.6. Preparation of inclusion complex

The two solid ICs [IC1 (IM-β-CD) and IC2 (IM-HP-β-CD)] have been prepared by mixing IM and CD in 1:1 molar ratio. 1.0 mmol CD was dissolved in 25 mL distilled water. Then predissolved 1.0 mmol IM in acetonitrile (AcN) [25 mL] was added slowly to an aqueous CD solution. This mixed solution was then kept at 48–50 °C with continuous stirring for 36 h. The stirred solution'was filtered and then stored into refrigerator for 24 h. The obtained suspension was filtered followed by drying in an oven at 70 °C for 9 h. Finally, the solid inclusion powder was collected and preserved in dessicator for latter use.

3. Results and discussion

3.1. Job plot determines the stoichiometry of the inclusion complex

In order to get an idea about the stoichiometry of the ICs a popularly known Job's method was applied using UV-Visible spectroscopic technique [37]. Job plots were obtained by plotting $\Delta A \times R$ against R (where ΔA denotes the difference in absorbance of IM in absence and presence of CD, and $R = [IM]/([IM] + [CD])$. The solutions were prepared taking 1:5 (V:V) AcN:H_2O as solvent because of the poor water solubility of IM. Absorption maximum values were obtained at λ_{max}= 279 nm for a series of solutions in such a manner that the overall concentration, [IM] + [CD], remains fixed

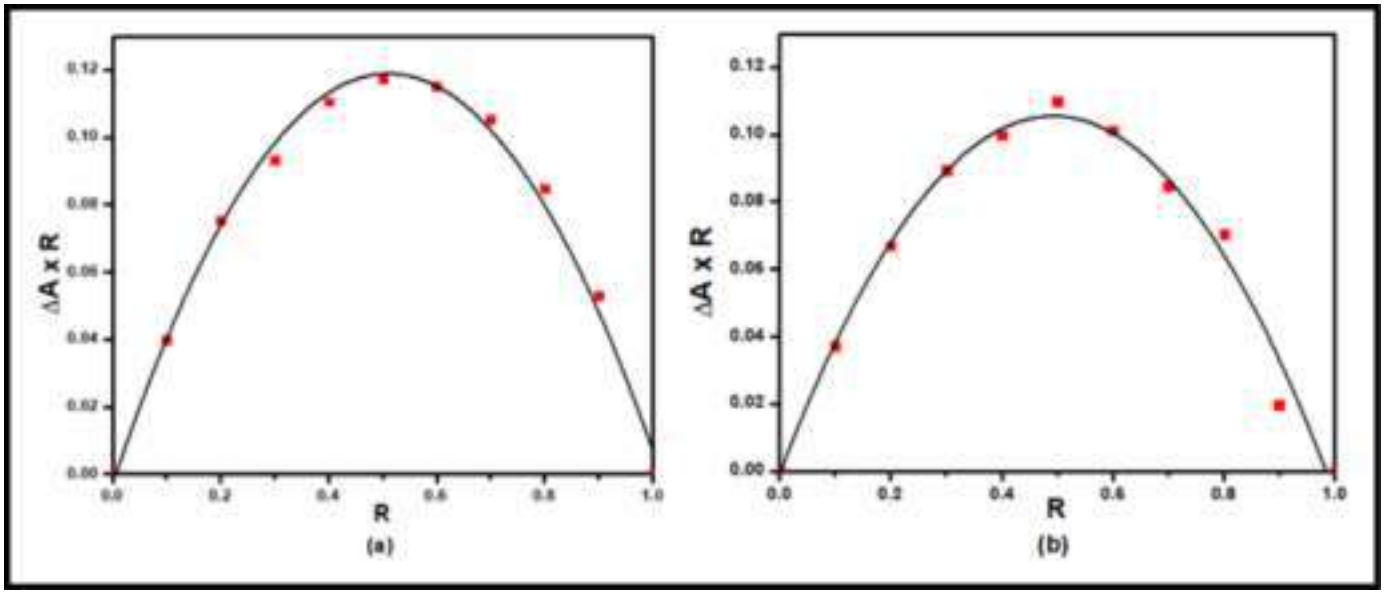

Fig. 1. Job plots of the (a) IM-β-CD and (b) IM-HP-β-CD systems at 298.15 K in 1:5 (V:V) AcN:H_2O at λ_{max} = 279 nm. ΔA = difference in absorbance of IM in absence and presence of CD, R = [IM]/([IM] + [CD]).

with varying mole fraction of IM in the range of 0–1 at 298.15 K (Tables S1 and S2). The maximum R value on the plot gives the stoichiometry of the complexation. In our present work, for both the systems IM-β-CD and IM-HP-β-CD, the observed maxima at R = 0.5 clearly indicates 1:1 stoichiometric ratio of the ICs (Fig. 1) [38].

3.2. Surface tension study demonstrates the inclusion and stoichiometric ratio

The formation of host-guest IC and its stoichiometry can be evaluated by surface tension (γ) study [39–41]. In this study, IM and CDs solutions were prepared taking 1:5 (V:V) AcN:H_2O as solvent because of the poor water solubility of IM. IM solution was found to have lower surface tension than the pure 1:5 (V:V) AcN:H_2O suggesting that IM is surface active, which may be ascribed to the presence of a hydrophobic indole moiety and a carbinol (-CH_2OH) group [42,43]. While CDs, having hydrophilic rims and hydrophobic external surface, does not display any alteration in γ of 1:5 (V:V) AcN:H_2O when dissolved in it in a significant range of concentration [44,45]. In our surface tension study, γ of IM solution were found to increase with increasing concentration of both β- and HP-β-CD (Tables S3 and S4, Fig. 2) indicating the inclusion of surface-active IM molecules into the central hydrophobic cavity of CD molecules from the surface of the solution forming ICs (Scheme 2) [46]. There was appearance of a break point in both the plots suggesting the formation of IC and also its 1:1 stoichiometry (Fig. 2) [39,40]. The concentrations of IM and CDs at each break point with corresponding γ values are listed in Table 1. The break points were observed at certain concentration where the molar concentration ratio of host CD and guest IM molecule are nearly 1:1 [46,43].

Table 1
Surface tension (γ) values at the break point and the corresponding concentrations of CD and IM at 298.15 K[a].

	Conc. of IM	Conc. of CD	γ^a
	(mM)	(mM)	(mNm^{-1})
β-CD	4.55	5.45	44.0
HP-β-CD	5.56	4.44	43.2

Table 2
Stability constant of different IM-CD ICs obtained from UV-Visible (K_a) and spectrofluorometric data (K_a^F) using Benesi-Hildebrand method; ± indicates the standard deviation.

Guest	Host	Temperature(K[a])	$K_a \times 10^{-3}$ (M^{-1})	$K_a^F \times 10^{-3}$ (M^{-1})
IM	β-CD	298.15	4.33±0.17	5.18±0.24
		303.15	4.17±0.09	
		308.15	4.04±0.12	
IM	HP-β-CD	298.15	17.60±0.99	21.98±1.42
		303.15	16.75±0.47	
		308.15	16.16±0.61	

3.3. Stability constants and thermodynamic parameters

The binding affinity of IM with β- and HP-β-CD can be determined by measuring association constant or stability constant (K_a) using UV-Visible spectroscopy [46]. For spectral measurement, 1:5 (V:V) AcN:H_2O was used as solvent because of the poor water solubility of IM. When IM molecules are encapsulated into the hydrophobic cavity of CD molecules, the environment of IM changes which results in the changes of molar extinction coefficient (ε) [47,48]. The change in absorbance (ΔA) of IM was checked out at the temperature range 298.15 K to 308.15 K by varying the concentration of β- and HP-β-CD (Tables S5 and S6) [42]. Based on Benesi-Hildebrand method for 1:1 complexes, the double reciprocal plots are drawn to calculate the K_a value using the following equation (Fig. S1) [49,38].

$$\frac{1}{\Delta A} = \frac{1}{\Delta\varepsilon[IM]K_a}\frac{1}{[CD]} + \frac{1}{\Delta\varepsilon[IM]} \quad (1)$$

where ΔA denotes the difference in absorbance of IM in absence and presence of CD. [IM] is the concentration of IM. The values of K_a for both IM-β-CD and IM-HP-β-CD ICs are determined from intercept/slope of the plots using Eq. (1) (Table 2) [50,46,42]. The smaller value of IM-β-CD ($\simeq$4.33 $\times$ 10^3 M^{-1} at 298.15 K) compared to that of IM-HP-β-CD ($\simeq$17.60 $\times$ 10^3 M^{-1} at 298.15 K) reveals that the binding capacity of β-CD is lower than HP-β-CD. This could

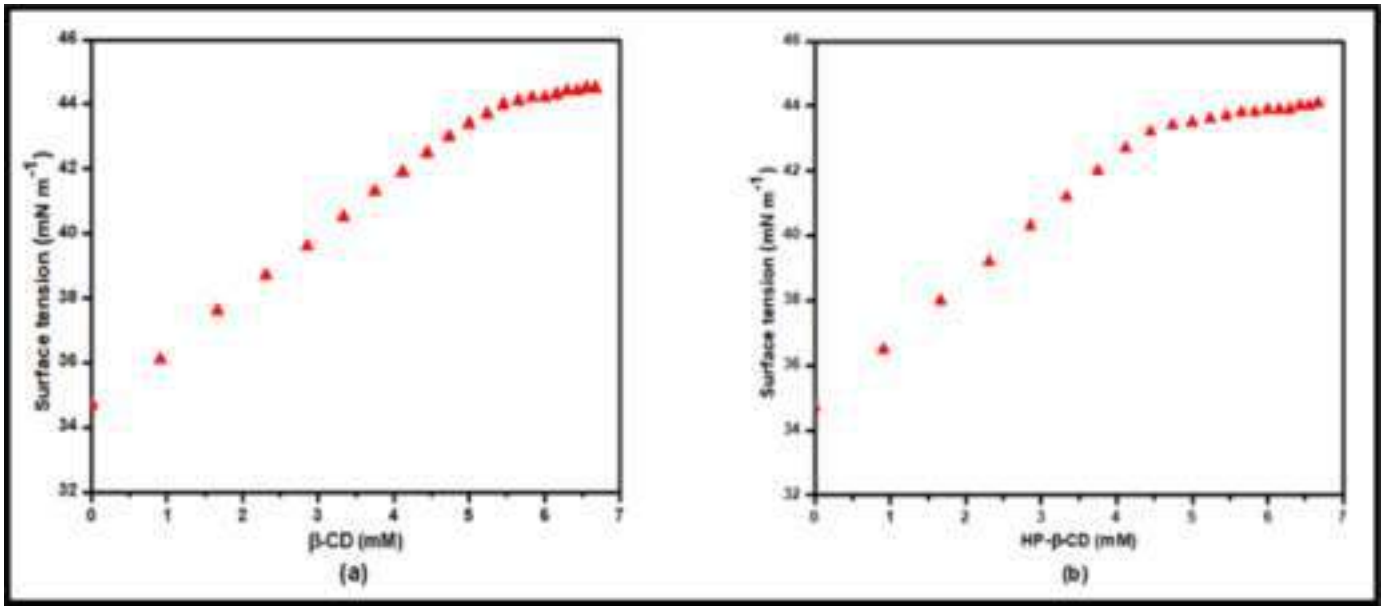

Fig. 2. Variation of surface tension of (a) IM with increasing β-CD concentration and (b) IM with increasing HP-β-CD concentration at 298.15 K.

Table 3
Thermodynamic parameters ΔH^0, ΔS^0, ΔG^0 obtained from van't Hoff equation using K_a value of different IM-CD ICs; ± indicates the standard deviation.

Guest	Host	Application of (K_a) to van't Hoff equation	
IM	β-CD	ΔH^0 (kJ mol^{-1})	−5.15±0.17
		ΔS^0 (J mol^{-1} K^{-1})	52.33±0.57
		ΔG^0 (kJ mol^{-1})	−20.75±0.08
	HP-β-CD	ΔH^0 (kJ mol^{-1})	−6.46±0.23
		ΔS^0 (J mol^{-1} K^{-1})	59.57±0.76
		ΔG^0 (kJ mol^{-1})	−24.23±0.11

be due to the steric hindrance induced by the substituted hydroxypropyl groups in HP-β-CD, which may lead to the widening of the cavity of HP-β-CD compared to that of β-CD.

The thermodynamic parameters ΔG^0, ΔS^0 and ΔH^0 can be obtained for the formation of inclusion complex from van't Hoff equation using values of K_a found at different temperatures.

$$lnK_a = -\frac{\Delta H^o}{RT} + \frac{\Delta S^o}{R} \quad (2)$$

The above linear equation involving $\ln K_a$ versus 1/T (Fig. S3) provides the value of ΔH^0, ΔS^0 and ΔG^0 for the formation of ICs (Table 3 and S9) [51,42,48]. The changes in enthalpy, entropy and free energy were found to be negative, positive and negative, indicating that the encapsulation process is exothermic, entropy-driven and spontaneous respectively. The large increase in entropy may be attributed to the release of highly ordered and restricted hydrogen-bonded water molecules in the direct vicinity of hydrophobic component of the drug or inside the CDs into the bulk water during encapsulation of IM into CDs [52]. Therefore, the negative ΔH^0, positive ΔS^0 and negative ΔG^0 values reveals that the overall encapsulation process is thermodynamically favourable.

3.4. Fluorescence study: modified Benesi–Hildebrand equation and stability constants

The stability constants (K_a^F) of ICs can also be derived from the spectrofluorometric data using modified Benesi–Hildebrand equation [53–55]. A 1:5 (V:V) AcN:H_2O was used as solvent for spectral measurement because of the poor water solubility of IM. The K_a^F values obtained from fluorescence study are found in good agreement with that obtained from the UV-Visible spectroscopic study (Table 2). It was observed that there was enhancement of fluorescence intensities of IM (at λ_{max} = 358 nm) with increasing concentration of CDs (Tables S7 and S8) suggesting an encapsulation of IM molecule into an apolar cavity of CDs. Such enhancement in the intensities may be attributed to the screening of the excited singlet state of fluorophore with the apolar cavity of the CDs [56,57]. The stability constants (K_a^F) of ICs have been obtained using double reciprocal plots:

$$\frac{1}{F - F_o} = \frac{1}{(F_\infty - F_o)K_a^F}\frac{1}{[CD]} + \frac{1}{F_\infty - F_o}$$

Table 4
^{1}HNMR data of the Indole-3-methanol (IM), β-Cyclodextrin (β-CD), Hydroxypropyl-β-Cyclodextrin (HP-β-CD) and the solid inclusion complexes IM-β-CD (IC1) and HP-β-CD (IC2). ND: not detected.

H protons	ppm (DMSO–d_6)			H protons	ppm (DMSO–d_6)		
	IM	β-CD	IM-β-CD (IC1)		IM	HP-β-CD	IM-HP-β-CD (IC2)
H2	7.23	–	7.19	H2	7.23	–	7.22
H6	7.58	–	7.52	H6	7.58	–	7.51
H7	6.97	–	6.89	H7	6.97	–	6.92
H8	7.08	–	7.03	H8	7.08	–	7.03
H9	7.34	–	7.32	H9	7.34	–	7.31
H2	–	3.42	3.41	H2	–	3.27	ND
H3	–	3.81	3.71	H3	–	3.84	3.71
H4	–	3.28	3.28	H4	–	3.15	ND
H5	–	3.63	3.58	H5	–	3.65	3.60

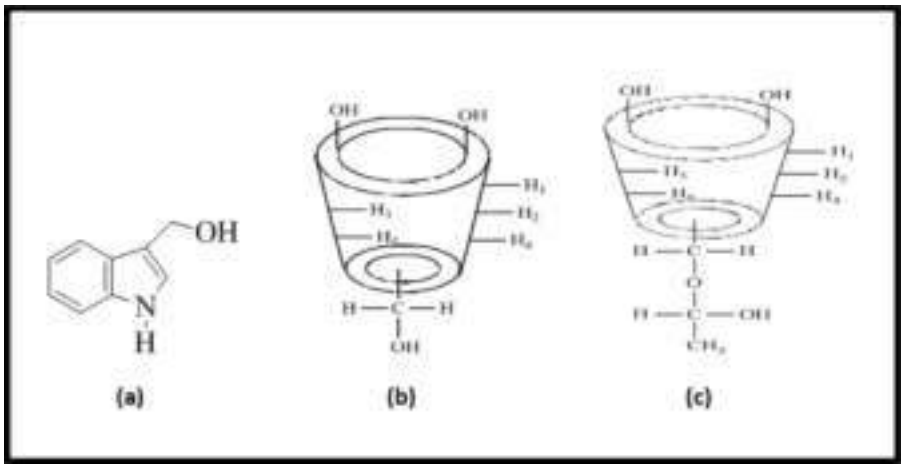

Scheme 1. Molecular Structures of (a) Indole-3-methanol, (b) β-Cyclodextrin and (c) Hydroxypropyl-β-Cyclodextrin.

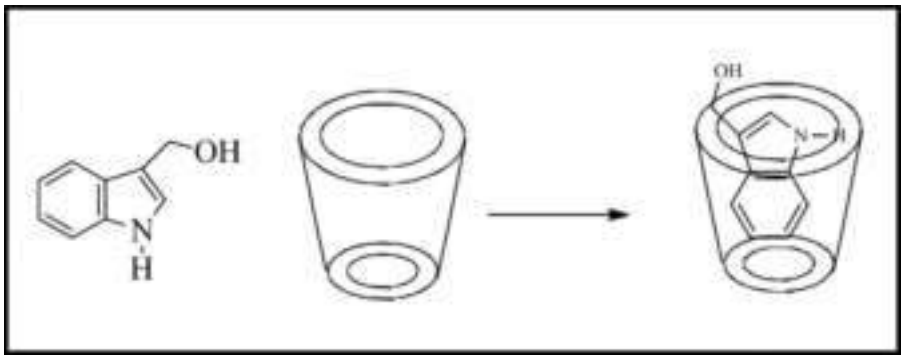

Scheme 2. Complexation of indole-3-methanol with cyclodextrin forming 1:1 inclusion complex.

where F and F_0 represents the fluorescence intensities of IM with and without CDs respectively, F_∞ is the fluorescence intensity of completely complexed IM and K_a^F is the stability constant of IC.

Plots of $1/(F - F_o)$ against 1/[CD] showed a good linear relationship suggesting 1:1 complexation (Fig. S2). The stability constants (K_a^F) of IM-β-CD and IM-HP-β-CD ICs, evaluated by the intercept/slope, were found to be 5.18×10^3 M^{-1} and 21.98×10^3 M^{-1} respectively at 298.15 K, which are in good agreement with that determined by the UV-Visible spectroscopic study (Table 2).

3.5. ^{1}H NMR spectral analysis

^{1}H NMR is a powerful tool in studying solid ICs, which provides quantitative information on the possible inclusion mode of ICs [58,59]. The encapsulation of a guest into a CD cavity causes changes in the chemical shift (δ) values of the guest as well as CD protons [60]. Usually the guest protons undergoes upfield chemical shifts upon inclusion into a CD cavity indicating that the protons of guest molecule were enclosed by electron density of the CDs [61,62]. The upfield shifts of the CD protons may also be observed owing to the induced anisotropic magnetic shielding produced by the encapsulated aromatic moiety of guest molecule [63,64]. In CD, H5 and H3 protons are situated in the interior of the cavity with H5 nearer to the narrower side and H3 to the wider side, whereas H4, H2 and H1 protons are placed at the outer surface (Scheme 1) [65,66]. In the present work, the molecular encapsulation of IM with β- and HP-β-CD has been explored using ^{1}H NMR spectroscopy. The NMR signals of IM protons and H5, H3 protons of β- and HP-β-CD were shown in Figures S4, S5 with their corresponding values of δ in Table 4. In case of solid ICs [IC1 (IM-β-CD) and IC2 (IM-HP-β-CD)], the NMR signals of the internal H5, H3 protons of β-CD and HP-β-CD along with the NMR signals of IM protons exhibited considerable upfield shifts, which confirms that IM is included inside the cavity of β- and HP-β-CD (Figures S4 and S5) [67]. Looking at these chemical shifts, we can also notice that the H3 proton undergoes significantly higher upfield shift compared to H5 proton (Table 4), indicating the preferential insertion of the aromatic moiety of IM into the cavity of both β- and HP-β-CD from the wider rim (Scheme 2) [68].

Table 5
The observed peaks at different *m/z* with corresponding ions for the solid inclusion complexes.

IM-β-CD inclusion complex		IM-HP-β-CD inclusion complex	
m/z	Ion	*m/z*	Ion
148.09	$[IM+H]^+$	148.09	$[IM+H]^+$
1135.31	$[\beta\text{-CD}+H]^+$	1542.35	$[HP\text{-}\beta\text{-CD}+H]^+$
1283.14	$[IM+\beta\text{-CD}+H]^+$	1689.42	$[IM+HP\text{-}\beta\text{-CD}+H]^+$
1305.13	$[IM+\beta\text{-CD}+Na]^+$	1711.33	$[IM+HP\text{-}\beta\text{-CD}+Na]^+$

3.6. High resolution mass spectrometric analysis

The solid ICs were analysed using mass spectroscopic study. The peaks observed in the spectra shown in Figure S6 with their corresponding *m/z* values are listed in Table 5. The observed peaks with *m/z* values 1305.13, 1283.11, 1711.33 and 1689.42 corresponds to the molecular ions $[IM+\beta\text{-CD}+Na]^+$, $[IM+\beta\text{-CD}+H]^+$, $[IM+HP\text{-}\beta\text{-CD}+Na]^+$ and $[IM+HP\text{-}\beta\text{-CD}+H]^+$ respectively. The appearance of these distinct peaks supports the formation of the ICs, IM-β-CD and IM-HP-β-CD, and their stoichiometric ratio should be 1:1

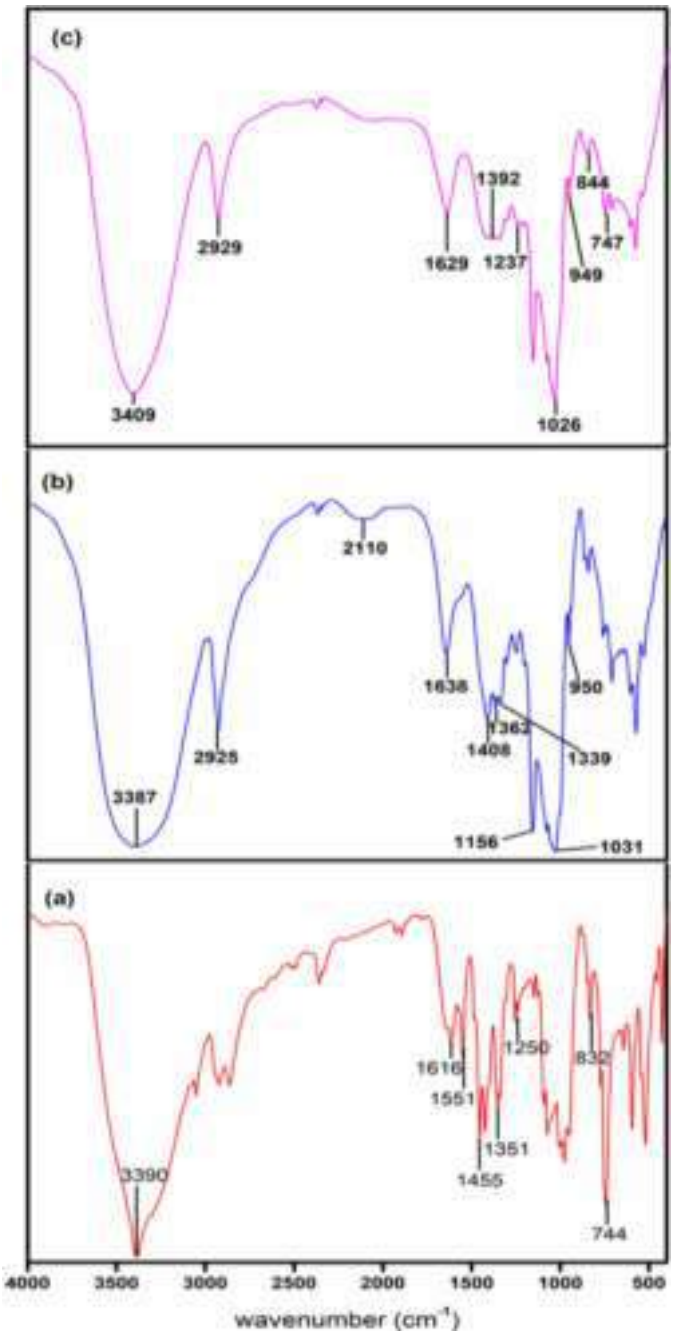

Fig. 3. FTIR spectra of (a) IM, (b) β-CD and (c) IM-β-CD inclusion complex.

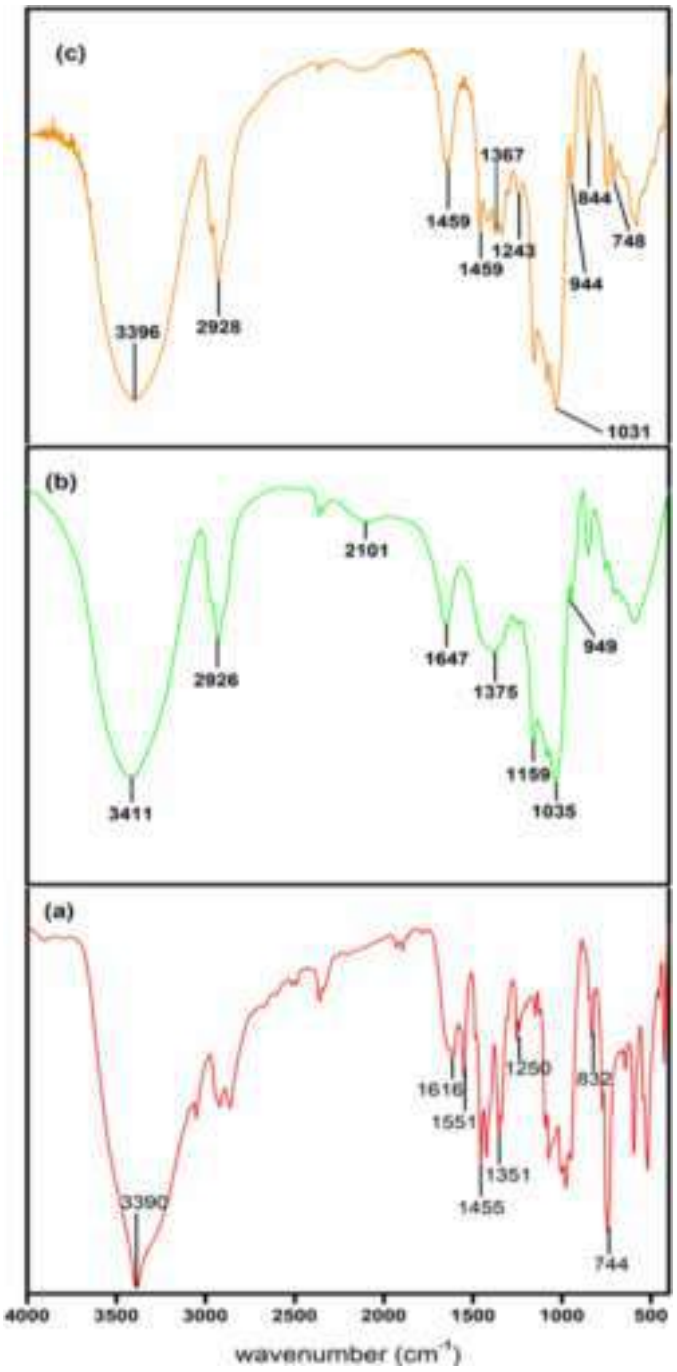

Fig. 4. FTIR spectra of (a) IM, (b) HP-β-CD and (c) IM-HP-β-CD inclusion complex.

(Scheme 2) [69,70] which is in accordance with the Job's method and surface tension study.

3.7. FTIR spectral analysis

FTIR study was performed to examine the characteristic changes in the IR spectra supporting the formation of ICs of IM with β- and HP-β-CD [71,67]. The spectra are shown in Figs. 3 and 4, and the vibrational frequencies with their corresponding chemical bonds have been set into Table S10.

The following changes in the IR spectra were observed for IM-β-CD IC (Fig. 3): The stretching vibrations involving O–H/N–H groups of IM at 3390 cm^{-1} and that of O–H of β-CD at 3387 cm^{-1} were appeared at 3409 cm^{-1} as a broad peak in the IC. The aromatic C=C skeletal stretching vibrations in IM were found to appear at 1616, 1551, 1455 cm^{-1}, and the aromatic C–H bending vibrations were observed at 1250 cm^{-1} (in-plane) and 744, 832 cm^{-1} (out-of-plane). Such C–H bending vibrations for IC were shifted to 1237 cm^{-1} (in-plane) and 747, 844 cm^{-1}(out-of-plane), along with disappearance of aromatic skeletal C=C stretching vibrations. The observed alteration of C–H bending modes and the disappearance of aromatic C=C skeletal stretching vibrations in IC indicates the encapsulation of aromatic indole moiety into the β-CD cavity with restriction of some modes of vibration of the IM within the cavity. The C–H bending modes were appeared at 1408, 1362, 1339 cm^{-1} for β-CD, and these bending modes were found to shift at 1392 cm^{-1}, which may be due to the close proximity of aromatic moiety of IM.

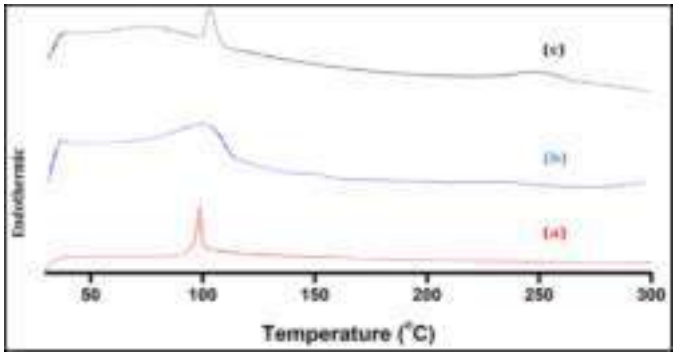

Fig. 5. DSC thermograms of (a) IM, (b) β-CD and (c) IM-β-CD inclusion complex.

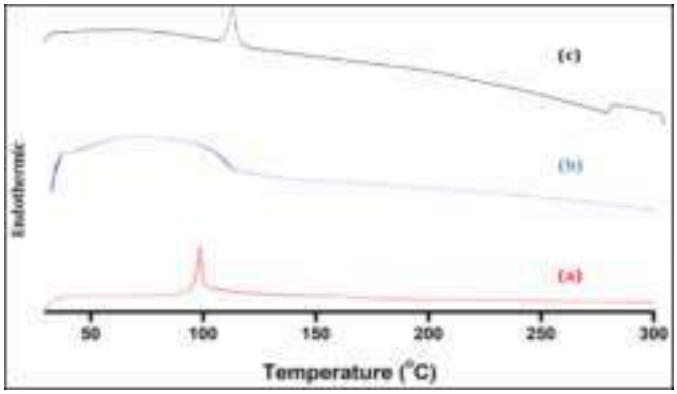

Fig. 6. DSC thermograms of (a) IM, (b) HP-β-CD and (c) IM-HP-β-CD inclusion complex.

Similarly, the following IR spectral shifts were observed for IM-HP-β-CD IC (Fig. 4): The stretching vibrations involving O–H/N–H groups of IM at 3390 cm^{-1} and that of O–H of HP-β-CD at 3411 cm^{-1} were appeared at 3396 cm^{-1} as a broad peak in the IC. The aromatic C=C skeletal stretching vibrations in pure IM were observed at 1616, 1551, 1455 cm^{-1}, and the aromatic C–H bending vibrations were noticed at 1250 cm^{-1} (in-plane) and 744, 832 cm^{-1} (out-of-plane). These C–H bending vibrations for IC were shifted to 1243 cm^{-1} (in-plane) and 748, 844 cm^{-1}(out-of-plane), along with appearance of only one skeletal stretching vibration involving aromatic C=C at

1455 cm^{-1}. The observed shifts of C–H bending modes and the disappearance of other two aromatic C=C skeletal stretching vibrations (1616 and 1551 cm^{-1}) in IC suggest the encapsulation of aromatic indole ring into the HP-β-CD cavity with restriction of some vibrational modes of the IM within the host cavity. The C–H bending frequency of HP-β-CD at 1375 cm^{-1} was found to shift at 1367 cm^{-1} for IC, which may be due to the close proximity of aromatic moiety of IM,

All these observations suggest that the appearance of shifting in IR spectra indicates the formation of IM-β-CD and IM-HP-β-CD ICs. Thus the results observed from FTIR study are in good correlation with the results of ^{1}H NMR.

3.8. DSC analysis

The differential scanning calorimetry (DSC) analysis was further utilized to provide additional evidence for the formation of inclusion complexes. The DSC curve of IM showed a sharp endothermic peak at 98^{0}C, which corresponds to its melting point. Broader endothermal peaks provided with water loss for β-CD around 101^{0}C and HP-β-CD around 85^{0}C were registered. However, there was disappearance of endothermic peak at about 98^{0}C corresponding to the pure IM in the DSC thermograms of complexes, and the appearance of a new endothermic peak with a lower intensity at 106^{0}C and 115^{0}C for IM-β-CD and IM-HP-β-CD complexes respectively, were encountered (Figs. 5 and 6). These outcomes not only confirm the formation of inclusion complexes, but also suggest that these inclusion complexes are comparatively stable than the pure IM from a thermal point of view.

3.9. SEM technique: surface morphology analysis

The surface morphological studies of solid samples can be carried out by scanning electron microscopy (SEM) [72,73]. The SEM image analysis provides an additional evidence in support of the formation of ICs of IM with β- and HP-β-CD. The surface morphology of IM, HP-β-CD, its physical mixture (PM2) and solid inclusion complex (IC2) are shown in Fig. 7(A). HP-β-CD consisted of round amorphous particle with aperture on its surface, and IM showed a group of plate shaped crystal in an aggregated form. Particles of HP-β-CD were found on the surface of IM in case of physical mixture. In contrast, inclusion complex was found to appear as irregular shaped crystal with a significant change in the morphology and crystalline nature. Similarly, the surface morphology of IM, β-CD, its physical mixture (PM1) and inclusion complex (IC1) are presented in Fig. 7(B). In β-CD, the particles were observed as uneven cubic crystal with large dimensions. The physical mixture displayed some similarities with the free components and has morphology comparable with these pure components. However, the particles of solid complex appeared as tiny flakes with a drastic change in the morphological structure and crystalline nature. These results confirms the formation of the inclusion complexes of IM with β- and HP-β-CD, i.e., IM-β-CD (IC1) and IM-HP-β-CD (IC2).

3.10. Molecular docking studies

Molecular docking studies were implemented to come up with useful insight on the encapsulation mode of guest molecule into the cavity of CD in previous literatures, which may aid the experimental estimations [74–76,82]. In this study, Molecular Operating Environment (MOE) docking method was used to explore the 3-D supramolecular structures of inclusion complexes, IM-β-CD (IC1) and IM-HP-β-CD (IC2). On the basis of the outcome of Job's method, surface tension study and HRMS analysis, a 1:1 stoichiometry of IM and the CDs was selected for molecular docking. The best docked conformation of IC1 (a, side view; b, top view) and IC2 (c, side view; d, top view) are presented in Fig. 8. The previous literature [77] reports the inclusion of the indole ring of 3-substituted indole derivatives through the wider rim of β-CD. There are also literature[78] based on molecular modeling which reports the inclusion of the hydrocarbon chain of 3H-indole derivatives within the β-CD cavity through the wider rim and the enhancement of complex stability or binding ability with the increase in the length of alkyl chain. However, in our present work, the observed ^{1}H NMR and IR spectral shifts suggested the entrance of indole moiety from the benzene ring side of IM into the hydrophobic cavity of β- and HP-β-CD rather than the entrance from polar –CH_2OH side of IM, which is in agreement with our findings from docking. Based on our docking study, the inclusion or binding mode of indole moiety through the wider side of β- and HP-β-CD cavity can be accounted by the fact that the indole ring being more hydrophobic than the small hydrophilic carbinol (–CH_2OH) group, the probable inclusion occurs from the benzene ring side of IM with carbinol group surrounded by hydrophilic secondary –OH group network near the wider rim. Further, molecular docking indicates that the additional H-bonding interaction of pyrrole –NH group with glucoside ether linkage in docked conformation of

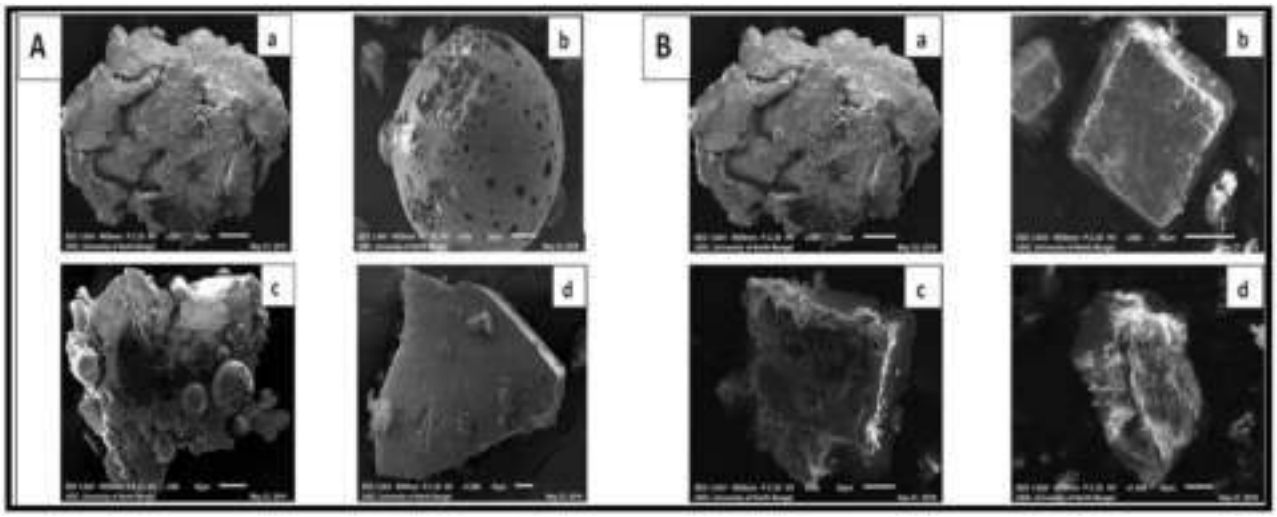

Fig. 7. (A) SEM images of (a) IM, (b) HP-β-CD, (c) physical mixture of IM and HP-β-CD [PM2], (d) IM-HP-β-CD inclusion complex [IC2]; (B) SEM images of (a)IM, (b) β-CD, (c) physical mixture of IM and β-CD [PM1], (d) IM-β-CD inclusion complex [IC1].

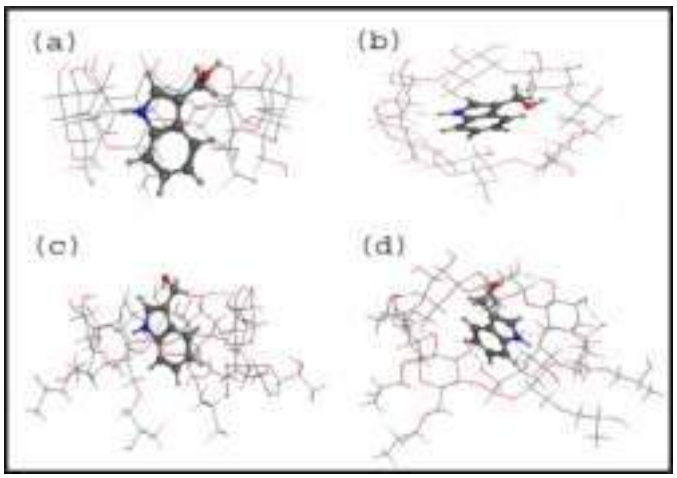

Fig. 8. Binding mode of IM into β-CD [IC1] (a) side view; (b) top view, and IM into HP-β-CD [IC2] (c) side view; (d) top view.

IM-β-CD (IC1) and the similar type of interaction of carbinol –OH group with secondary –OH group in docked conformation of IM-HP-β-CD (IC2) provides more stability with better binding to the ICs (Fig. 8), which is clearly reflected from the binding constant values of IC1 ($\simeq$4.33 $\times$ 10^3 M^{-1}) and IC2 ($\simeq$17.60 $\times$ 10^3 M^{-1}) obtained from UV-visible spectroscopic studies. The binding energy of IC2 (- 19.25 kJ mol^{-1}) was found to be lower than that of IC1 (- 17.15 kJ mol^{-1}) [Table 6], which indicates that the substitution of hydroxypropyl group improved the inclusion capacity of β-CD, as determined by the UV-visible spectroscopic studies. This could be probably attributed to the extension of the size of β-CD cavity on derivatization with hydroxypropyl group, which makes IM penetrate conveniently into the cavity improving complex forming ability [79,80].

Table 6
Binding affinity of IM with β-CD and HP-β-CD derived from molecular docking.

Ligand with receptor	Binding affinity(ΔG^0) in kJ mol^{-1}
IM-β-CD (IC1)	-17.15
IM-HP-β-CD (IC2)	-19.25

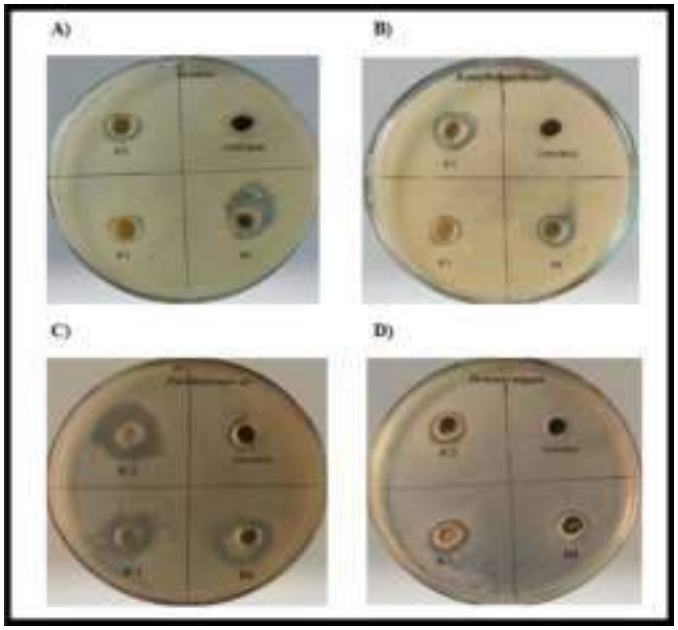

Fig. 9. Antibacterial efficiency of free IM, IM-β-CD (IC1) and IM-HP-β-CD (IC2) against two gram-positive bacteria (A) *B. subtilis* (B) *B. amyloliquefaciens*, and two gram-negative bacteria (C) *Pseudomonas* sp. (D) *Proteus vulgaris*.

3.11. In vitro biological activity study

3.11.1. Antimicrobial activity

About 70% of death cases have been found to be caused by bacterial infections [81]. In the present work, we have analyzed IM and its inclusion complexes IC1 and IC2 for their antimicrobial efficiency against some pathogenic bacteria.

The antibacterial effect has been examined taking four different bacteria, namely, *Proteus vulgaris, Pseudomonas* sp., *Bacillus amyloliquefaciens* and *Bacillus subtilis* by agar well diffusion technique (Figs. 9 and 10). The results listed in Table S11 showed that the IM and its complexes possesses antibacterial effect against gram-

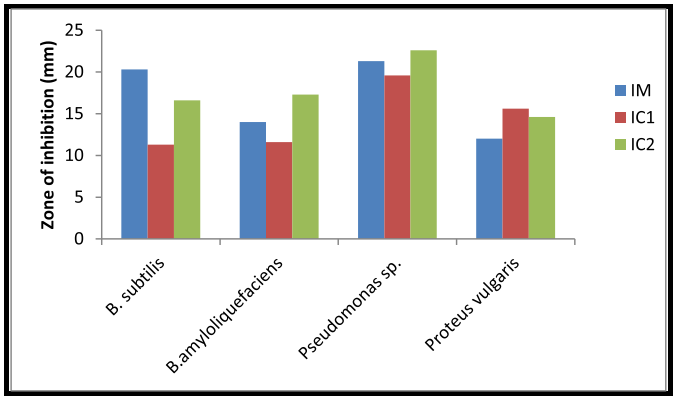

Fig. 10. Zone of inhibition (mm) examined during antibacterial activity analysis of pure IM, IM-β-CD [IC1] and IM-HP-β-CD [IC2] against two gram-positive bacteria: *B. subtilis, B. amyloliquefaciens*, and two gram-negative bacteria: *Pseudomonas* sp., *Proteus vulgaris*.

positive as well as gram-negative pathogenic bacteria. IC2 showed relatively greater inhibitory effect than free IM against *B. amyloliquefaciens, Pseudomonas* sp. and *P. vulgaris*, with 54, 51 and 45% inhibition respectively, whereas IC1 had greater inhibitory effect of 49% than pure IM against *P. vulgaris* only. The IM and its inclusion complexes inhibited the growth of bacterial cultures irrespective of their gram nature. Ultimately this relative study confers that the inclusion complexes displayed fairly better antibacterial efficacy than pure IM, which probably may be due to the ability of CDs to release the IM readily from the ICs or due to the increase of solubility of IM after complexation. However, IC2 provided greater activity than IC1.

Table 7
Values of "Half maximal inhibitory concentration" of pure IM, IM-β-CD [IC1] and IM-HP-β-CD [IC2].

	IM	IC1	IC2
Half maximal inhibitory concentration	107 μM	264 μM	301 μM

3.11.2. *In vitro cytotoxic activity*

The cytotoxicity of pure IM, IM-β-CD (IC1) and IM-HP-β-CD (IC2) complexes has been investigated by exposing normal liver cell line WRL-68 to a series of five sets of free IM, IC1 and IC2 with each set having different concentrations (50, 100, 150, 200, 250 μM), and the cell viability was analyzed by means of an MTT assay. From Fig. 11(a,b), it can be seen that for each of the five sets, IC1 and IC2 complexes showed lower cytotoxicity or lower percentage inhibition than pure IM. The mean concentration of IC1 and IC2 that caused 50% cell inhibition was increased to 264 and 301 μM respectively compared with 107 μM of free IM (Table 7). Interestingly, these results suggested that IC1 and IC2 inhibits the cell growth of tested cells minorly than free IM, showing inclusion complexes of IM to be less cytotoxic than pure IM. This may be probably due to the fact that the sustained release of IM from inclusion complexes makes IM less exposed to the cell, which may result in low endocytic uptake of IM from the inclusion complex compared to the pure IM [82,83].

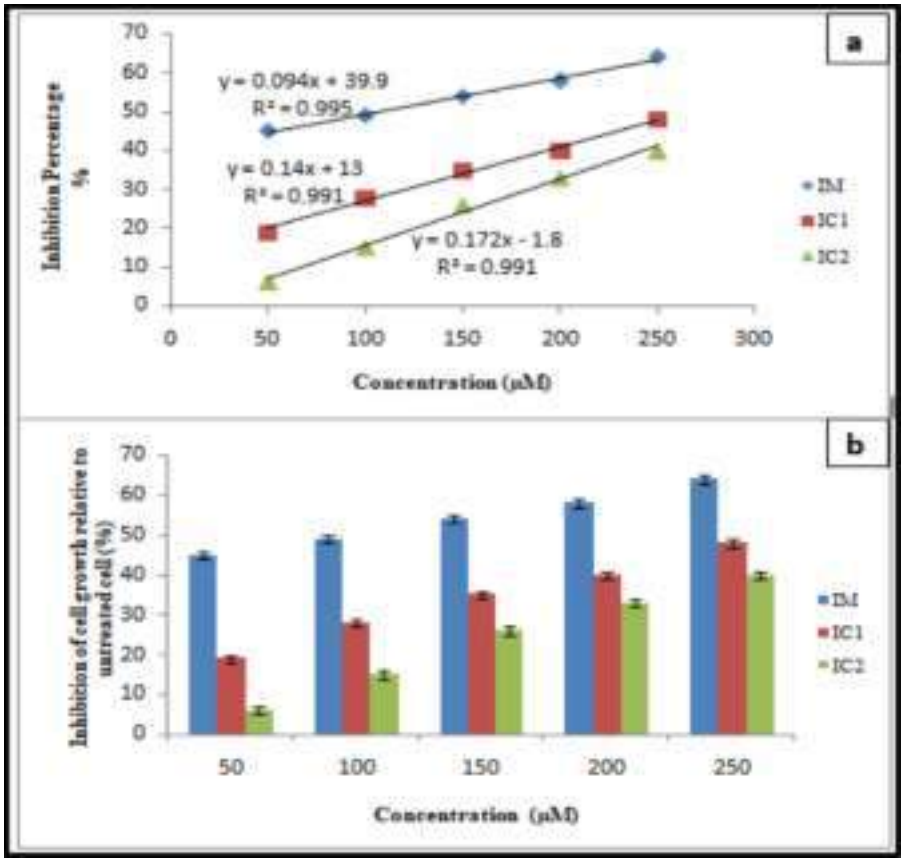

Fig. 11. Cytotoxicity potential of pure IM, IM-β-CD [IC1] and IM-HP-β-CD [IC2] against normal liver cell line WRL-68 at different concentration a) Graph represents the linear regression and b) Percentage inhibition of cell growth. Data represent the mean of three replicates.

4. Conclusions

In this study, we report herein the supramolecular interactions of macrocyclic host (β-CD and HP-β-CD) with important phytochemical compound IM and formation of their ICs, which can be used in near future for an efficient regulatory delivery of IM retaining its bioactivity. The surface tension study and Job's method suggested the formation of mono-molecular encapsulated complex, which was further confirmed by mass spectral analysis. The stability constants and thermodynamic parameters determined from the reliable spectroscopic methods accounts for the stability of ICs formed and the thermodynamic feasibility of inclusion process respectively. The increase in ΔS^0 and a drop in ΔG^0 indicates the inclusion process to be thermodynamically favourable. The greater value of association constant, and hence more stability of IM-HP-β-CD IC compared to IM-β-CD IC is attributed to the larger cavity diameter of HP-β-CD than β-CD. FTIR study and SEM image analysis confirmed the formation of IC from structural and morphological details. ^{1}H NMR spectroscopic analysis provided a deep insight towards the mode of complexation in which aromatic ring of IM was encapsulated from the wider rim side of the cavity of CDs. DSC study revealed that the inclusion into CDs can enhance the thermal stability of IM. The molecular docking simulation revealed the possible interaction of IM with β- and HP-β-CD giving stable 3-D structures of the ICs. The antimicrobial activity of IM was considerably improved after its encapsulation in CDs, however, IM-HP-β-CD IC provided better activity than IM-β-CD IC. Further, both IM-β-CD and IM-HP-β-CD ICs expressed low cytotoxic effect than free IM on the normal liver cell line WRL-68. Therefore, the encapsulation of IM into CDs can be a potential approach to improve stability and biological activity of IM for applications in the pharmaceutical industries and biomedical sciences.

Credit author statement

M N Roy* and P Bomzan put forwarded the concept; P Bomzan, N Roy, A Sharma, V Rai acquired the data; M N Roy, P Bomzan, N Roy, S Ghosh and A Kumar analyzed the data. M N Roy and P Bomzan wrote the first original draft; N Roy, A Sharma and V Rai reviewed and edited the draft.

Declaration of Competing Interest

The authors declare no conflict of interest.

Acknowledgement

The authors are very much grateful to SAP, Department of Chemistry, University of North Bengal under University Grants Commision, New Delhi for financial support to complete this research work. P.B. is also thankful to University Grants Commission, New Delhi for giving fellowship (Ref No. 222/CSIR-UGC NET DEC. 2017). Moreover, the authors express sincere gratitude to the Department of Biotechnology, University of North Bengal for carrying out the biological work. Corresponding author Prof. M.N. Roy is very much grateful to University Grants Commision, New Delhi for awarding One Time Grant of seven lakh under BSR.

Supplementary materials

Supplementary material associated with this article can be found, in the online version, at doi:10.1016/j.molstruc.2020.129093.

References

[1] H. Li, D. Chen, Y. Sun, Y. Zheng, L. Tan, P. Weiss, Y. Yang, Viologen-mediated assembly of and sensing with carboxylatopillar[5]arene-modified gold nanoparticles, J. Am. Chem. Soc. 135 (2013) 1570–1576.
[2] N. Qiu, B. Shen, X. Li, X. Zhang, Z. Sang, T. Yang, L. An, J. Liu, L. Chen, L. Wang, Inclusion complex of magnolol with hydroxypropyl-β-cyclodextrin: characterization, solubility, stability and cell viability, J. Incl. Phenom. Macrocycl. Chem. 85 (2016) 289–301.
[3] W. Saenger, Cyclodextrin inclusion compounds in research and industry, Angew. Chem. Int. Ed. 19 (1980) 344–362.
[4] E.M. Del Valle, Cyclodextrins and their uses: a review, Process Biochem. 39 (9) (2004) 1033–1046.
[5] B.G. Mathapa, V.N. Paunov, Cyclodextrin stabilised emulsions and cyclodextrinosomes, Phys. Chem. Chem. Phys. 15 (2013) 17903–17914.
[6] Y. Kang, K. Guo, B.J. Li, S. Zhang, Nanoassemblies driven by cyclodextrin-based inclusion complexation, Chem. Commun. 50 (2014) 11083–11092.
[7] S. Alberti, G.J.A.A. Soler-Illia, O. Azzaroni, Gated supramolecular chemistry in hybrid mesoporous silica nanoarchitectures: controlled delivery and molecular transport in response to chemical, physical and biological stimuli, Chem. Commun. 51 (2015) 6050–6075.
[8] Y. Liu, Y. Chen, Cooperative binding and multiple recognition by bridged bis(-cyclodextrin)s with functional linkers, Acc. Chem. Res. 39 (2006) 681–691.
[9] W. Misiuk, M. Zalewska, Investigation of inclusion complex of trazodone hydrochloride with hydroxypropyl-β-cyclodextrin, Carbohydr. Polym. 77 (2009) 482–488.
[10] H. Wu, H. Liang, Q. Yuan, T. Wang, X. Yan, Preparation and stability investigation of the inclusion complex of sulforaphane with hydroxypropyl-β-cyclodextrin, Carbohydr. Polym. 82 (2010) 613–617.
[11] E. Pinho, M. Grootveld, G. Soares, M. Henriques, Cyclodextrins as encapsulation agents for plant bioactive compounds, Carbohydr. Polym. 101 (2014) 121–135.
[12] H. Bian, J. Chen, X. Cai, P. Liu, H. Liu, X. Qiao, Inclusion complex of butachlor with β-cyclodextrin: characterization solubility, and speciation dependent adsorption, J. Agric. Food Chem. 57 (2009) 7458–7543.
[13] K. Uekama, F. Hirayama, T. Irie, Cyclodextrin drug carrier systems, Chem. Rev. 98 (1998) 2045–2076.
[14] J. Wang, Z. Cai, Investigation of inclusion complex of miconazole nitrate with β-cyclodextrin, Carbohydr. Polym. 72 (2008) 255–260.
[15] A. Ueno, Review: fluorescent cyclodextrins for molecule sensing, Supramol. Sci. 3 (1996) 31–36.
[16] R. Breslow, S.D. Dong, Biomimetic reactions catalyzed by cyclodextrins and their derivatives, Chem. Rev. 98 (1998) 1997–2012.
[17] J. Szejtli, Introduction and general overview of cyclodextrin chemistry, Chem. Rev. 98 (1998) 1743–1753.
[18] G. Yu, K. Jie, F. Huang, Supramolecular amphiphiles based on host–guest molecular recognition motifs, Chem. Rev. 115 (2015) 7240–7303.
[19] Z. Aytac, Z.I. Yildiz, F. Kayaci-Senirmak, N.O.S. Keskin, S.I. Kusku, T.E. Durgun, T. Tekinay, T. Uyar, Fast-Dissolving, Prolonged release, and antibacterial cyclodextrin/limonene-inclusion complex nanofibrous webs via polymer-free electrospinning, J. Agric. Food Chem. 64 (2016) 7325–7334.
[20] H. Zhou, T. Yamada, N. Kimizuka, Supramolecular thermo-electrochemical cells: enhanced thermoelectric performance by host–guest complexation and salt induced crystallization, J. Am. Chem. Soc. 138 (2016) 10502–10507.
[21] L. Stricker, E.C. Fritz, M. Peterlechner, N.L. Doltsinis, B.J. Ravoo, Arylazopyrazoles as light-responsive molecular switches in cyclodextrin-based supramolecular systems, J. Am. Chem. Soc. 138 (2016) 4547–4554.
[22] M. Xue, W. Wei, Y. Su, D. Johnson, J.R. Heath, Supramolecular probes for assessing glutamine uptake enable semi-quantitative metabolic models in single cells, J. Am. Chem. Soc. 138 (2016) 3085–3093.
[23] P. Díez, A. Sánchez, M. Gamella, P. Martínez-Ruíz, E. Aznar, C. de la Torre, J.R. Murguía, R. Martínez-Máñez, R. Villalonga, J.M. Pingarrón, Toward the design of smart delivery systems controlled by integrated enzyme-based biocomputing ensembles, J. Am. Chem. Soc 136 (2014) 9116–9123.
[24] B.B. Aggarwal, H. Ichikawa, Molecular targets and anticancer potential of indole-3-carbinol and its derivatives, Cell Cycle 4 (9) (2005) 1201–1215.
[25] N. Fujioka, V. Fritz, P. Upadhyaya, Research on cruciferous vegetables, indole-3-carbinol, and cancer prevention: a tribute to Lee W. Wattenberg, Mol. Nutr. Food Res. 60 (6) (2016) 1228–1238.
[26] D.T. Verhoeven, H. Verhagen, R.A. Goldbohm, A review of mechanisms underlying anticarcinogenicity by brassica vegetables, Chem. Biol. Interact. 103 (2) (1997) 79–129.
[27] S.Y. Kim, D.S. Kima, Y.M. Jeong, S.I. Moon, S.B. Kwon, K.C. Park, Indole-3-carbinol and ultraviolet B induce apoptosis of human melanoma cells via down-regulation of MITF, Pharmazie 66 (2011) 982–987.
[28] H.L. Bradlow, Review. Indole-3-carbinol as a chemoprotective agent in breast and prostate cancer, In Vivo (Brooklyn) 22 (4) (2008) 441–445.
[29] R.N. El-Naga, H.I. Ahmed, E.N.A. Al Haleem, Effects of indole-3-carbinol on clonidine-induced neurotoxicity in rats: impact on oxidative stress, inflammation, apoptosis and monoamine levels, Neurotoxicology 44 (2014) 48–57.
[30] J.M. Song, X. Qian, K. Molla, F. Teferi, P. Upadhyaya, G. OSullivan, X. Luo, F. Kassie, Combinations of indole-3-carbinol and silibinin suppress inflammation-driven mouse lung tumorigenesis by modulating critical cell cycle regulators, Carcinogenesis 36 (2015) 666–675.
[31] K.R. Grose, L.F. Bjeldanes, Oligomerization of indole-3-carbinol in aqueous acid, Chem. Res. Toxicol. 5 (1992) 188–193.
[32] F. Vallejo, F.A. Tomas-Barberan, C. Garcia-Viguera, Glucosinolates and vitamin C content in edible parts of broccoli florets after domestic cooking, Eur. Food Res. Technol. 215 (4) (2002) 310–316.
[33] O. Adeoye, J. Conceição, P.A. Serra, A.B.D. Silva, N. Duarte, R.C. Guedes, M.C. Corvod, A.A. Ricardo, L. Jicsinszky, T. Casimiro, H.C. Marques, Cyclodextrin solubilization and complexation of antiretroviral drug lopinavir: in silico

prediction; effects of derivatization, molar ratio and preparation method, Carbohydr. Polym. 227 (2020) 115287.
[34] Q. Geng, T. Li, X. Wang, W. Chu, M. Cai, J. Xie, H. Ni, The mechanism of bensulfuronmethyl complexation with β-cyclodextrin and 2-hydroxypropyl-β-cyclodextrin and effect on soil adsorption and bio-activity, Sci. Rep. 9 (1) (2019) 1–11.
[35] F.A. Wintol, The antibacterial, phytochemicals and antioxidants evaluation of the root extracts of Hydnora africana Thunb. Used as antidysenteric in eastern Cape Province, South Africa, Comp. Alter. Med. 15 (2015) 1–12.
[36] M. Balouiri, M. Sadiki, S.K. Ibnsouda, Methods for in vitro evaluating antimicrobial activity: a review, J.Pharm. Anal. 6 (2016) 71–79.
[37] P. Job, Ann. Chim., Formation and Stability of Inorganic Complexes in Solution, 1928, 9, 113−203.
[38] J.V. Caso, L. Russo, M. Palmieri, G. Malgieri, S. Galdiero, A. Falanga, C. Isernia, R. Iacovino, Investigating the inclusion properties of aromatic amino acids complexing beta-cyclodextrins in model peptides, Amino Acids 47 (2015) 2215–2227.
[39] Y. Gao, X. Zhao, B. Dong, L. Zheng, N. Li, S. Zhang, Inclusion complexes of α-cyclodextrin with ionic liquid surfactants, J. Phys. Chem. B 110 (2006) 8576–8581.
[40] A. Piñeiro, X. Banquy, S. Pérez-Casas, E. Tovar, A. Garcia, A. Villa, A. Amigo, A.E. Mark, M. Costas, On the characterization of host-guest complexes: surface tension, calorimetry, and molecular dynamics of cyclodextrins with a non-ionic surfactant, J. Phys. Chem. B 111 (2007) 4383–4392.
[41] A. Roy, S. Saha, M.N. Roy, Study to explore host-guest inclusion complexes of cyclodextrins with biologically active molecules in aqueous environment, Fluid Phase Equilib. 425 (2016) 252–258.
[42] M.N. Roy, S. Saha, M. Kundu, B.C. Saha, S. Barman, Exploration of inclusion complexes of neurotransmitters with β-cyclodextrin by physicochemical techniques, Chem. Phys. Lett. 656 (2016) 43–50 655W22.
[43] A. Roy, S. Saha, B. Datta, M.N. Roy, Insertion behavior of imidazolium and pyrrolidinium based ionic liquids into α- and β- cyclodextrins: mechanism and factors leading to host-guest inclusion complexes, RSC Adv. 6 (2016) 100016–100027.
[44] M.N. Roy, S. Saha, S. Barman, D. Ekka, Host−guest inclusion complexes of RNA nucleosides inside aqueous cyclodextrins explored by physicochemical and spectroscopic methods, RSC Adv. 6 (2016) 8881–8891.
[45] M.N. Roy, D. Ekka, S. Saha, M.C. Roy, Host−guest inclusion complexes of α- and β-cyclodextrins with α-amino acids, RSC Adv. 4 (2014) 42383–42390.
[46] S. Saha, A. Roy, K. Roy, M.N. Roy, Study to explore the mechanism to form inclusion complexes of β-cyclodextrin with vitamin molecules, Sci. Rep. 6 (2016) 35764.
[47] M.N. Roy, S. Saha, S. Barman, D. Ekka, Host−guest inclusion complexes of RNA nucleosides inside aqueous cyclodextrins explored by physicochemical and spectroscopic methods, RSC Adv. 6 (2016) 8881–8891.
[48] F. Cramer, W. Saenger, H. Spatz, Inclusion Compounds. XIX[1a]. The formation of inclusion compounds of α-cyclodextrin in aqueous solutions. Thermodynamics and kinetics, J. Am. Chem. Soc. 89 (1967) 14–20.
[49] H.A. Benesi, J.H. Hildebrand, A spectrophotometric investigation of the interaction of iodine with aromatic hydrocarbons, J. Am. Chem. Soc. 71 (1949) 2703–2707.
[50] Y. Dotsikas, E. Kontopanou, C. Allagiannis, Y.L. Loukas, Interaction of 6-p-toluidineylnaphthalene-2-sulphonate with β-cyclodextrin, J. Pharm. Biomed. Anal. 23 (2000) 997–1003.
[51] Y. He, X. Shen, Interaction between β-cyclodextrin and ionic liquids in aqueous solutions investigated by a competitive method using a substituted 3H-indole probe, J. Photochem. Photobiol., A 197 (2008) 253–259.
[52] A. Ignaczak, B. Pałecz, S. Belica-Pacha, Quantum chemical study and isothermal titration calorimetry of β-cyclodextrin complexes with mianserin in aqueous solution, Org. Biomol. Chem. 15 (2017) 1209.
[53] S. Prabu, M. Swaminathan, K. Sivakumar, R. Rajamohan, Preparation, characterization and molecular modeling studies of the inclusion complex of caffeine with beta-cyclodextrin, J. Mol. Struct. 1099 (2015) 616–624.
[54] C.N. Sanrame, R.H. de Rossi, G.A. Arguello, Effect of β-cyclodextrin on the excited state properties of 3-substituted indole derivatives, J. Phys. Chem. 100 (1996) 8151–8156.
[55] M. Oana, A. Tintaru, D. Gavriliu, O. Maior, M. Hillebrand, Spectral study and molecular modeling of the inclusion complexes of β-cyclodextrin with some phenoxathiin derivatives, J. Phys. Chem. B 106 (2002) 257–263.
[56] Q.F. Zhang, Z.T. Jiang, Y.X. Guo, R. Li, Complexation study of brilliant cresyl blue with β-cyclodextrin and its derivatives by UV–vis and fluorospectrometry, Spectrochimica Acta Part A 69 (2008) 65–70.
[57] M. Zhang, J. Li, W. Jia, J. Chao, L. Zhang, Theoretical and experimental study of the inclusion complexes of ferulic acid with cyclodextrins, Supramol. Chem. 21 (2009) 597–602.
[58] W. Li, X. Liu, Q. Yang, N. Zhang, Y. Du, H. Zhu, Preparation andcharacterization of inclusion complex of benzyl isothiocyanate extracted frompapaya seed with β-cyclodextrin, Food Chem. 184 (2015) 99–104.
[59] K. Srinivasan, K. Sivakumar, T. Stalin, 2, 6-Dinitroaniline and beta-cyclodextrin inclusion complex properties studied by different analytical methods, Carbohydr. Polym. 113 (2014) 577–587.
[60] V. Sindelar, M.A. Cejas, F.M. Raymo, W. Chen, S.E. Parker, A.E. Kaifer, Supramolecular assembly of 2, 7-dimethyldiazapyrenium and cucurbit[8]uril: a new fluorescent host for detection of catechol and dopamine, Chem. Eur. J. 11 (2005) 7054–7059.
[61] K.H. Kim, Y.H. Park, Enantioselective inclusion between terbutaline enantiomers and hydroxypropyl-β-cyclodextrin, Int. J. Pharm. 175 (1998) 247.
[62] L. Ribeiro, R.A. Carvalho, D.C. Ferreira, F.J. Veiga, Multicomponent complex formation between vinpocetine, cyclodextrins, tartaric acid and water-soluble polymers monitored by NMR and solubility studies, Eur. J. Pharm. Sci. 24 (1) (2005) 1–13.
[63] L.J. Yang, S.X. Ma, S.Y. Zhou, W. Chen, M.W. Yuan, Y.Q. Yin, X.D. Yang, Preparation and characterization of inclusion complexes of naringenin with β-cyclodextrin or its derivative, Carbohydr. Polym. 98 (2013) 861–869.
[64] F.J.B. Veiga, C.M. Fernandes, R.A. Carvalho, C.F.G.C. Geraldes, Molecular modelling and H-NMR: ultimate tools for the investigation of tolbutamide: β-cyclodextrin and tolbutamide: hydroxypropyl-β-cyclodextrin complexes, Chem. Pharm. Bull. 49 (2001) 1251–1256.
[65] A. Fernandes, G. Ivanova, N.F. Bras, N. Mateus, M.J. Ramos, M. Rangel, V. de Freitas, Structural characterization of inclusion complexes between cyanidin-3-O-glucoside and β-cyclodextrin, Carbohydr. Polym. 102 (2014) 269–277.
[66] B. Yang, J. Lin, Y. Chen, Y. Liu, Artemether/hydroxypropyl-b-cyclodextrin host–guest system: characterization, phase-solubility and inclusion mode, Bioorg. Med. Chem. 17 (2009) 6311–6317.
[67] C.F. Xiao, K. Li, R. Huang, G.J. He, J.Q. Zhang, L. Zhu, Q.Y. Yang, K.M. Jiang, Y. Jin, J. Lin, Investigation of inclusion complex of epothilone A with cyclodextrins, Carbohydr. Polym. 102 (2014) 297–305.
[68] T. Wang, M.D. Wang, C. Ding, J. Fu, Mono-benzimidazole functionalized β-cyclodextrins as supramolecular nanovalves for pH triggered release of p–coumaric acid, Chem. Commun. 50 (2014) 12469–12472.
[69] Y. Okada, K. Ueyama, J.I. Nishikawa, M. Semma, A. Ichikawa, Effect of 6-O-α-maltosyl-β cyclodextrin and its cholesterol inclusion complex on cellular cholesterol levels and ABCA1 and ABCG1 expression in mouse mastocytoma P-815 cells, Carbohydr. Res. 357 (2012) 68–74.
[70] J.Q. Zhang, K.M. Jiang, K. An, S.H. Ren, X.G. Xie, Y. Jin, J. Lin, Novel water-soluble fisetin/cyclodextrins inclusion complexes: preparation, characterization, molecular docking and bioavailability, Carbohydr. Res. 418 (2015) 20–28.
[71] W. Zhang, X. Gong, Y. Cai, C. Zhang, X. Yu, J. Fan, G. Diao, Investigation of water-soluble inclusion complex of hypericin with β-cyclodextrin polymer, Carbohydr. Polym. 95 (2013) 366–370.
[72] J. Wang, Y. Cao, B. Sun, C. Wang, Characterisation of inclusion complex of trans-ferulic acid and hydroxypropyl-β-cyclodextrin, Food Chem. 124 (2011) 1069–1075.
[73] R. Ghosh, D. Ekka, B. Rajbanshi, A. Yasmin, M.N. Roy, Synthesis, characterization of 1-butyl-4-methylpyridinium lauryl sulfate and its inclusion phenomenon with β-cyclodextrin for enhanced applications, Colloids Surf. 548 (2018) 206–217.
[74] S. Basak, S. Mondal, S. Dey, P. Bhattacharya, A. Saha, V. Deep Punetha, A. Abbas, N. Gopal Sahoo, Fabrication of β-cyclodextrin-mediated single bimolecular inclusion complex: characterization, molecular docking, in-vitro release and bioavailability studies for gefitinib and simvastatin conjugate, J. Pharm. Pharmacol. 69 (2017) 1304–1317.
[75] N. Issaraseriruk, A. Shitangkoon, T. Aree, Molecular docking study for the prediction of enantiodifferentiation of chiral styrene oxides by octakis (2,3-di-O-acetyl-6-O-tert -butyldimethylsilyl)-γ-cyclodextrin, J. Mol. Graphics Modell. 28 (2010) 506–512.
[76] P. Sompornpisut, N. Deechalao, J. Vongsvivut, An inclusion complex of β-Cyclodextrin-L-Phenylalanine: 1H NMR and molecular docking studies, Sci. Asia. 28 (2002) 263–270.
[77] C.N. Sanrame, R.H. Rossi, G.A. Arguello, Effect of β-cyclodextrin on the excited state properties of 3-substituted indole derivatives, J. Phys. Chem. 100 (1996) 8151–8156.
[78] K.A. Al-Sou'od, M.B. Zughul, A.A. Badwan, Experimental and molecular mechanical studies of complexation of some 2h- and 3h- indole derivatives with aqueous β;-cyclodextrin, J. Solut. Chem. 35 (2006) 1377–1388.
[79] F.M. Mady, U.F. Aly, Experimental, molecular docking investigations and bioavailability study on the inclusion complexes of finasteride and cyclodextrins, Drug Des. Dev. Ther. 11 (2017) 1681.
[80] C.L. Zhang, J.C. Liu, W.B. Yang, D.L. Chen, Z.G. Jiao, Experimental and molecular docking investigations on the inclusion mechanism of the complex of phloridzin and hydroxypropyl-β-cyclodextrin, Food Chem. 215 (2017) 124–128.
[81] T.R. Walsh, M.A. Toleman, L. Poirel, P. Nordmann, Metallo-β-lactamase: the quiet before the storm, Clin. Microbiol. Rev. 18 (2005) 306–325.
[82] M.A.A. Maki, P.V. Kumar, S.C. Cheah, Y.S. Wei, M.A. Nema, O. Bayazeid, A.B.B.A. Majeed, A molecular modeling-based delivery system enhances everolimus-induced apoptosis in Caco-2 cells, ACS Omega 4 (2019) 8767–8777.
[83] L. Rena, J. Wang, G. Chen, Preparation, optimization of the inclusion complex of glaucocalyxin A with sulfobutylether-β-cyclodextrin and antitumor study, Drug Deliv. 26 (1) (2019) 309–317.

Food Chemistry Advances 1 (2022) 100015

Contents lists available at ScienceDirect

Food Chemistry Advances

journal homepage: www.elsevier.com/locate/focha

Inclusion of an antiplatelet agent inside into β-cyclodextrin for biochemical applications with diverse authentications

Pranish Bomzan[a], Niloy Roy[a], Vijeta Rai[b], Debadrita Roy[a], Shilpi Ghosh[b], Anoop Kumar[b], Kanak Roy[c], Rinku Chakrabarty[c], Jyotsna Das[d], Vikas Kumar Dakua[c], Kumar Basnet[e], Mahendra Nath Roy[a,c,*]

[a] Department of Chemistry, University of North Bengal, Raja Rammohanpur, Darjeeling, West Bengal 734013, India
[b] Department of Biotechnology, University of North Bengal, Darjeeling 734013, India
[c] Department of Chemistry, Alipurduar University, Alipurduar 736122, India
[d] Department of Botany, Alipurduar University, Alipurduar 736122, India
[e] Department of Zoology, Alipurduar University, Alipurduar 736122, India

ARTICLE INFO

Keywords:
Ticlopidine hydrochloride
β-cyclodextrin
Thermogravimetric analysis
Molecular docking
Antibacterial activity
Cytotoxicity

ABSTRACT

We aim to develop the complex of ticlopidine hydrochloride (TCP) with β-cyclodextrin (β-CD) and to investigate its antibacterial and cytotoxic activities. The complex was characterized by various physicochemical as well as spectroscopic techniques suggesting the successful inclusion of TCP molecule into the β-CD cavity. TG analysis showed that the thermal stability of TCP was found to improve after complexation. Molecular docking study speculated the most preferred orientation of TCP molecule within the binding pocket of β-CD cavity. *In vitro* antibacterial activity test demonstrated that the TCP-β-CD complex displayed better activity than pure TCP. TCP-β-CD complex (IC_{50} = 24 μM) also exhibited significant *in vitro* cytotoxic activity than pure TCP (IC_{50} = 44 μM) towards human kidney cancer cell line (ACHN). Furthermore, the complex induces the ROS generation in ACHN cells more pronouncedly than TCP alone, suggesting the increased apoptotic activity of TCP after complexation. These results reveals that inclusion of TCP using β-CD could lead to stabilization of TCP and efficient display of its antibacterial and cytotoxic activities.

1. Introduction

Thienopyridine compounds act as antiplatelet agents which inhibit the formation of thrombus without markedly affecting other coagulation segments. They promote inhibition of platelet secretion reaction, inhibit platelet functions such as aggregation, adhesion, and lower circulating platelet aggregates, in addition to clotting of blood in coronary artery disease, peripheral vascular disease and cerebrovascular disease (Ferri et al., 2013; Rao et al., 2013; Wu et al., 2012). Beside their anti-aggregating effects, thienopyridines has other pharmacological effects which include lowering circulating fibrinogen (Mazoyer et al., 1994) as well as erythrocyte filterability (Hayakawa et al., 1991), and stimulation of NO production (De Lorgeril et al., 1998). Even though the actual mechanism is not understood till date, thienopyridine derivatives have demonstrated pro-apoptotic effect towards cancer cells (Calvisi et al., 2013) as well as anti-proliferative and anti-cancer activity against hepatocellular carcinoma (Zeng et al., 2010).

Ticlopidine Hydrochloride (TCP) is one of the FDA approved drugs belonging to the family of thienopyridines which has its wide applications as antiplatelet agent. It exhibits its therapeutic effect by blocking ADP receptors irreversibly on the surface of platelets. Studies suggest that the TCP prevents clot formation and platelet aggregation inside blood vessels inhibiting development of thrombus by interacting with the $P2Y_{12}$ receptor ADP at the site of the vascular lesion through bioactivation by cytochrome P450 (CYP) (Gachet et al., 1990; Saltiel et al., 1987). Beside antiplatelet property, TCP is also reported to have antibacterial (Veloso et al., 2015) and anticancer (Wojtukiewicz et al., 2017) activities. However, TCP is sensitive to external conditions such as light, alkaline and acidic environment, temperature changes and oxidation (Ram et al., 2011), which considerably demarcate its utility in terms of its anticancer and antibacterial activities. To overcome these problems one approach is encapsulation with β-cyclodextrin (β-CD). From the point of the solubilization, stabilization and delivery of the bioactive compounds, encapsulation technology is extensively used by

Abbreviations: TCP, Ticlopidine hydrochloride; β-CD, β-cyclodextrin; FDA, Food and Drug Administration; ACHN, Kidney cancer cell line; ROS, Reactive oxygen species.

* Corresponding author at: Department of Chemistry, University of North Bengal, Raja Rammohanpur, Darjeeling, West Bengal 734013, India.
E-mail address: mahendraroy2002@yahoo.co.in (M.N. Roy).

https://doi.org/10.1016/j.focha.2022.100015
Received 30 October 2021; Received in revised form 12 January 2022; Accepted 13 January 2022

pharmaceutical and food industries (Ozdemira et al., 2018). According to the previous literature, inclusion complex of β-CD improved *in vitro* antimicrobial activity of *Euterpe oleracea* Mart-oil (Magalhães et al., 2020) and *in vivo* anti-cancer activity of curcumin (Zhang et al., 2016). Similarly, encapsulated lycorine (Liu et al., 2017) was observed to have better *in vitro* cytotoxic activities. It should also be noted that β-CD was included into GRAS (generally recognized as safe) protectants and carriers by US Food and Drug Administration (USFDA, 2001). β-CD is a member of cyclic oligosaccharides containing seven glucopyranose units linked via α-1,4-linkages (Gong et al., 2016). Along with physical and chemical stability, β-CD is characterized with a relatively hydrophilic outer surface and hydrophobic central cavity. This cyclic carbohydrate, having specific cavity size (6.0–6.5 Å diameter) as well as low cost, becomes ideal for inclusion of guest molecules with molecular weights ranging from 200 to 800 g/mol (Li et al., 2018). After incorporation of bioactive compounds into β-CD cavity, outer microsphere of inclusion complex keeps guest molecules protected from oxygen and light (Gong et al., 2016). To the best of our knowledge, investigation on encapsulation of TCP with β-CD and its specific antibacterial and cytotoxic activities, has not been yet studied.

Therefore, in this research, we have prepared the inclusion complex of TCP and β-CD. The physicochemical properties of prepared TCP-β-CD complex were characterized by UV-Visible spectroscopy, surface tension study, PXRD, FTIR spectroscopy, ^{1}H NMR, TGA analysis, SEM study and mass spectroscopy. Molecular docking was performed as well to recognize the best orientation of included TCP into the cavity of β-CD. Finally, the antibacterial and cytotoxic activities of the complex were studied and compared with that of pure TCP.

2. Experimental section

2.1. Materials

Ticlopidine Hydrochloride (purity > 98%) and β-Cyclodextrin (purity 98%) were purchased from TCI Chemicals (India) and Sigma-Aldrich (India), respectively. Human kidney cancer cell lines (ACHN) were obtained from National center for Cell Science, Pune, India. Media component used for animal cell were purchased from Hi-media Laboratory Pvt. Ltd. MTT was purchased from Hi-media, India and DCDF dye was obtained from Sigma India Pvt. Ltd. All chemicals and media components used were of analytical grade from Sigma India Pvt. Ltd; Himedia, India; Sisco Research Laboratories, India, TCI Chemicals, India, and E. Merck, Germany.

2.2. Instruments

All the UV-visible absorption spectra were assembled at 298.15 K using the Agilent 8453 spectrophotometer, with an uncertainty of wavelength resolution of ±0.5 nm. An automated digital thermostat was used to keep the measuring temperature constant.

The surface tension was measured using a digital K9 Tensiometer (Kruss, Germany) at 298.15 K by platinum ring detachment method with measurement accuracy within ±0.1 mN m^{-1}. Temperature was maintained by auto-thermostat.

500 μL of each sample were taken into Bruker NMR tubes. Then, ^{1}HNMR spectra were acquired in D_2O at 298.15 K using Bruker Avance 300 MHz NMR spectrometer. The chemical shift values, δ, are presented in ppm. The peak of HDO at 4.70 ppm was taken as an internal standard reference.

The FT-IR spectra were recorded by KBr disk technique using Perkin-Elmer spectrometer with a 2 cm^{-1} spectral resolution at room temperature and 45% humidity. The disks were prepared by taking sample and KBr in the ratio of 1:100. The spectra were collected in the wavenumber region of 4000−400 cm^{-1}.

ESI-MS spectra were acquired on a high-resolution Q-TOF mass spectrometer with a positive-mode electrospray ionization taking the methanol solution of the solid inclusion complexes.

The samples were subject to Thermogravimetric analysis (TGA) using TA Instrument Q-50 TGA in the temperature range of 30–600 °C with the heating rate of 10° per minute.

Powder XRD data were collected on a Bruker SMART APEX diffractometer using graphite-monochromated MoK_α (λ=0.71073 Å) radiation equipped with CCD area detector at 273 K with scan rate 1^0/min and step size 0.042.

The surface morphological structure of the samples was analyzed using a JSM-6360 Scanning Electron Microscope (SEM).

2.3. Preparation of inclusion complex

Inclusion complex of TCP with β-CD (i.e., TCP-β-CD IC) was prepared by mixing TCP and β-CD in a molar ratio 1:1. Initially, TCP (30 mg, 4.0 mmol) and β-CD (113.5 mg, 4 mmol) were dissolved separately in 25 mL distilled water. These two solutions were then mixed in a beaker and kept for 30 min under moderate stirring at room temperature. Then the mixed solution was heated upto 50 ^{0}C under continuous stirring of 450 r/min for 30 hrs till the appearance of a precipitate. The obtained precipitate was filtered and stored in an oven at 60 ^{0}C for 9 h to draw out solvent. The final solid white powder of inclusion complex was collected and kept in a dessicator for further analysis.

2.4. Job's method for stoichiometric determination of inclusion complex

Job plot was obtained by a very reliable Job's method (also known as the continuous variation method) using UV-Visible spectroscopy to determine the complexation stoichiometry of inclusion complex formed (Rajbanshi et al., 2018). To perform the experiment, stock solutions with equimolar concentrations of β-CD and TCP were prepared. From these two stock solutions a series of sample solutions were prepared in such a way that the overall molar concentration, [TCP]+[β-CD], was kept fixed while the mole fraction of TCP altered within the range of 0–1 (Table S1). The values of absorption maximum were recorded at λ_{max} = 214 nm for a set of solutions at 298.15 K.

2.5. Surface tension measurement

Ten milliliters of 10 mM TCP solution was taken in a 100 ml beaker and surface tension was measured. Then 1 ml of β-CD was added to the TCP solution for 20 times. During each addition of β-CD, surface tension reading was collected (Rajbanshi et al., 2018).

2.6. Absorption spectral titrations

The inclusion complex formation phenomenon of β-CD with guest TCP in aqueous solution was examined by means of UV–visible spectral titration (Rajbanshi et al., 2018). During titration, one milliliter 140 μM solution of TCP was taken in a cuvette and then a series of 1.0 ml β-CD solution was added to it, so that the concentrations of β-CD ranged from 1.0 to 5.0 mM and that of TCP becomes 70 μM.

2.7. Molecular docking study

Molecular docking was conducted to predict the most probable binding mode and binding free energy (ΔG) of TCP with β-CD using automated docking program, AutoDock 4.2 (Alshehri et al., 2020). The 3D structure of TCP was downloaded as SDF file from the PubChem and converted into a PDB (protein data bank) file using OpenBabel 2.4.1 software. From the RCSB Protein Data Bank, the PDB file 3CGT was downloaded and the 3D structure of β-CD was extracted from the PDB file. The optimization of the molecular structures of TCP and β-CD was performed using Gaussian 09 software with the 6-311++G (d, p) basis

set and B3LYP method. Before carrying out docking, the ligand (TCP) and receptor (β-CD) coordinate files were converted into PDBQT format using MGL Tools (version 1.5.6). In our docking study, β-CD was set as a rigid receptor, and TCP molecule as the flexible ligand. To seek for favorable binding mode of TCP with β-CD, a 3D docking grid box of dimension 41 Å × 41 Å × 41 Å with grid spacing 0.375 Å was constructed. Autogrid4 parameter was employed to achieve a rigid grid box. Further to acquire best docking conformations, autodock4 with Lamarckian genetic algorithm using default values was applied. On the basis of docking score, the most favorable docked conformer with lowest binding energy was selected.

2.8. In vitro *antibacterial activity assay*

The antibacterial activity of TCP and TCP-β-CD complex was studied using the agar well diffusion method (Rai et al., 2019). The bacterial cultures (*Shigella sp., Salmonella* sp., *Bacillus amyloliquefeciens* and *Bacillus subtilis*) were grown overnight in nutrient broth at 37 ^{0}C, which were further swabbed over the surface of an agar plate. Three wells were prepared in each agar plates with the help of sterile cork-borer, and 40 μL 6 mM solutions of β-CD, TCP and TCP-β-CD complex were introduced into their respective wells. These solutions inside the well were allowed to diffuse for an hour. Then the plates were incubated at 37 ^{0}C for 24 h. Following incubation, plates were observed for evaluating zone of inhibition.

2.9. *Cell line culture*

For this purpose, human kidney cancer (ACHN) cell line was obtained from Cell Repository, National center for Cell Sciences (NCCS), Pune, India. ACHN was cultured in Dulbecco's modified eagle medium (DMEM), supplemented with 5% FBS, 100 IU ml^{-1} Penicillin and 100 μgml^{-1} Streptomycin, in 100 mm petri dishes and incubated in 5% CO_2 incubator at 37 °C.

2.10. In vitro *cell viability assay*

Anticancer screening of TCP and TCP-β-CD complex was carried out against human kidney cancer cell line (ACHN) by MTT [(3-(4,5-dimethylthiazol-2-yl)-2,5-diphenyltetrazolium bromide] reduction assay (Rai et al., 2019). For a typical *in vitro* anticancer screening experiment, each well of 96-well microtiter plates were inoculated with 100 µl volume of cells at a concentration of 1 × 10^5 cells ml^{-1}. After cell inoculation, the microtiter plates were incubated at 37 ^{0}C for 24 h in 5% CO_2, 95% air and 100% relative humidity. Following incubation, the cells were treated with different concentrations of TCP and its complex. After 24 h of treatment, 10 μl of MTT (5 mg ml^{-1}) was added to each well and incubated further for 4 h. The MTT solution was replaced by 50 μl of isopropanol which was used to dissolve the insoluble formazan product. The extent of formazan product produced due to the reduction of MTT into formazan within the cells was calculated by measuring the absorbance at 540 nm using spectrostarnano plate reader (BMG Labtech). All experiments were repeated at least three times in triplicates. The relative percentage of cell viability was evaluated by using the formula:

$$\text{Percent inhibition}(\%) = \frac{Y - X}{Y} \times 100$$

Where, Y is the mean absorbance of control and X is the mean absorbance of cells treated with TCP and its complex. The stock solutions of TCP and complex were prepared using distilled water and the same solvent was kept as control.

2.11. *Determination of ROS (reactive oxygen species) generation*

Intracellular ROS generation can be detected using 2,7-dichlorodihydrofluorescein diacetate (DCF-DA) as a fluorescent probe (Rai et al., 2019). DCF-DA undergoes oxidation in presence of free oxygen radicals inside the cell to fluorescent 2,7-dichlrofluorescein (DCF), which can be visualized under fluorescent microscope. Kidney cancer cell line (ACHN) were grown over the cover slip and incubated in CO_2 incubator for 24 h. Further these cells were treated with TCP and TCP-β-CD complex at their IC_{50} values. 1.5 mM H_2O_2 treated cells were considered as positive control whereas the untreated cells were set as a control. Following a 24 h incubation period, the cells were washed thrice with PBS and fresh serum medium containing DCF-DA dye was added to it. It was then subjected to an incubation period of 30 min in a CO_2 incubator. After incubation, the extra dye was washed by using PBS and coverslip was flipped upside down on slide having 2,3 drops of glycerin on it. Then the cells were observed under florescence phase contrast microscope with excitation wavelength at 480 nm and emission was photographed by using Olympus digital camera.

2.12. *Statistical analysis*

All the results were processed in Origin Pro 8.5 and SPSS and all the experimental results are mean ± SD of three parallel measurements. The data were analyzed by analysis of variance ($P < 0.05$). The graph and tables have been represented with standard deviation and perform statistical analysis.

3. Results and discussion

3.1. *Determination of stoichiometric ratio of the inclusion complex by Job's method*

In order to obtain the Job plot, ΔA x R versus R was plotted (where ΔA is the changes in the absorbance of TCP without and with the presence of β-CD, and R = [TCP]/([TCP] + [β-CD])). The maximal peak value of R on the plot provides the complexation stoichiometry. From Fig. 1(a), the observed maximum value of ΔA x R at $R = 0.5$ confirms the complexation stoichiometry of 1:1 for the inclusion complex of TCP and β-CD.

3.2. *Surface tension studies*

Surface tension (γ) evaluation provides noteworthy evidence with regard to the formation and stoichiometry of the inclusion complex (Rajbanshi et al., 2018). No any significant change in γ was observed when β-CD was dissolved in aqueous medium in an appreciable range of concentration. However, TCP solution was found to possess low γ value compared to that of pure aqueous solvent indicating that TCP is surface active molecule consisting of a hydrophobic portion and also a charged end. In this study, the γ of TCP solution was determined at 298.15 K with increasing β-CD concentration (Table S2 and Fig. 1(b)). A regular increasing trend of γ was observed with increase in the concentration of β-CD, which may be possibly due to the encapsulation of TCP molecules from the solution surface into the hydrophobic nano cavity of β-CD forming inclusion complex. A noticeable break point was found to appear in the plot indicating not only the formation of inclusion complex but also defines 1:1 stoichiometric ratio of the formed complex (Fig. 1(b)). The γ value and the corresponding TCP and β-CD concentrations at the break point (point of intersection) of the surface tension curve are listed in Table S3. The ratio of the concentrations of TCP and β-CD at the break point was found to be nearly 1:1 suggesting the emergence of 1:1 inclusion complex between TCP and β-CD.

3.3. *Absorption spectral analysis*

The affinity for binding of TCP with β-CD was determined by evaluating binding constant (K_a) using UV spectral studies (Rajbanshi et al., 2018). The encapsulation of TCP molecules into the apolar β-CD cavity results in the gradual increase of TCP absorbance. The occurrence

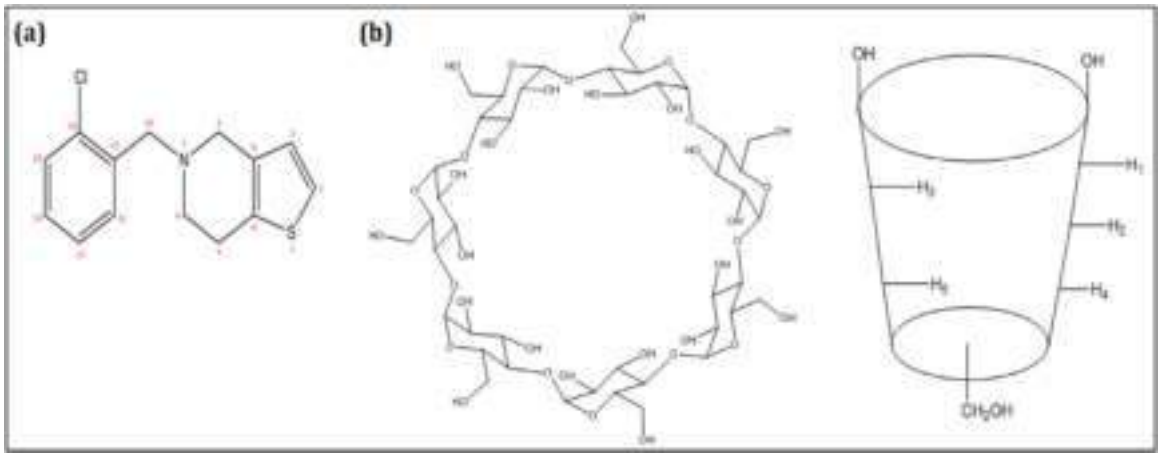

Scheme 1. Molecular structures of (a) TCP and (b) β-CD.

of such hyperchromic shift is attributed to the decrease in polarity of the environment of β-CD cavity encountered by the TCP molecules during formation of inclusion complex (Cramer et al., 1967). The binding constant (K_a) of TCP-β-CD complex at 298.15 K was evaluated from the changes in the absorption intensity (ΔA) of TCP (at λ_{max} = 214 nm) with the increasing β-CD concentration by means of Benesi-Hildebrand equation (Table S4). According to the Benesi-Hildebrand method, a double reciprocal plot is drawn for 1:1 complexation utilizing the following Benesi-Hildebrand equation

$$\frac{1}{\Delta A} = \frac{1}{\Delta\varepsilon[TCP]K_a}\frac{1}{[\beta - CD]} + \frac{1}{\Delta\varepsilon[TCP]} \quad (1)$$

where $\Delta\varepsilon$ is the difference in molar absorption coefficient of TCP in the presence and absence of β-CD. The plot of $1/\Delta A$ against $1/[\beta\text{-CD}]$ (Fig. S1) presents a good linear correlation (R^2 =0.99554) indicating 1:1 stoichiometry of the TCP-β-CD complex. The value of binding constant (K_a) for 1:1 TCP-β-CD complex, obtained from the intercept/slope of Benesi-Hildebrand plot using Eq. (1) [21] was found to be 25.16×10^3 M^{-1}.

For the encapsulation process between β-CD and TCP, the Gibb's free energy of binding (ΔG) can be deduced from the value of binding constant K_a at 298.15 K using Eq. (2).

$$\Delta G = -RTlnK_a \quad (2)$$

The value of ΔG was found to be -6.0 kcal/mol, which indicates that the encapsulation process is spontaneous.

3.4. ^1H NMR analysis

^1H NMR study is performed for investigating the detailed information on the inclusion mechanism of guest molecule with the CDs (Alshaer et al., 2019). The complexation of a guest molecule with the CD usually results in the upfield chemical shifts of both the guest and CD protons owing to the enclosure of guest molecule by the electron clouds of CD and the anisotropic ring-current effects of the encapsulated guest molecule, respectively (Alshaer et al., 2019). In CD, H-5′ and H-3′ hydrogen atoms are positioned within the cavity in the vicinity of the narrower rim and wider rim, respectively, whereas the other H-4′, H-2′, H-1′ hydrogen atoms are located on the outside of the surface (Scheme 1). In our present work, we have explored the encapsulation of TCP with β-CD using ^1H NMR spectroscopy. The NMR spectra of TCP, β-CD and TCP-β-CD inclusion complex were shown in Fig. S2 with their corresponding chemical shift (δ) values enlisted in Table S5. After the formation of complex, H-4′, H-2′ and H-1′ protons of β-CD were observed to possess negligible changes in their chemical shift values with $\Delta\delta$ –0.01, –0.01 and –0.02, respectively. However, H-5′ ($\Delta\delta$ = –0.09) and H-3′ ($\Delta\delta$ = –0.12) protons exhibited relatively considerable chemical shift changes, indicating the inclusion of TCP into the cavity of β-CD (Fig. S2). Since H-3′ proton was found to undergo significant upfield shift than H-5′ proton (Table S5), therefore, it can be suggested that the encapsulation of TCP occurs through the wider rim of β-CD cavity.

Further, when we compared the ^1H NMR spectrum of free TCP with TCP-β-CD complex, appreciable variation in the chemical shift values was monitored for most of the TCP protons in TCP-β-CD inclusion complex. It was observed that chlorophenyl ring, piperidine ring and methylene protons such as H-12, H-13/H-14, H-15, H-4 and H-10 were greatly upfield shifted with $\Delta\delta$ –0.04, –0.03, –0.05, –0.04 and –0.04, respectively (Fig. S2 and Table S5). In contrast, H-2 ($\Delta\delta$ = –0.00) and H-3 ($\Delta\delta$ = –0.01) protons of thiophene ring along with H-7 proton ($\Delta\delta$ = –0.02) of piperidine ring showed relatively negligible or no changes in their chemical shift values, suggesting that the thiophene ring along with C-7 carbon of piperidine ring resides outside the wider rim of β-CD with the preferential occupancy of hydrophobic cavity by the chlorophenyl ring, piperidine ring and methylene group of TCP (Fig. S2 and Table S5).

3.5. ESI-MS studies

The stoichiometry of solid TCP-β-CD inclusion complex was figured out using electronspray ionization mass spectroscopy (ESI-MS) (Benkovics et al., 2017). The peaks at m/z values 1399.72 and 1421.69 were observed corresponding to the molecular ions $[TCP+\beta\text{-CD+H}]^+$ and $[TCP+\beta\text{-CD+ Na}]^+$, respectively (Fig. S3). This clearly indicates the formation of TCP-β-CD inclusion complex with 1:1 stoichiometric ratio, which is in conformity with the results obtained from surface tension study and Job's method.

3.6. Powder XRD analysis

The XRD analysis results further provides strong evidence for ensuring the inclusion complex formation (Rani et al., 2020). The XRD patterns of β-CD, TCP and TCP-β-CD complex were shown in Fig. 2(a). β-CD showed a crystalline diffractogram with sharp peaks at 4.64^0, 9.11^0, 12.47^0, 19.52^0, 21.25^0, 22.82^0, 24.30^0, 25.64^0, 27.04^0, 31.12^0, 32.06^0, 34.80^0 and 35.90^0. The TCP also exhibited a distinctive sharp peaks at 14.50^0, 16.4^0, 17.96^0, 19.29^0, 20.15^0, 22.97^0, 25.32^0, 26.03^0, 26.89^0, 27.52^0, 32.29^0 and 34.48^0, indicating the existence of TCP in a crystalline state. However, the XRD spectrum of TCP-β-CD complex displayed a broad diffraction profile with reduced number as well as intensity of peaks and showed no reflections due to either TCP or β-CD. This suggested that the moiety responsible for the crystalline nature of TCP got encapsulated into the cavity of β-CD which results in the change in environment of TCP and β-CD. This observation indicates the formation of solid inclusion complex. The appearance of new diffraction peaks

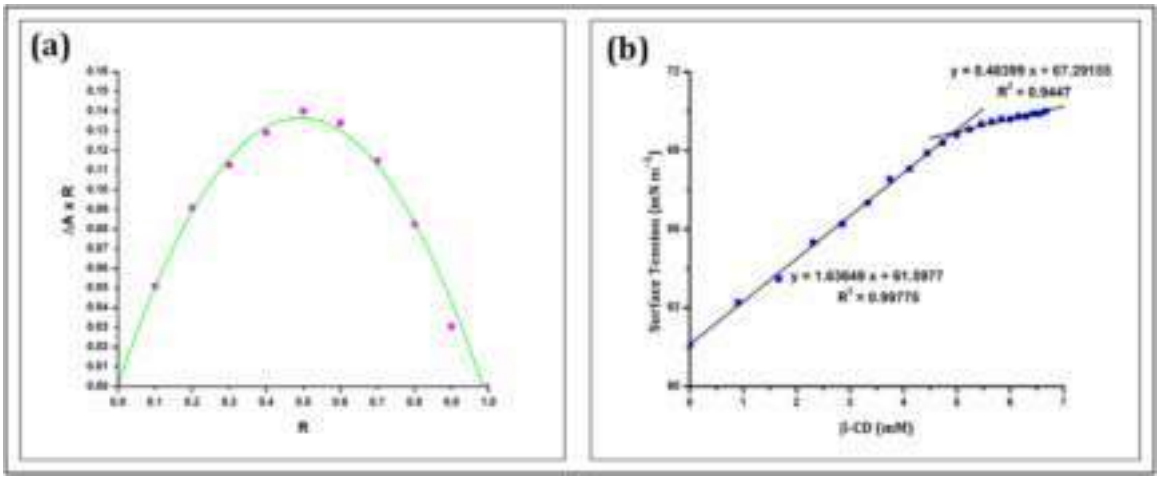

Fig. 1. **(a)** Job plot for TCP-β-CD system at 298.15 K (λ_{max} = 214 nm); **(b)** Surface tension variation of aqueous TCP solution with increasing β-CD concentration at 298.15 K.

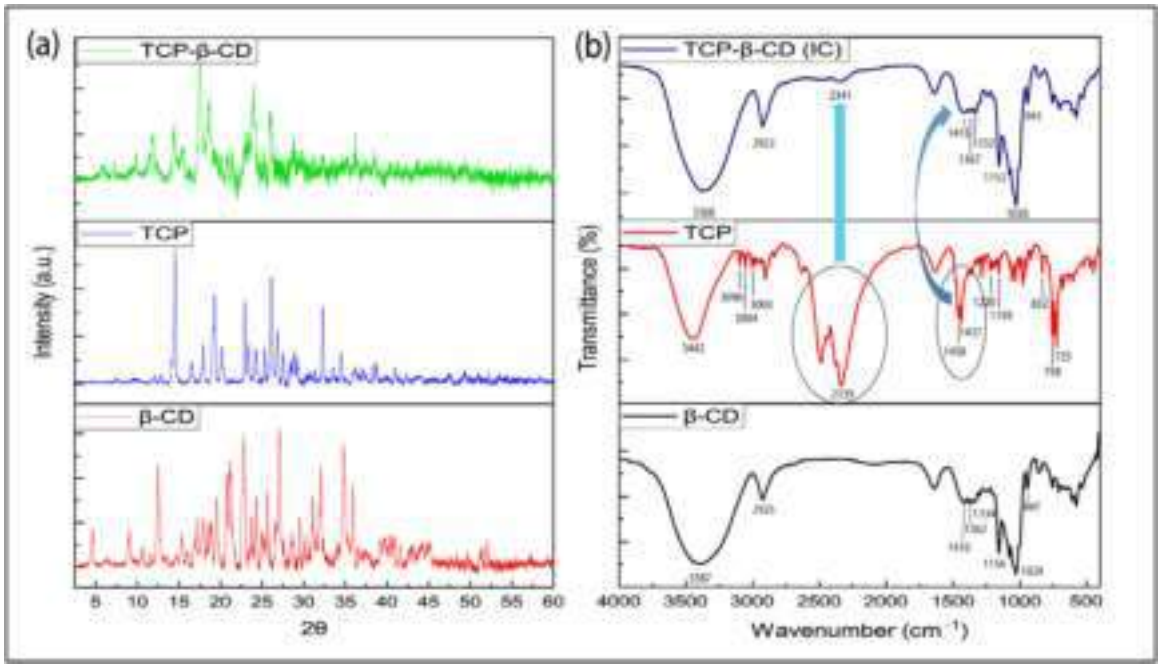

Fig. 2. **(a)** PXRD profiles and **(b)** FTIR spectra of β-CD, TCP and solid TCP-β-CD inclusion complex (IC).

at diffraction angles (2θ) of 11.80^0, 14.38^0, 15.44^0, 17.58^0, 18.64^0 and 23.94^0 revealed that the formed TCP-β-CD inclusion complex achieved a new solid state having amorphous structure, as indicated by the less intense broader diffraction peaks.

3.7. Analysis of FT-IR spectra

The analysis of prepared solid inclusion complex can be performed using a very useful FT-IR spectroscopic method. FT-IR spectral analysis highlights the molecular interaction of guest with host (Roy et al., 2020). The formation of solid inclusion complex is confirmed by the variation in the peak intensity, position, shape, and its disappearance in the spectra (Roy et al., 2020). The infrared spectra of β-CD, TCP and TCP-β-CD complex are depicted in Fig. 2(b), and the chemical bonds with their corresponding vibrational frequencies are presented in Table S6. The N-H stretching band of TCP at 3442 cm^{-1} and that of β-CD O-H at 3387 cm^{-1} were shifted to 3368 cm^{-1} as a broad band in the complex. In the case of TCP, chlorophenyl ring stretching at 1458, 1437 cm^{-1}, chlorophenyl C-H stretching at 3098, 3054, 3003 cm^{-1}, chlorophenyl C-H bending at 832, 758, 725 cm^{-1} (out-of-plane) & 1220 cm^{-1}(in-plane), C-S-C stretching at 2339 cm^{-1} and piperidine ring stretching at 1159 cm^{-1}, were observed. However, bands related to the chlorophenyl and piperidine rings in the spectrum of TCP were found to disappear in the TCP-β-CD complex spectrum, while that of C-S-C stretching observed in TCP was slightly shifted and appeared at 2341 $cm^{-1}$with much reduced intensity in TCP-β-CD complex. Such disappearance of IR peaks related to the chlorophenyl and piperidine rings, and the emergence of C-S-C stretching with reduced intensity indicates the inclusion of only the chlorophenyl and piperidine moieties (and not the thiophene ring) into the nano hydrophobic cavity of β-CD. The IR spectra of β-CD is characterized by C-H stretching band at 2925 cm^{-1}, C-H bending vibrations at 1410, 1362, 1334 cm^{-1}, C-O-C bending vibration at 1156 cm^{-1}, C-C-O stretching frequency at 1029 cm^{-1} and skeletal vibration involving α-1,4-linkage at 947 cm^{-1}. These vibrational bands of β-CD were

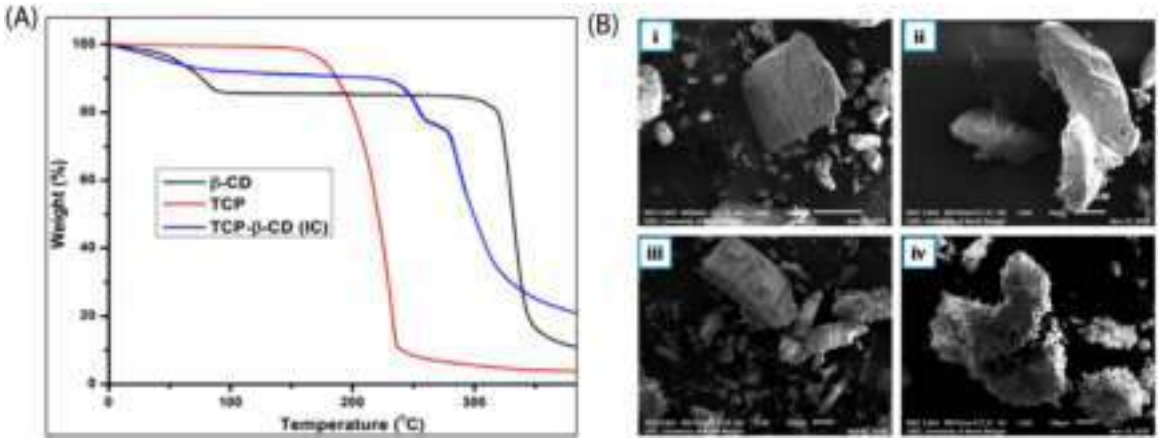

Fig. 3. **(A)** TGA thermograms of TCP, β-CD and TCP-β-CD inclusion complex (IC); **(B)** Scanning electron micrographs: (i) β-CD, (ii) TCP, (iii) physical mixture of TCP and β-CD, (iv) TCP-β-CD inclusion complex (IC).

shifted to 2922 cm^{-1} (C-H stretching), 1415, 1367, 1332 cm^{-1} (C-H bending), 1152 cm^{-1} (C-O-C bending), 1026 cm^{-1} (C-C-O stretching) and 943 cm^{-1} (skeletal vibration involving α-1,4-linkage) in the spectrum of solid inclusion complex, which may be possibly due to the incorporation of TCP into the β-CD cavity. All these observed variations of intensity and shifts in the IR spectra provides us the evidence of inclusion complex formation. These results suggest that the chlorophenyl and piperidine moieties (not the thiophene ring) are included into the hydrophobic cavity of β-CD, which are in good agreement with the ^{1}H NMR observations.

3.8. Thermal analysis

The TG analysis was performed on solid TCP-β-CD complex, pure TCP and β-CD to verify the thermal stability of TCP after its inclusion into CD cavity (Fig. 3A). The TGA curve of β-CD exhibits a weight loss below 100 ^{0}C corresponding to the water loss and a major weight loss between 280 ^{0}C and 388 ^{0}C due to the decomposition of β-CD. For TCP, a significant weight loss was observed indicating the degradation of TCP in the range 126–250 ^{0}C. On the other hand, it can be observed from the TGA thermogram of TCP-β-CD complex that the first stage weight loss below 89 ^{0}C is due to dehydration, the second one in the range 190–269 ^{0}C is attributed to the degradation of TCP, and the considerable weight loss after 269 ^{0}C indicates the main thermal decomposition of β-CD. It is evident from the TGA thermogram that the thermal decomposition of prepared complex was observed to occur at a higher range of temperature (190–269 ^{0}C) compared to pure TCP (126–250 ^{0}C), confirming that the inclusion complexation has enhanced the thermal stability of TCP.

3.9. SEM analysis

The study of SEM image was conducted to obtain a supporting evidence for the formation of inclusion complex by analyzing the surface morphology of solid samples (Pal et al., 2020). Fig. 3B shows the SEM microphotographs of β-CD, TCP, physical mixture and solid TCP-β-CD inclusion complex. Pure β-CD (Fig. 3B (i)) had a parallelogram-like crystal structure, while TCP (Fig. 3B (ii)) appeared as irregularly shaped crystal particles. In physical mixture (Fig. 3B (iii)), hybrids of parallelogram-like and irregularly shaped crystals were observed, i.e., crystalline nature of both β-CD and TCP were depicted. However, solid TCP-β-CD complex (Fig. 3B (iv)) appeared as unevenly shaped amorphous aggregates. Such significant modification in the surface morphology of complex confirms the encapsulation of TCP into β-CD cavity leading to the formation of solid TCP-β-CD inclusion complex.

3.10. Molecular docking studies

Molecular docking has been carried out for the prediction of most feasible conformation of TCP-β-CD inclusion complex with lowest binding energy (ΔG) (Alshehri et al., 2020). AutoDock 4.2 was used to dock a guest molecule, TCP, into the pocket of β-CD. The program produced various possible docked models according to the energetic parameters of TCP-β-CD complex. The computationally calculated free energies of binding corresponding to the ten docked conformations were listed in Table S7. Out of these ten docked conformations, four conformations 4, 5, 8 and 9 were observed to have identical structures which is reflected from their same lowest free energy of binding, -5.62 kcal/mol.One among the four lowest energy docked models of TCP-β-CD complex is shown in Fig. 4. The lowest negative binding energy value (-5.62 kcal/mol)is very close to the value (-6.0 kcal/mol) calculated from the binding constant (K_a) obtained from UV-visible spectroscopic studies, which suggest that the binding energy based on docking result is in accordance with that deduced from UV-visible absorption analysis. In all these four identical conformations, chlorophenyl and piperidine moieties are almost completely included into the binding pocket of β-CD, while thiophene ring was observed to lie nearly outside the wider rim. These interactions of TCP with β-CD resulted from docking analysis are in good agreement with the FT-IR and ^{1}H NMR results.

3.11. In vitro *studies of biological activity*

3.11.1. In vitro *cytotoxicity studies*

In this study, the cytotoxic effect of TCP and TCP-β-CD complex was explored against human kidney cancer cell line (ACHN). The ACHN cells were treated with various concentrations (5 μM, 10 μM, 15 μM, 20 μM and 25 μM) of TCP and complex, and the percentage inhibition of cell growth was measured by MTT assay. Fig. 5 represents the dose-dependent growth inhibition of human kidney cancer cell line (ACHN) after exposure with TCP and TCP-β-CD complex. When ACHN cells are exposed with pure TCP, the IC_{50} value was found to be 44 μM. Treating the similar cells with TCP-β-CD complex gives an IC_{50} value of 24 μM. These results suggest that the complex has higher cytotoxicity and reduces the viability of tested ACHN cells more effectively than TCP alone. Hence, complexation of TCP with β-CD was found to improve the anticancer activity of TCP towards ACHN cells. This may be probably due to the sustained release of TCP from the microsphere of β-CD, which leads to greater bioavailability thus enhancing the drug effect (Ren et al., 2019). In addition, the anticancer activity enhancement of TCP by complexation with β-CD is also likely due to the reason that β-CD can infiltrate into the drug permeation barrier, called unstirred water layer

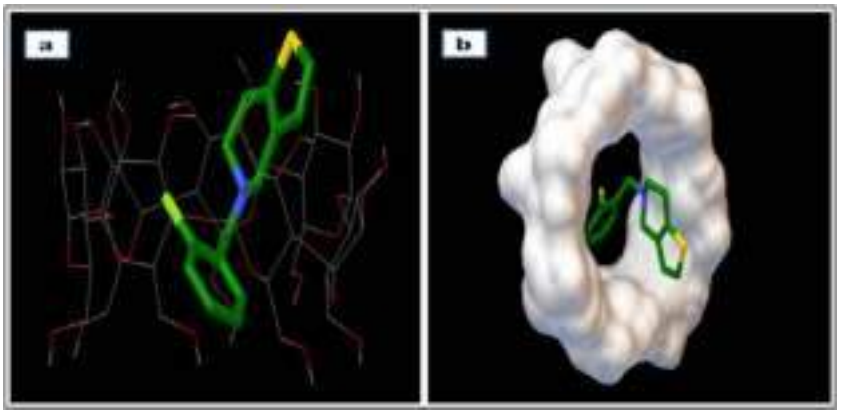

Fig. 4. Docked conformation of TCP-β-CD inclusion complex (IC), side view **(a)** and top view **(b)**.

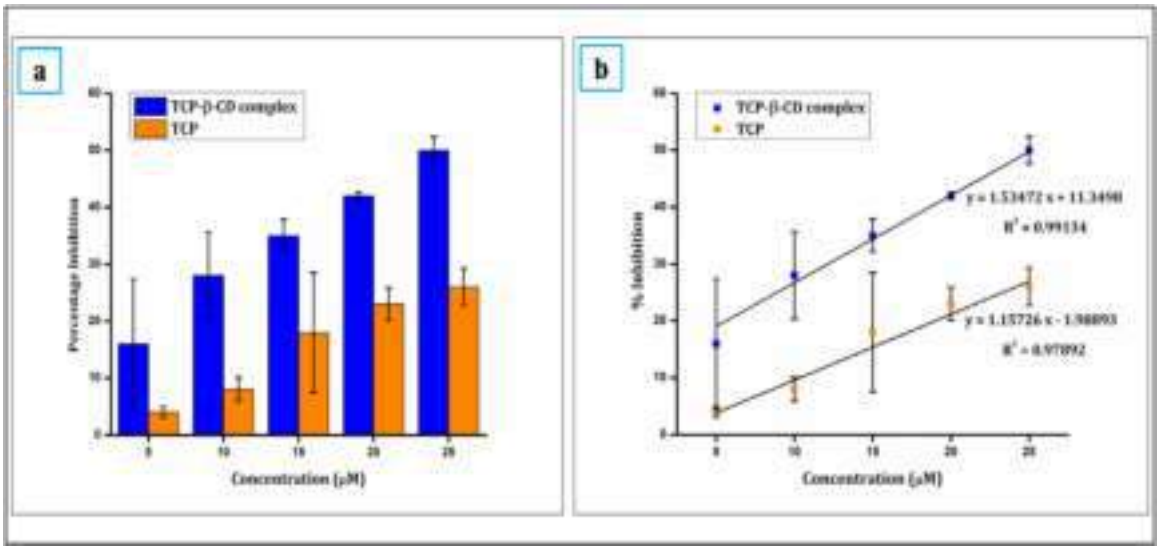

Fig. 5. **(a)** Dose-dependent growth inhibition of human kidney cancer cell line (ACHN) after exposing with TCP and TCP-β-CD complex for 48 h, **(b)** Linear regression analysis to calculate IC_{50} values. The obtained results are from three separate experiments presented as mean ± standard deviation.

(UWL) consisting of a large number of strong H-bond networks, better than the free form of TCP (Loftsson, 2012).

3.11.2. Assessment of ROS generation in ACHN cells

The overproduction of intracellular ROS (oxidative stress) could be generated not only by abnormal metabolism, but also by various drugs therapy. Oxidative stress has been widely implicated in drug-induced cytotoxicity (Deavall et al., 2012). Therefore, we evaluated the ROS production in ACHN cancer cells treated with TCP and TCP-β-CD complex at their IC_{50} values of 44 μM and 24 μM, respectively. 1.5 mM H_2O_2 treated cells were considered as positive control whereas the untreated cells were set as a control. Since in apoptosis ROS generation is an early event, the production of ROS in ACHN cells was determined after 24 h (Tian et al., 2012). Fig. 6(a) showed that a faintly green fluorescence was observed for control indicating the formation of ROS at basal level. On the other hand, bright green fluorescence was induced in cells treated with TCP, complex and positive control, displaying a substantial amount of ROS generation (Fig. 6(a)).

ROS generation was found a bit higher for TCP treated cells compared to cells exposed with positive control (Fig. 6(b)). However, TCP-β-CD complex induces significantly higher ROS generation in ACHN cells than TCP and positive control (Fig. 6(b)), which reveal that the complexation with β-CD increases the apoptotic activity of TCP. These findings demonstrates that the TCP in its complex form is more effective for oxidative mediated apoptosis than TCP alone due to ROS hyper-generation. Therefore, the induction of increased intracellular ROS (oxidative stress) production by TCP-β-CD complex could be one of the reasons for the observation of greater cytotoxicity of the complex towards ACHN cells compared to free TCP.

3.11.3. In vitro *antibacterial activity studies*

The treatment of cancer with chemotherapeutic agents/drugs may lead to secondary complications of weakening the immune system and in some cases causing immunodeficiency. Therefore, cancer patients are more vulnerable to develop various types of microbial infections. According to reports, microbial infections remain a significant cause of mortality among cancer patients (Bhat et al., 2021). Thus, there is an unfulfilled and unresolved need for a drug which not only has anti-cancer properties but also has antibacterial properties. The drug having such effect could lead to reduce the secondary complications and thus improve the chances of recovery and survival of cancer patients. Therefore, we performed the antibacterial test using the agar diffusion technique with four bacteria, namely, *Salmonella sp., Shigella sp., B. amyloliquefaciens* and *B. subtilis*, to evaluate the antibacterial activity of TCP and TCP-β-CD complex. Both TCP and TCP-β-CD complex showed noteworthy antibacterial activity against these bacteria (Fig. S4). However, it can be seen from the Tables S8 and S9 that the complex was found to possess relatively greater inhibitory effect than TCP alone. This indicates that the complex possessed effectively higher antibacterial activity than pure TCP, which may be possibly due to the fact that β-CD transports TCP readily to the surface of bacterial cells (Inoue et al., 2020). Another factor for this is presumably the complexation of TCP with β-CD signif-

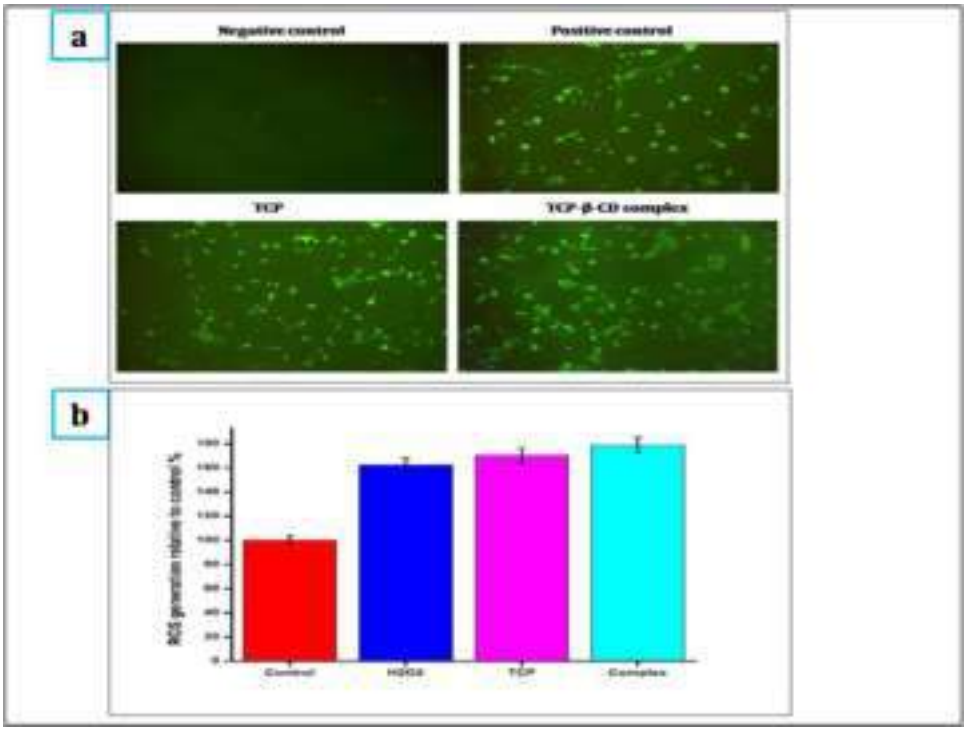

Fig. 6. Evaluation of intracellular ROS generation in ACHN cells using the fluorescent probe DCF-DA. **(a)**Photomicrographs of the untreated cells (negative control) and the cells treated with TCP (IC_{50} = 44 μM), TCP-β-CD complex (IC_{50} = 24 μM) and positive control (1.5 mM H_2O_2) for 24 h. **(b)** Percentage of ROS generation relative to control. The obtained results are presented as mean ± standard deviation.

icantly improved the bioavailability of TCP due to the improvement of the solubility (Savic et al., 2019).

4. Conclusions

We have reported the successful preparation of TCP-β-CD complex and examined the effect of inclusion on the *in vitro* bioactivity of TCP. The formulation of complex was confirmed by ^{1}H NMR, ESI-MS, FT-IR, TGA, SEM, PXRD, surface tension and UV-vis spectroscopic studies. The Job's method, surface tension study and ESI-MS experiment confirmed 1:1 stoichiometry of the TCP-β-CD complex. Higher binding constant value ($K_a = 25.16 \times 10^3$ M^{-1}) accounts for the higher binding affinity of TCP with β-CD and the thermodynamic spontaneity of binding process was validated by the negative Gibb's free energy change (ΔG). ^{1}H NMR, FT-IR and molecular docking studies suggested a possible stable molecular conformation for TCP-β-CD complex in which the chlorophenyl and piperidine moieties are almost completely included into the cavity of β-CD, and the thiophene ring lie nearly outside the wider rim. PXRD and SEM analysis showed that the prepared complex has amorphous nature which is unlike from its pure components. From TGA analysis we observed that encapsulation has enhanced the thermal stability of TCP. *In vitro* antibacterial test showed that the better activity was displayed by TCP after its complexation with β-CD. TCP-β-CD complex (IC_{50} = 24 μM) expressed significant cytotoxic effect than pure TCP (IC_{50} = 44 μM) towards human kidney cancer cell line (ACHN). Furthermore, the complex was found to induce the intracellular ROS generation more prominently than TCP, suggesting the enhancement in the apoptotic activity of TCP after complexation. Thus, TCP-β-CD inclusion complex can be a promising approach for designing a novel formulation of TCP in drug delivery, thereby, extending the potential clinical purpose of TCP in pharmaceutical industries and biomedical sciences.

Funding

This research did not receive any specific grant from funding agencies in the public, commercial, or not-for-profit sectors.

Declaration of Competing Interest

The authors declare no conflict of interest.

Supplementary materials

Supplementary material associated with this article can be found, in the online version, at doi:10.1016/j.focha.2022.100015.

CRediT authorship contribution statement

Pranish Bomzan: Conceptualization, Data curation, Investigation, Formal analysis, Writing – original draft. **Niloy Roy:** Data curation, Investigation, Writing – review & editing. **Vijeta Rai:** Data curation, Investigation, Writing – review & editing. **Debadrita Roy:** Formal analysis, Writing – review & editing. **Shilpi Ghosh:** Formal analysis. **Anoop Kumar:** Formal analysis. **Kanak Roy:** Formal analysis, Writing – review & editing. **Rinku Chakrabarty:** Formal analysis, Writing – review & editing. **Jyotsna Das:** Formal analysis, Writing – review & editing. **Vikas Kumar Dakua:** Formal analysis, Writing – review & editing. **Kumar Basnet:** Formal analysis, Writing – review & editing. **Mahendra Nath Roy:** Writing – original draft.

References

Alshaer, W., Zraikat, M., Amer, A., Nsairat, H., Lafi, Z., Alqudah, D. A., et al. (2019). Encapsulation of echinomycin in cyclodextrin inclusion complexes into liposomes: *In vitro* antiproliferative and anti-invasive activity in glioblastoma. *RSC Advances, 9*(53), 30976–30988.

Alshehri, S., Imam, S. S., Hussain, A., & Altamimi, M. A. (2020). Formulation of piperine ternary inclusion complex using β-CD and HPMC: Physicochemical characterization, molecular docking, and antimicrobial testing. *Processes, 8*(11), 1450.

Benkovics, G., Afonso, D., Darcsi, A., Béni, S., Conoci, S., Fenyvesi, É., et al. (2017). Novel β-cyclodextrin–Eosin conjugates. *Beilstein Journal of Organic Chemistry, 13*, 543–551.

Bhat, S., Muthunatarajan, S., Mulki, S. S., Bhat, K. A., & Kotian, K. H. (2021). Bacterial infection among cancer patients: Analysis of isolates and antibiotic sensitivity pattern. *International Journal of Microbiology*, 1–7 . Article ID 8883700. 10.1155/2021/8883700.

Calvisi, D. F. (2013). Inhibition of hepatitis B virus-associated liver cancer by antiplatelet therapy: A revolution in hepatocellular carcinoma prevention? *Hepatology, 57*(2), 848–850 (Baltimore, Md.).

Cramer, F., Saenger, W., & Spatz, H. (1967). Inclusion Compounds. XIX 1a. The formation of inclusion compounds of α-cyclodextrin in aqueous solutions, Thermodynamics and kinetics. *Journal of the American Chemical Society, 89*(1), 14–20.

De Lorgeril, M., Bordet, J. C., Salen, P., Durbin, S., Defreyn, G., Delaye, J., et al. (1998). Ticlopidine increases nitric oxide generation in heart-transplant recipients: A possible novel property of ticlopidine. *Journal of Cardiovascular Pharmacology, 32*(2), 225–230.

Deavall, D. G., Martin, E. A., Horner, J. M., & Roberts, R. (2012). Drug-induced oxidative stress and toxicity. *Journal of Toxicology*, 1–13.

Ferri, N., Corsini, A., & Bellosta, S. (2013). Pharmacology of the new P2Y12 receptor inhibitors: Insights on pharmacokinetic and pharmacodynamic properties. *Drugs, 73*(15), 1681–1709.

Gachet, C., Stierle, A., Cazenave, J. P., Ohlmann, P., Lanza, F., Bouloux, C., et al. (1990). The thienopyridine PCR 4099 selectively inhibits ADP-induced platelet aggregation and fibrinogen binding without modifying the membrane glycoprotein IIb-IIIa complexin rat and in man. *Biochemical Pharmacology, 40*(2), 229–238.

Gong, L., Li, T., Chen, F., Duan, X., Yuan, Y., Zhang, D., et al. (2016). An inclusioncomplex of eugenol into β-cyclodextrin: Preparation, and physicochemical and antifungal characterization. *Food Chemistry, 196*, 324–330.

Hayakawa, M., & Kuzuya, F. (1991). Effects of ticlopidine on erythrocyte aggregation in thrombotic disorders. *Angiology, 42*(9), 747–753.

Inoue, Y., Suzuki, R., Murata, I., Nomura, H., Isshiki, Y., & Kanamoto, I. (2020). Evaluation of antibacterial activity expression of the hinokitiol/cyclodextrin complex against bacteria. *ACS Omega, 5*(42), 27180–27187.

Li, Q., Pu, H., Tang, P., Tang, B., Sun, Q., & Li, H. (2018). Propyl gallate/cyclodextrin supramolecular complexes with enhanced solubility and radical scavenging capacity. *Food Chemistry, 245*, 1062–1069.

Liu, D. D., Guo, Y. F., Zhang, J. Q., Yang, Z. K., Li, X., Yang, B., et al. (2017). Inclusion of lycorine with natural cyclodextrins (α-, β- and γ-CD): Experimental and *in vitro* evaluation. *Journal of Molecular Structure, 1130*, 669–676.

Loftsson, T. (2012). Drug permeation through biomembranes: Cyclodextrins and the unstirred water layer. *Die Pharmazie, 67*(5), 363–370.

Magalhães, T. S. S. A., Macedo, P. C. O., Pacheco, S. Y. K., Santos da, Sofia, Silva, S. S. S., Barbosa, E. G., et al. (2020). Development and evaluation of antimicrobial and modulatory activity of inclusion complex of Euterpe oleracea mart oil and β-cyclodextrin or HP-β–cyclodextrin. *International Journal of Molecular Sciences, 21*(3), 942.

Mazoyer, E., Ripoll, L., Boisseau, M. R., & Drouet, L. (1994). How does ticlopidine treatment lower plasma fibrinogen? *Thrombosis Research, 75*(3), 361–370.

Ozdemira, N., Polab, C. C., Teixeirac, B. N., Hilld, L. E., Bayraka, A., & Gomesd, C. L. (2018). Preparation of black pepper oleoresin inclusion complexes based on beta-cyclodextrinfor antioxidant and antimicrobial delivery applications usingkneading and freeze drying methods: A comparative study. *LWT-Food Science and Technology, 91*, 439–445.

Pal, A., Roy, S., Kumar, A., Mahmood, S., Khodapanah, N., Thomas, S., et al. (2020). Physicochemical characterization, molecular docking, and *in vitro* dissolution of glimepiride–captisol inclusion complexes. *ACS Omega, 5*(32), 19968–19977.

Rai, V., Kumar, A., Das, V., & Ghosh, S. (2019). Evaluation of chemical constituents and *in vitro* antimicrobial, antioxidant and cytotoxicity potential of rhizome of Astilbe rivularis (Bodho-okhati), an indigenous medicinal plant from Eastern Himalayan region of India. *BMC Complementary and Alternative Medicine, 19*(1), 200.

Rajbanshi, B., Saha, S., Das, K., Barman, B. K., Sengupta, S., Bhattacharjee, A., et al. (2018). Study to probe subsistence of host-guest inclusion complexes of α and β-cyclodextrins with biologically potent drugs for safety regulatory dischargement. *Scientific Reports, 8*(1), 13031.

Ram, V., Kher, G., Dubal, K., Dodiya, B., & Joshi, H. (2011). Development and validation of a stability indicating UPLC method for determination of ticlopidine hydrochloride in its tablet formulation. *Saudi Pharmaceutical Journal, 19*(3), 159–164.

Rani, D., Sethi, A., Kaur, K., & Agarwa, J. (2020). Ultrasonication-assisted synthesis of a D-glucosamine-based β-CD inclusion complex and its application as an aqueous heterogeneous organocatalytic system. *The Journal of Organic Chemistry, 85*(15), 9548–9557.

Rao, A., K. (2013). Acquired disorders of platelet function. *Platelets; Academic Press, San Diego, CA.*, 1051–1076.

Ren, L., Wang, J., & Chen, G. (2019). Preparation, optimization of the inclusion complex of glaucocalyxin Awith sulfobutylether-β-cyclodextrin and antitumor study. *Drug Delivery, 26*(1), 309–317.

Roy, N., Ghosh, B., Roy, D., Bhaumik, B., & Roy, M. N. (2020). Exploring the inclusion complex of a drug (Umbelliferone) withα-cyclodextrin optimized by molecular docking and increasing bioavailability with minimizing the doses in human body. *ACS Omega, 5*(46), 30243–30251.

Saltiel, E., & Ward, A. (1987). Ticlopidine. A review of its pharmacodynamic and pharmacokinetic properties, and therapeutic efficacy in platelet-dependent disease states. *Drugs, 34*(2), 222–262.

Savic, I. M., Jocic, E., Nikolic, V. D., Popsavin, M. M., Rakic, S. J., & Savic-Gajic, I. M. (2019). The effect of complexation with cyclodextrins on the antioxidant and antimicrobial activity of ellagic acid. *Pharmaceutical Development and Technology, 24*(4), 410–418.

Tian, L., Yin, D., Ren, Y., Gong, C., Chen, A., & Guo, F. (2012). Plumbagin induces apoptosis via the p53 pathway and generation of reactive oxygen species in human osteosarcoma cells. *Molecular Medicine Reports, 5*(1), 126–132.

USFDA, (2001). U.S. food and drug administration. Agency response letter Gras notice 000074. CFSAN/Office of Food Additive Safety. <https://www.fda.gov/downloads/food/ingredientspackaginglabeling/gras/noticeinventory/ucm261320.pdf/> (Accessed date: 5 May 2017).

Veloso, T. R., Oechslin, F., Que, Y., Moreillon, P., Entenza, J. M., & Mancini, S. (2015). Aspirin plus ticlopidine prevented experimental endocarditis due to Enterococcus faecalisand Streptococcus gallolyticus. *FEMS Pathogens and Disease, 73*(8), ftv060.

Wojtukiewicz, M. Z., Hempel, D., Sierko, E., Tucker, S. C., & Honn, K. V. (2017). Antiplatelet agents for cancer treatment: A real perspective or just an echo from the past? *Cancer Metastasis Reviews, 36*(2), 305–329.

Wu, Y. (2012). Heterocycles and medicine: A survey of the heterocyclic drugs approved by the U.S. FDA from 2000 to present. *Progress in Heterocyclic Chemistry, 24*, 1–53.

Zeng, X. X., Zheng, R. L., Zhou, T., He, H. Y., Liu, J. Y., Zheng, Y., et al. (2010). Novel thienopyridine derivatives as specific anti-hepatocellular carcinoma (HCC) agents: Synthesis, preliminary structure-activity relationships, and *in vitro* biological evaluation. *Bioorganic & Medicinal Chemistry Letters, 20*(21), 6282–6285.

Zhang, L., Man, S., Qiu, H., Liu, Z., Zhang, M., Ma, L., et al. (2016). Curcumin-cyclodextrin complexes enhanced the anti-cancer effects of curcumin. *Environmental Toxicology and Pharmacology, 48*, 31–38.